

Recombinant expression of the pRb- and p53-interacting domains from the human
RBBP6 protein for *in vitro* binding studies

Nonkululeko Ndabambi

A thesis submitted in partial fulfilment of the requirements for the degree of Magister
Scientiae in the Faculty of Sciences, University of the Western Cape.



Supervisor: Dr DJR Pugh

December 2004

**Recombinant expression of the pRb- and p53-interacting domains from the human
RBBP6 protein for *in vitro* binding studies**

Nonkululeko Ndabambi

Keywords:

DWNN

Expression

Protein-protein interactions

NMR

p53

Rb

Recombinant

RBBP6

Tumour suppressor

Structural biology



Abstract

Recombinant expression of the pRb- and p53-interacting domains from human RBBP6 for *in vitro* binding studies

N. Ndabambi

M.Sc. thesis, Department of Biotechnology, Faculty of Natural Science, University of the Western Cape.

This thesis describes the cloning and recombinant expression of domains from the human RBBP6 protein for future *in vitro* binding studies with pRb and p53. RBBP6 is a splicing-associated protein that is known to interact with both p53 and the Retinoblastoma gene product (pRb), and has recently been shown to be highly upregulated in oesophageal cancer. The pRb binding domain (RbBD) and the p53 binding domain (p53BD) were each expressed using the glutathione-S-transferase (GST) tag affinity system, and affinity purified using a glutathione-linked agarose column. Purified fusion proteins were cleaved to separate the target protein from GST using PreScission™ Protease, for which there is a recognition sequence located immediately upstream of the multiple cloning site on the pGEX-6P series of plasmids. The pRb binding and p53 binding domains were further purified using cation exchange chromatography.

Mass spectrometry confirmed that the RbBD was expressed as a single species of the expected molecular weight. However preliminary NMR analysis suggested that the domain was not fully folded. A total yield of 8 mg of protein was achieved from 1l of culture, which make it feasible to express ^{15}N and ^{12}C labelled samples for NMR. The p53BD was found to be expressed at lower levels and subject to C-terminal degradation, which suggest that the C-terminus is unstructured most likely due to the presence of poly-lysine tail.

Human pRb protein was also successfully expressed and purified using the GST affinity system. Human p53 protein was expressed but was found to be insoluble and attempts to purify it were not pursued. Attempts to confirm the interactions between human RBBP6 and p53 and pRb proteins are on-going but fall outside the scope of this thesis.



Expression constructs for the RING and zinc finger domains from human RBBP6 were also cloned into the pGEX system for future structural studies using NMR. Both domains were found to be expressed as soluble fusion proteins in preliminary expression studies.

Declaration

I declare that “*Recombinant expression of the pRb- and p53-interacting domains from the human RBBP6 protein for in vitro binding studies*” is my own work that has not been submitted for any degree or examination in any other university and that all the sources I have used or quoted have been indicated and acknowledged by complete references.

Nonkululeko Ndabambi

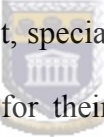


December 2004


Signed:.....

Acknowledgements

I would like to thank my supervisor Dr David Pugh and co-supervisor Prof Jasper Rees for their help and support during the course of this project.

I would also like to thank Dr Anne-Lee Gall of Cambridge University and Prof Iqbal Parker of the University of Cape Town for their reagents. I wish to extend my sincere gratitude to the DWNN research group, and most especially to Dr Amanda Skepu for generating a full-length human RBBP6 cDNA construct and other members of the Rees research lab for their valuable input on my project and for creating a warm and memorable environment. I am grateful to the National Research Foundation (NRF) for their financial support. Last, but not least,  special thanks to my family and especially my mother Nonceba and my father Sipho for their moral support, endless love and their patience throughout the past years.

ABBREVIATIONS

Amp	Ampicillin
Bax	Bcl-2-associated x protein
Bid	B cell leukaemia-2
BLAST	Basic Local Alignment Search Tool
bp	base pair
BCL-2	B cell leukaemia lymphoma-2
BSA	Bovine serum albumin
cDNA	complementary DNA
cdk	Cyclin-D dependent kinase
Caspase	 Cysteine aspartic acid-specific protease
CHO	Chinese Hamster Ovary
CTL	Cytotoxic T lymphocyte
D ₂ O	Deuterium oxide
DMSO	Dimethyl sulphoxide
DNA	Deoxyribonucleic acid
DR	Death receptor
DTT	Dithioreitol
DWNN	Domain With No Name
EDTA	Ethylene diamine tetra acetic acid
FADD	Fas-associated death domain
GST	Glutathione-S-Transferase

hnRNP	heterogeneous nuclear ribonucleoprotein
HPV	Human papilloma virus
hr	hour
ICE	Interleukin-1 β -converting enzyme
IPTG	Isopropyl- β -D-thiogalactopyranoside
kbp	kilo base pair
kDa	kilo Dalton
l	litre
LB	Luria Broth
MHz	MegaHertz
MW	Molecular weight
MCS	Multiple cloning site
MDM2	Murine double minute clone 2
min	minute
MOPS	4-Morpholine-propanesulfonic acid
mRNA	messenger RNA
NMR	Nuclear Magnetic Resonance
PACT	p53 associated cellular-protein testis-derived
PAGE	Polyacrylamide gel electrophoresis
PARP	Poly (ADP-ribose) Polymerase
PBS	Phosphate buffered saline
PCR	Polymerase chain reaction
PMSF	Phenylmethanesulphonyl fluoride


P2P-R	Proliferation potential related protein
Rb	Retinoblastoma gene
pRb	Retinoblastoma gene product
RBBP6	Retinoblastoma binding protein 6
RNA	Ribonucleic acid
RING	Really Interesting New Gene
SDS	Sodium dodecyl sulphate
s	seconds
SR domain	serine/arginine rich domain
TBP	TATA binding protein
TAFs	TBP-associated factors
TEMED	 <i>N, N, N', N'</i> -Tetramethylethylenediamine
TNF	Tumour necrosis factor
TRADD	TNFR-associated death domain
UV	Ultra violet
V	Volts

TABLE OF CONTENTS

Title.....	i
Keywords.....	i
Abstract.....	ii
Declaration.....	iv
Acknowledgements.....	v
Abbreviations.....	vi
Table of contents.....	ix

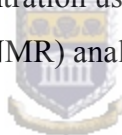
Chapter 1: Introduction ----- 1

1.1 The RBBP6 family of proteins.....	1
1.2 Tumour suppressor genes and apoptosis.....	5
1.3 p53.....	10
1.4 Retinoblastoma gene product (pRb).....	15
1.5 Aims.....	18

Chapter 2: Materials and Methods----- 20

2.1 Bacterial strains used.....	20
2.2 Preparation of bacterial (<i>E. coli</i>) competent cells.....	20
2.3 Cloning vectors.....	21
2.3.1 Cloning into the pGEM [®] -T Easy vector.....	21
2.3.2 Cloning into the pGEX-6P-2 expression vector.....	21
2.4 Bacterial transformation.....	23
2.5 Preparation of plasmid DNA.....	23
2.5.1 Small-scale preparation of plasmid DNA.....	23
2.5.2 Large-scale preparation of plasmid DNA.....	24
2.6 Agarose gel electrophoresis of DNA.....	26

2.7 DNA quantification-----	26
2.8 Manipulation of DNA -----	26
2.8.1 Restriction enzyme digestion-----	26
2.8.2 Cloning of DNA -----	27
2.9 PCR amplification of DNA fragments -----	27
2.10 Gel purification of DNA and PCR products -----	27
2.11 DNA sequencing-----	28
2.12 Colony PCR -----	29
2.13 Expression and purification of GST fusion proteins -----	29
2.13.1 Expression screen -----	29
2.13.2 Large-scale expression-----	30
2.13.3 Glutathione affinity chromatography -----	31
2.14 Cation exchange chromatography -----	31
2.15 SDS-PAGE analysis-----	32
2.16 Determination of protein concentration using the Bradford assay -----	33
2.17 Nuclear Magnetic Resonance (NMR) analysis -----	33



Chapter 3: Cloning, expression and purification of the pRb and p53 binding domains from human RBBP6 -----	35
3.1 Introduction-----	35
3.2 Construction of expression plasmids for the Rb and p53 binding domains -----	35
3.2.1 Amplification of RbBD and p53BD using PCR -----	35
3.2.2 Cloning of the pRb and p53 binding domains into pGEM [®] -T Easy -----	36
3.2.3 Sub-cloning of the pRb and p53 binding domains into pGEX-6P-2 -----	37
3.3 Expression and purification of the pRb and p53 binding domains -----	38
3.3.1 Expression screen of the pRb and p53 binding domains -----	38
3.3.2 Large-scale expression and purification of the pRb and p53 binding domains	38
3.4 Physical analysis of the RbBD -----	39
3.4.1 Mass spectrometric analysis-----	40
3.4.2 Determination of the concentration of the pRb binding domain-----	40
3.4.3 1D NMR analysis of pRb binding domain -----	42

Chapter 4: Recombinant expression of p53 and Rb A/B -----	43
4.1 Introduction-----	43
4.2 Construction of an expression plasmid for full-length p53 -----	44
4.2.1 Amplification of p53 using PCR-----	44
4.2.2 Cloning of p53 into pGEM [®] -T Easy -----	44
4.2.3 Sub-cloning of p53 into pGEX-6P-2 -----	44
4.3 Expression and purification of p53 and Rb A/B -----	45
4.3.1 Expression screen of the p53 and Rb A/B-----	45
4.3.2 Large-scale expression of and purification of p53 and Rb A/B-----	45
Chapter 5: Generation of recombinant expression constructs for the RING and zinc finger domains from human RBBP6 -----	47
5.1 Introduction-----	47
5.2 PCR amplification of RING and zinc finger domains-----	48
5.3 Cloning of RING and zinc finger domains into pGEM [®] -T Easy -----	48
5.4 Sub-cloning the RING and zinc finger domains into pGEX-6P-2-----	49
5.5 Expression screen of RING and zinc finger constructs -----	49
Chapter 6: Discussion and Conclusion -----	50
6.1 Introduction-----	50
6.2 Expression and purification of the pRb binding domain from human RBBP6 and the pocket domain from pRb-----	50
6.3 Generation of recombinant expression constructs for the p53 binding domain from human RBBP6 and for full-length p53 -----	51
6.4 Generation of reagents for structural analysis of the RING and zinc finger domains of the human RBBP6.-----	53

References

Appendix 1: Human RBBP6 sequence

Appendix 2: Human p53 sequence

Appendix 3: General stock solution and buffers

Appendix 4: General chemicals and enzymes



Chapter 1: Introduction

1.1 The RBBP6 family of proteins

RBBP6 (Retinoblastoma binding protein 6) is a 250 kDa splicing-associated protein that has previously been shown to interact *in vivo* with two major tumour suppressor proteins, p53 and the Retinoblastoma gene product pRb, in both human and mouse [1]. Using pRb as a probe, a 140 kDa truncation of the human protein was originally isolated from a small lung carcinoma H69c expression library and named Retinoblastoma binding protein 6 (RBBP6) or RBQ-1 [2]. RBBP6 was shown to bind to the under-phosphorylated form of pRb but not to the phosphorylated [3]. The binding can be interrupted by adenovirus E1A protein, which is known to bind to the pocket domain of pRb, suggesting that RBBP6 also binds to the pocket domain of pRb. A region of 34 amino acids corresponding to exon 16 of the full-length gene was found to be alternatively spliced [1]. The 140 kDa protein originally named RBBP6 results from a truncation caused by a mutational event in the small lung carcinoma H69c, leading to the introduction of a stop codon [1, 3]. The name RBBP6 is now applied to the full-length protein, which appears in the GenBank database under the accession number NP_008841.

Using p53 as a probe to screen a mouse testis expression library, a cDNA encoding a 250 kDa protein was subsequently isolated and denoted PACT (p53 Associated Cellular protein-Testis-derived) [1]. PACT was subsequently shown by sequencing to be a different truncation of the full-length RBBP6 protein. The C-terminal region of PACT was shown to be responsible for the binding to wild type p53, and two different mutations

in the core domain of p53 were shown to abolish this interaction [1]. PACT was also shown to interfere with the binding of p53 to specific sites on DNA. PACT contains a serine/arginine (SR) rich region near the N-terminus that is found in many pre-mRNA splicing factors [4]. The 250 kDa PACT protein can be precipitated from cell lysates using a method specific for SR proteins [4]. It was also shown by co-precipitation that PACT can bind p53 and pRb simultaneously [1].

Terminal differentiation occurs when cells lose their ability to proliferate and acquire specialized functions. It is associated with repression of the proliferation potential proteins (P2P) which are a subset of the heterogeneous nuclear ribonucleoproteins (hnRNP) that are involved in RNA processing [4]. Antibodies specific for the class of P2P proteins were used to isolate a protein, denoted Proliferation Potential Related (P2P-R) that was subsequently shown to be yet another truncation of RBBP6 [4]. It was shown that P2P-R can precipitate pRb out of human K-562 cell extracts containing abundant pRb [4]. The P2P-R/Rb complex was reported to be reduced by competition with adenovirus E1A protein, suggesting that the interaction occurs through the pocket domain of pRb. Expression of P2P-R is repressed during terminal differentiation [4]. P2P-R lacks the 34 amino acids first shown to be alternatively spliced in RBBP6 [1], which appears to be the dominant isoform expressed in murine cell lines [5].

Mpe1 is the yeast homologue of RBBP6, identified by Vo and co-workers, and encodes a protein of 441 amino acids with a molecular weight of 49.5 kDa [6]. Mpe1 is essential for yeast viability and is required for the specific cleavage and polyadenylation of pre-

mRNA. It has been shown to interact with the PCF11 protein, which encodes a subunit of cleavage factor I (CFI), which is responsible for the specific cleavage and polyadenylation of pre-mRNA [6]. Mpel has also been shown to be a component of the cleavage and polyadenylation factor complex (CPF) although it is not essential for the stability of the CPF [6].

It has recently been shown that RBBP6 is highly up-regulated in oesophageal cancer cells [7]. Yoshitake and co-workers showed that the cell growth rate was reduced in RBBP6 knockdown oesophageal cell line TE13, which suggests that RBBP6 is also important in the cell cycle progression. Cytotoxic T cell lines specific for RBBP6 were able to kill tumour cells *in vitro* and also inhibited the growth of oesophageal tumours in mice xenograft models.



Bioinformatic and structural analysis carried out at the University of the Western Cape has shown that homologues of RBBP6 occur in all completely sequenced eukaryotic genomes analysed to date, in most cases at single copy number [8]. All homologues contain a previously uncharacterised ubiquitin-like domain at the N-terminus, which has been named the DWNN domain (Domain With No Name). The structure of the 80 residue DWNN domain was determined using heteronuclear NMR and shown to be most similar to that of human ubiquitin. Human and mouse homologues contain a DWNN domain, a zinc knuckle and a RING finger domain, as well as an SR domain and the domains previously shown to interact with pRb and p53 respectively [1, 3]. RBBP6 homologues are shorter in invertebrates than in vertebrates, containing only the DWNN

domain, zinc knuckle, and RING finger domain and lacking both the p53 binding domain and the pRb binding domain (see Fig 1.1).

Zinc knuckles form a subgroup of zinc finger domains, which are small protein motifs that fold around a single zinc ion [9]. The zinc ion is coordinated by four conserved cysteine or histidine residues, with the classical zinc finger having the CCHC consensus motif. Many proteins containing classical zinc fingers are known to bind DNA, and they are typically found in transcription factors [10], and are also thought to bind preferentially to mRNA. Zinc knuckles have also been found in viral proteins and proteins involved in mRNA processing.

RING fingers bind two zinc ions through a conserved set of eight cysteine (C) or histidine (H) residues [11]. They are similar to double zinc fingers, except that the zinc ions are coordinated in a cross-brace fashion, with the first ion being coordinated by the first and third pair of C/H residues, and the second ion being coordinated by the second and fourth C/H pair. RING finger domains are found in proteins involved in a diverse range of cellular processes, including apoptosis, oncogenesis, ubiquitination and viral infections [12]. They also have an ability to mediate protein-protein interactions, particularly in the formation of large macromolecular scaffolds [13]. Recently, RING fingers have been shown to play a role in the ubiquitination of proteins, and many are found within E3 ubiquitin-ligase enzymes which catalyse the attachment of ubiquitin [14]. The presence of the ubiquitin-like DWNN domain, the mRNA binding zinc knuckle and the RING finger domain within a protein that is also known to be involved in mRNA

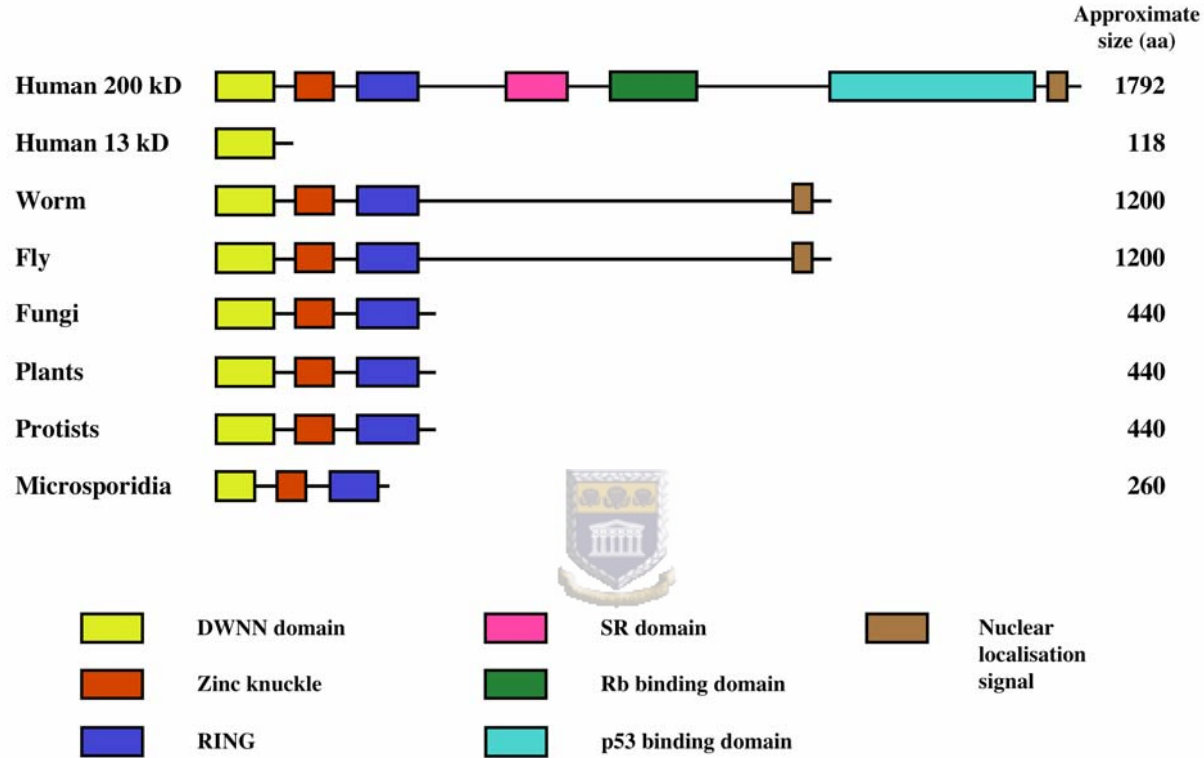


Fig. 1.1: Arrangement of the RBBP6/PACT domains in various eukaryotic species. All eukaryotes contain the ubiquitin-like DWNN domain, the zinc knuckle and the RING finger domain. Higher eukaryotes contain an additional C-terminal extension containing the p53 interacting domain and the pRb interacting domain.

processing suggest that RBBP6 may play a role in transcriptional regulation involving a ubiquitin-conjugation type mechanism.

The role of p53 and pRb in this scenario is still unclear. Vertebrate and insect homologues of RBBP6 contain long C-terminal extensions containing the domains shown to interact with pRb and p53 *in vivo* [1, 3]. Neither of these domains contains any identifiable motifs previously associated with p53 or pRb binding and it is therefore difficult to predict whether they will be folded if expressed recombinantly *in vitro*

1.2 Tumour suppressor genes and apoptosis

Tumour suppressor genes regulate cell division or cause cells to die by apoptosis [15]. They play a central role in regulating molecular pathways that have evolved to integrate positive and negative growth signals during normal development and repair [16]. *p53* and *Rb* represent two of the most important tumour suppressor genes. Both are activated following tumour formation and mutation of *p53* or *Rb* frequently leads to disruption of their anti-tumour activity, leading to cancer. *Rb* is frequently found to be mutated in osteosarcoma and in small-lung carcinomas, whereas *p53* is mutated more frequently in malignant melanoma [17]. Overall, *p53* is found to be mutated in over 50% of all human cancers [18]

Apoptosis is a naturally occurring process of cellular suicide that occurs in all animals during normal development. Two forms of cell death have been described: necrosis and apoptosis. Cells die either because of an attained injury in the case of necrosis or because

they commit suicide in the case of apoptosis. There is a distinct difference between these two processes based on structural changes to the cell. Necrosis is a pathological form of cell death resulting from an acute cellular injury, leading to an influx of water and extracellular ions. Intracellular organelles and the entire cell swell, leading to rupture of the plasma membrane, followed by leakage of the cytoplasmic contents into the extracellular fluid. Necrosis is associated with tissue damage, which leads to an inflammatory response. In apoptosis, the process is characterised by chromatin condensation, internucleosomal fragmentation of DNA, blebbing of the cell membrane and vesicularisation of the cell contents into apoptotic bodies [19, 20]. The apoptotic bodies are then engulfed by phagocytes or neighbouring cells through phagocytosis resulting in suppression of the inflammatory response.



Apoptosis plays an important role in normal development, in tumour suppression and as a defence mechanism against viral infections [21]. Defects in the regulation of apoptosis contribute to a number of human diseases. For example, excessive down-regulation of apoptosis has been linked to the development of cancer and viral infections, while excessive up-regulation causes autoimmune disorders, neurodegenerative diseases such as Alzheimer's disease and ischaemic injury [22, 23]. Many genes involved in tumour suppression are also involved in regulating apoptosis and there is an increased frequency of tumours when these genes are inactivated.

The development of human cancers is frequently associated with the inactivation of two major suppression pathways associated with the Retinoblastoma gene product (pRb) and

p53 respectively. pRb and p53 negatively regulate critical steps in the cell cycle commonly known as checkpoints [24, 25]. Two checkpoints monitor DNA damage: one at the G₁/S transition and the other at the G₂/M transition. The G₁/S checkpoint prevents replication of damaged DNA: arrest at this point is thought to give cells time to repair critical damage before DNA replication occurs, thereby avoiding the propagation of genetic lesions to progeny cells. The cell cycle will either resume once the damage has been repaired or, if the damage is too extensive, apoptosis will be initiated.

During the gap between DNA synthesis and mitosis, the cell will continue to grow and produce new proteins. At the end of this gap another checkpoint, the so-called G₂/M checkpoint, monitors whether the cell is ready to enter M phase (mitosis) and divide. p53 also has a role in regulating the G₂/M transition [26]. However, the G₂/M transition can also be regulated independently in p53^{-/-} cells. p53 promotes apoptosis only under certain circumstances, such as in response to DNA damage [27]. p53-dependent apoptosis occurs predominantly in the G₁ phase when cells are in growth arrest. Although the exact mechanism is unclear, it may involve the levels of the pro-apoptotic proteins *bax* and *bcl-2*, which p53 controls by activating expression of the *bax* gene and repressing expression of *bcl-2* gene [28].

The product of the *bcl-2* (B cell leukaemia lymphoma-2) gene is an important regulator of apoptosis, which was first identified not due to its role in cellular proliferation, but rather due to its involvement in chromosome translocation in B cell follicular lymphoma in which the *bcl-2* oncogene is activated and enhances cell survival. In T cells the *bcl-2*

gene confers resistance to apoptosis induced by glucocorticoids, radiation and other agents. Expression of Bcl-2 is widespread during embryogenesis but is restricted to differentiated cells. A critical mediator of *bcl-2*-regulated apoptosis is interleukin-1 β -converting enzyme (ICE), a cysteine protease that processes IL-1 β during the inflammatory response. Mammalian cells express several cell death cysteine proteases that form a proteolytic cascade [29]. Over-expression of ICE in mammalian cells causes apoptosis that is inhibited by Bcl-2. In general, the activity of a family of ICE-related genes would appear to be critical in driving apoptosis. A number of ICE family substrates have been identified, including poly (ADP) ribose polymerase (PARP) and nuclear lamins. p53 is also implicated in the movement of Fas, a member of the tumour necrosis factor (TNF) receptor family involved in apoptosis, from the cytoplasmic pool to the membrane so that it can interact with Fas-ligand (FasL) and initiate apoptosis [30]. Like other TNF family members, FasL is a homo-trimeric molecule [31]. Therefore each FasL trimer on the membrane binds three Fas molecules, which leads to clustering of death domain receptors. An adapter protein called Fas-associated death domain (FADD) then binds through its own death domain to the clustered death receptor death domains. FADD contains its own death effector domain, which binds to and activates caspase-8, which then activates the downstream effector caspase-9, thereby committing the cell to apoptosis.

Retinoblastoma (*Rb*) is another tumour suppressor gene that suppresses cellular proliferation and is inactivated in various human cancers [32]. The product of the retinoblastoma gene, pRb, is a nuclear phosphoprotein that plays a crucial role in the

decision of the cell to enter or to exit the cell cycle [25]. It is present throughout the cell cycle, but its phosphorylation state changes in a cell cycle-dependent manner, catalysed by cyclin-dependent kinases (cdks) in late G₁ phase [33]. It acts by repressing transcription of particular genes in G₁ phase, including members of the E2F family of transcription factors, which are required for the G₁ to S phase transition, leading to cell cycle arrest [25]. Progression of the cell through G₁/S phase requires inactivation of pRb by phosphorylation by cdks, leading to release of pRb from E2F [34]. *Rb* is a critical negative regulator of the cell cycle and therefore prevents deregulation of proliferation and tumour formation. The pRb protein acts differently from other tumour suppressors in that it does not induce apoptosis directly, but rather acts by stabilising p53 by blocking degradation of p53 by the murine double minute clone 2 protein (MDM2) [32].



Phosphorylation of pRb at its serine and threonine residues leads to activation of E2F, allowing cells to progress from G₁ phase to S phase. E2F is a family of closely related group of transcription factors (E2F1, E2F2, E2F3, E2F4 and E2F5), which were first characterised for their role in mediating transcriptional activation of the adenovirus E2 promoter. E2F, together with the heterodimeric small subunit of DNA polymerase II known as DP1, regulates expression of genes required for progression into G₁ phase. Phosphorylation of pRb is regulated by cyclin-D-dependent kinases cdk4 and cdk6 [25]. Mutations in E2F block the interaction with pRb leading to accelerated onset of S phase and apoptosis.

1.3 *p53*

The *p53* tumour suppressor gene encodes a nuclear phosphoprotein with cancer-inhibiting properties. The gene is the most frequently mutated gene in human cancers [18] and the majority of mutations are point mutations falling within evolutionarily conserved domains of the gene. These mutations cause conformational changes in the protein, thereby rendering it inactive with respect to its normal function. *p53* was originally discovered in immunoprecipitates performed using the large tumour antigen (large T) from Simian virus 40 (SV40) transformed rodent cells [35]. The human *p53* gene contains 11 exons and spans 20 kbp on the short arm of chromosome 17 (17p13.1).

p53 protein structure

p53 is a protein of 393 amino acids, organised into four structural and functional regions, as shown in Fig. 1.2A: the amino-terminal transactivation domain, the core domain, the tetramerisation domain and the carboxy-terminal regulatory domain [36]. The four regions are highly conserved between species. The transactivation domain (residues 1-42) is highly hydrophobic and regulates gene expression by interacting with proteins such as MDM2 and transactivating factors. The core domain (residues 102-292) contains the sequence-specific DNA binding activity of the *p53* protein. Mutations in this domain result in a loss of DNA binding. The tetramerisation domain (residues 324-355) is responsible for *p53* forming a homo-tetramer in solution through dimerisation of two β -sheets and two α -helices within the domain [37]. The tetramerisation domain is linked to the core domain by a flexible linker of 37 residues. The C-terminal domain (residues

A.



B.

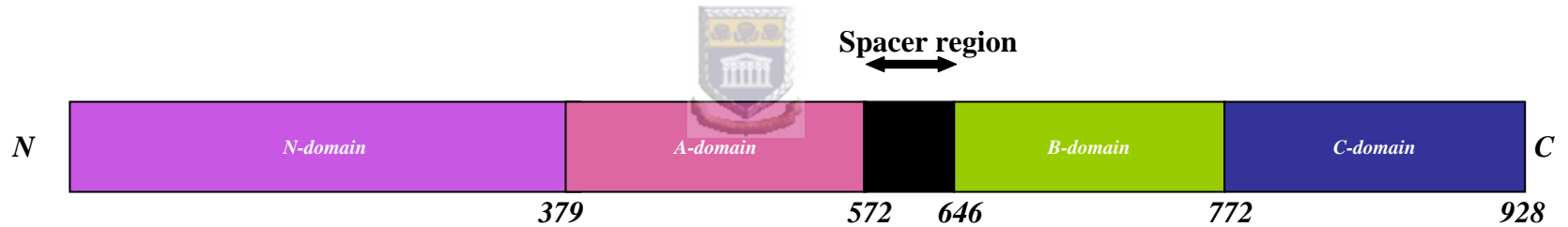


Fig. 1.2: (A) Structure of the p53 showing four different functional domains: the transactivation domain, the core domain, the tetramerisation domain and the regulatory domain. (B) The structure of the retinoblastoma (Rb) pocket domain showing the N-domain, A-domain, B-domain and the C-domain with the spacer region between the A-domain and B-domain (Morrison and Dyson *et al.*, 2001).

367-393) contains the nuclear localisation signal and also plays a role in non-specific DNA binding [38].

The function of p53

p53 functions as a sequence specific DNA binding protein and transcription factor that controls the expression of proteins involved in growth control, DNA repair, cell cycle arrest, apoptosis, and protein degradation [39-41]. There are several mechanisms by which p53 carries out these functions including blocking of the cell cycle before entry into S phase in response to various stimuli such as viral infection and agents that induce DNA damage, and the induction of apoptosis by activating the expression of *bax* genes. These responses allow p53 to inhibit the growth of stressed cells either by cycle arrest or by permanent removal of these cells from the organism by apoptosis [42].



The stress-regulated transactivation function of p53 is driven by its sequence-specific DNA binding domain and is co-ordinated by specific protein-protein interactions that can in turn be modulated by covalent and non-covalent modifications [43]. There is conclusive evidence that p53 behaves as a transcription factor as it contains an acidic domain on the N-terminus (residues 1 to 42) similar to that of other well characterised transcription factors [44, 45]. It has been shown that when this acidic domain is fused to the GAL4 DNA binding domain, the fusion protein is able to activate transcription from the GAL4 operon [46]. The central core domain of p53 (amino acids 90-295) contains the sequence specific DNA binding domain containing two copies of the 10-base pair consensus motif 5'-PuPuPuC(A/T)(A/T)GPyPyPy-3' [47]. Both copies are necessary for

DNA binding and can be separated by 13 base pairs of random DNA to preserve binding of p53 to the DNA. Most of the mutations found in human cancers occur within the core domain.

DNA binding has also been mapped to the C-terminal domain, which contains two motifs required for heterogeneous oligomerisation. The C-terminal domain maintains the p53 protein in a latent state for specific DNA binding and mutations of this domain at Ser³⁹² has been shown to activate the latent specific DNA binding function of p53 *in vitro* [48]. p53 has been shown to interact directly with the TATA binding protein (TBP) [49]. This may mediate the influence of p53 on transcription and involves TBP-associated factors (TAFs), such as TAF_{II}40, TAF_{II}60 and TAF_{II}230 [50]. p53 also interacts weakly with TFIID, a factor required for transcription initiation [51].



Regulation of p53 stability

Since p53 is such a potent inhibitor of cell growth, its function must be tightly controlled to allow for normal growth and development. This is achieved by several mechanisms that regulate its transcription, translation, stability, sub-cellular localisation and activity [52]. p53 has a very short half-life in normal cells and is present at very low levels. The levels increase by 10 to 20 fold in late G₁ phase, just prior to the onset of S phase. Similarly high levels are detected after DNA damage or following the induction of apoptosis [53].

One of the key regulators of p53 is the MDM2 protein, which can inhibit the transcriptional activity of p53 and target it for degradation via the ubiquitin proteasome pathway [54]. MDM2 binds to the N-terminal transactivation domain of p53 and also acts as a ubiquitin ligase [55]. Ubiquitin is a 76 amino acid residue protein that covalently attaches to substrate proteins at free amine groups [56] and marks the proteins for rapid proteolysis by the 26S proteasome [57]. Since the proteasome is located within the cytoplasm, p53 needs to be exported from the nucleus in order for degradation to take place [58]. Both the nuclear import and export of p53 are tightly regulated [28]. Nuclear import of p53 depends on its interaction with the microtubule network and dynein, indicating that p53 is actively transported towards the nucleus, and nuclear localisation signals within the C-terminus of p53 facilitate import into the nucleus [59]. p53 contains a nuclear export signal within its C-terminus but efficient export of p53 from the nucleus requires MDM2, which also needs to shuttle from the nucleus to the cytoplasm. MDM2 contains a leucine-rich domain which acts as the nuclear export signal that facilitates the transport of the MDM2/p53 complex from the nucleus back to the cytoplasm [60].

It was shown previously that the binding of pRb to MDM2 is essential for pRb to overcome both the anti-apoptotic function of MDM2 and MDM2-dependent degradation of p53 [32]. This interaction does not prevent MDM2 from inhibiting p53-dependent transcription and the pRb-MDM2 complex is still able to bind to p53. MDM2 ubiquitinates both p53 and itself, thereby contributing to the rapid turnover of both proteins [52]. The p53 protein itself binds to the regulatory region of the MDM2 gene and stimulates the transcription of the gene, resulting in increased protein levels [15]. The

MDM2 protein then binds to p53 and stimulates the addition of ubiquitin to the C-terminus of p53, which is then degraded. An autoregulatory feedback loop is then generated in which increased p53 activity leads to increased expression of its negative regulator.

In most cases, induction of p53 involves the inhibition of the p53/MDM2 interaction, which is achieved through several different and independent pathways, depending on the stress signal [15]. These include direct repression of MDM2 expression, post-translational modification of p53 and MDM2, expression of proteins that inhibit MDM2 function and regulation of the sub-cellular localisation of p53 or MDM2. For example, the DNA damaged induced kinases Chk1 and Chk2 have been shown to phosphorylate p53, a modification that inhibits the interaction of p53 with MDM2 and so prevents the degradation of p53 [61, 62].



Regulation of p53 transcriptional activity in response to DNA damage

In response to DNA damage, phosphorylation of the N-terminus of p53 leads to disruption of the p53/MDM2 interaction [63]. In addition, N-terminal phosphorylation of p53 enables interactions to take place between p53 and histone acetyltransferases such as p300/CBP and pCAF [64], facilitating acetylation of the C-terminus of p53. This phosphorylation of p53 establishes a phosphorylation/acetylation cascade, thereby enhancing p53 activity [60, 65]. Reduction of p53 acetylation by MDM2-mediated inhibition of acetyltransferases or direct binding to a deacetylase complex [66], inhibits p53 function. The ability of p53 to bind DNA and function as a transcription factor can

also be regulated. Post-translational modifications within the C-terminus of p53 have been shown to enhance sequence-specific DNA binding and transcriptional activities in response to stresses such as phosphorylation, sumoylation and acetylation [67-70]. Activation of DNA binding and subsequent transactivational activity of p53 occurs through phosphorylation-acetylation cascade [65]. It is the effects of the N and C-terminal modifications on p53 that determines its downstream specificity.

In addition to phosphorylation and acetylation, protein-protein interactions also play a role in the activity of p53 in response to DNA damage [60], particularly with proteins involved in DNA repair. For example, p53 interacts directly with the human RecA homologue, Rad51 [71], implicating p53 in DNA repair and recombination. It was previously shown that expression of p53-inducible gene products such as p21 and bax are enhanced by interactions between p53 and BRCA1 [72].

1.4 Retinoblastoma gene product (pRb)

Rb was one of the first tumour suppressor genes to be identified and characterised [73]. The human *Rb* gene is located on chromosome 13q14.2. The *Rb* gene product (pRb) restricts cell proliferation, inhibits apoptosis and promotes cell differentiation [74]. The frequent mutation of the *Rb* gene and the functional inactivation of pRb in a significant proportion of human cancers, including familial retinoblastoma, osteosarcomas, small lung carcinomas, breast cancer and some forms of leukaemias [75], have created interest in the mechanism of action of pRb. Initially the focus was on the role of pRb in the regulation of the E2F transcription factor [76], but biochemical studies have suggested

that E2F is only one of many binding partners of pRb. Nevertheless it is still unclear how most of these contribute to the normal function of pRb [77].

Structure of human pRb

Human pRb is a nuclear phosphoprotein with a relatively long half-life, containing 928 amino acids (see Fig. 1.2B). It is synthesised throughout the cell cycle and its activity is regulated by cell cycle dependent phosphorylation. pRb is known to bind to proteins from a number of small DNA viruses: E1A from adenovirus, T antigen (Tag) from SV40 and E7 from human papilloma virus (HPV) protein. Mutagenesis of E1A, Tag and E7 demonstrate that a conserved motif, Leu-x-Cys-x-Glu (LxCxE), is essential for the binding of these proteins to pRb. However, a much larger portion of pRb, called the pocket domain (residues 379-772), is required for tight binding and efficient complex formation. The pocket domain contains two regions essential for viral oncoprotein binding, the A-domain (residues 379-572) and the B-domain (residues 646-772), which are connected by a spacer region of 46 amino acids. In addition to the pocket domain, formation of the physiological complex of pRb and E2F, as well as its inhibition activity, requires the presence of the C-terminal domain of pRb [78].

pRb function

An important function of pRb is to regulate the G₁ to S phase transition in the cell cycle. When DNA is injured by foreign stimuli, a signal is immediately transmitted by the p53 protein that initiates either apoptosis or G₁ arrest to escape carcinogenesis, according to the degree of DNA injury [79]. If the DNA injury is so severe that it cannot be repaired

the injured cell undergoes apoptosis. In cases of slight DNA injury, pRb triggers G₁ arrest so that enzymes such as DNA polymerase and DNA ligase have time to repair the injured cell. pRb prevents premature G₁/S transition through interaction with a transcription factor E2F, which is necessary for activation of the S phase genes.

Phosphorylation of pRb is tightly regulated by the action of cyclin-dependent kinases (cdks) [80]. Normal progression of the cell cycle requires the pRb to be phosphorylated by G₁/S-phase-specific cdk complexes. The C-terminal domain of pRb is required for normal recruitment of cdks [81]. Sequences both N- and C-terminal to the pocket domain are highly conserved between pRb homologs of different species and most mutations of pRb are located in the N- and C-terminal regions of the pocket domain.



Regulation of pRb

pRb is a key cell cycle regulator that controls entry into the S-phase. The growth suppressor function of pRb is regulated primarily by cell cycle dependent phosphorylation [25]. pRb binds to E2F through its large pocket domain [25]. Inactivation of pRb by phosphorylation through cdks results in the release of pRb from E2F thereby leading to progression of the cell cycle. The activity of pRb as a repressor of G₁ progression is in turn regulated by cycles of phosphorylation and dephosphorylation on specific serine and threonine residues. Phosphorylation of pRb is controlled by cdk4 and cdk6 [82], which in turn are regulated by interactions with members of the p16^{INK4} family (p15, p16, p18 and p19), which are specific inhibitors of cdk4 and cdk6.

Wild-type p53 suppresses transcription of pRb through a cis-acting sequence in the *Rb* promoter [83]. This element overlaps the basal transcription of the *Rb* promoter leading to inhibition of the basal promoter activity. The N-terminal acidic and C-terminal basic domains of p53 are both required for the suppression of pRb.

1.5 Aims

The overall aim of this project was to investigate the feasibility of recombinantly expressing domains from human RBBP6 for future *in vitro* interaction studies with pRb and p53, and for future structural studies, using heteronuclear NMR. NMR interaction studies typically require 0.6 ml samples with concentrations in the range of 0.5-1 mM, necessitating yields of 5-10 mg or more of purified proteins in each case.



The first aim was therefore to investigate whether the pRb and the p53 binding domains could be expressed and purified in sufficient quantities and concentrated to the required concentration for NMR studies. Both domains corresponded to constructs used in previous studies in which they had been shown to interact *in vivo* [1, 4]. However, since neither of the domains had been previously characterised *in vitro*, the second aim was to use NMR to investigate whether either of the domains was folded. The third aim was to investigate the feasibility of expressing pRb and p53 themselves in bacteria. The portion of pRb expressed corresponded to the A and B domains (denoted pRb A/B), excluding the linker region, that had previously been used to solve the crystal structure of the protein [84]. It was therefore likely that pRb A/B could be successfully expressed. However p53 is reported to be a tetramer in solution and to be difficult to express solubly

in bacteria. The fourth aim of the project was to generate DNA expression constructs for the zinc knuckle and RING finger domains from human RBBP6. These were for use in future structural studies, which, however, are beyond the scope of this thesis.



Chapter 2: Materials and Methods

2.1 Bacterial strains used

1. *Escherichia coli* (*E. coli*) MC 1061: F⁻, araD139, (*ara*, *leu*) 7697, Δ lacX74, galU⁻, galK⁻, hsr⁻, hsm⁺, strA
2. *E. coli* BL21 (DE3) pLys S: F⁻ omp T hsdS_B (*rb*⁻ *m_B*⁻) gal dcm rem131 (DE3).

2.2 Preparation of bacterial (*E. coli*) competent cells

A glycerol stock of the chosen strain was used to streak out a nutrient agar plate containing 10 mM MgCl₂ and incubated overnight at 37°C. A single colony was then inoculated into 20 ml of TYM broth in a 11 flask and shaken vigorously at 37°C until the optical density at 550nm (OD₅₅₀) reached 0.2. The cells were then transferred into a 2l flask and 80 ml of fresh TYM broth added and allowed to grow until the OD₅₅₀ again reached 0.2. The culture was then transferred into a 2l flask and 400 ml of fresh TYM broth was added, and allowed to grow until the OD₅₅₀ reached 0.6. The culture was rapidly cooled by swirling the flask in ice water and then transferred to 250 ml polypropylene tubes and centrifuged at 6 000 x g for 10 minutes (min) at 4°C. After discarding the supernatant, the pellet was re-suspended in 250 ml ice cold Tfb1 buffer, incubated on ice water for 30 min and then centrifuged at 6 000 x g for 10 min at 4°C. The supernatant was discarded and the pellet gently re-suspended with 50 ml of Tfb2 buffer. The re-suspended cells were rapidly frozen in 300 µl aliquots using liquid nitrogen and stored at -80°C.

2.3 Cloning vectors

2.3.1 Cloning into the pGEM[®]-T Easy vector

The pGEM[®]-T Easy Vector system (Promega) is a 3 kbp plasmid vector that is optimised for the cloning of PCR products (see Fig. 2.1). The vector is supplied in a linearised form with 3'-T overhangs on both ends, which facilitates the cloning of PCR products that have 5'-A overhangs on both ends.

PCR products were visualized on a 1% agarose gel and purified using the GFX[™] DNA and Gel Band Purification kit (Amersham Pharmacia). The appropriate amount of PCR product to be used was calculated using the following equation:

$$\text{Mass of insert (ng)} = \mu \times \text{Mass of vector (ng)} \times \frac{\text{Size of insert (bp)}}{\text{Size of vector (bp)}}$$



where μ represents the desired molar ratio of insert to vector. The precise reaction conditions can be found in Table 1. The reactions were mixed and incubated at 22°C for 3 hrs, after which the ligation mix was used to transform competent cells as described in Section 2.4.

2.3.2 Cloning into the pGEX-6P-2 expression vector

The pGEX system (Amersham Pharmacia) is designed for inducible, high-level expression of proteins in *E. coli* as fusions with the 27 kDa glutathione-S-transferase (GST) protein from *Schistosoma japonicum* [85]. The incorporation of GST allows for the affinity purification of fusion proteins using a glutathione-linked agarose column. A recognition sequence for the Prescission[™] Protease, located immediately upstream of the

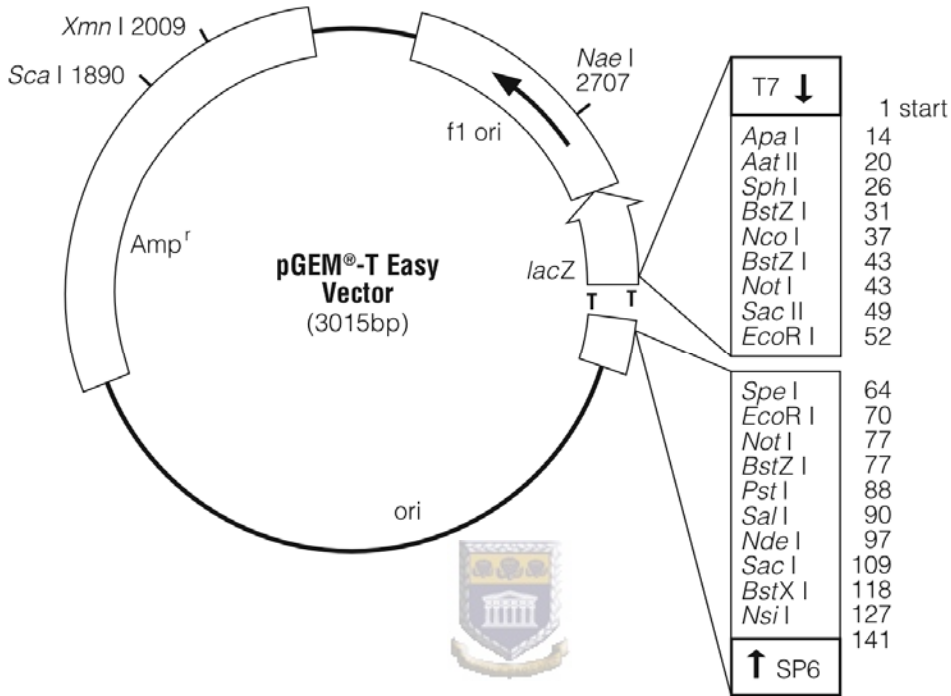


Fig. 2.1: A circular map of the pGEM®-T Easy Vector System. Neither *Bam* HI nor *Xho* I is present in the vector allowing re-excision of the cloned fragments using the *Bam* HI and *Xho* I sites incorporated into the primers. (Diagram courtesy of Promega).

multiple cloning site on the pGEX-6P series of plasmids, allows for removal of the GST fusion partner following affinity purification (see Fig. 2.2).

Table 1. Cloning of PCR products into the pGEM[®]-T Easy vector

The amount of PCR product used (denoted x) is as determined in Section 2.3.1.

Reagent	Standard Reaction	Positive Control	Negative Control
2x Rapid ligation buffer	5 µl	5 µl	5 µl
pGEM [®] -T Easy vector (1 ng/µl)	1 µl	1 µl	1 µl
PCR product	x µl	-	-
Control insert DNA (1 µg/µl)	-	2 µl	-
T4 DNA ligase (3 Weiss U/µl)	1 µl	1 µl	1 µl
dH ₂ O to a final volume	10 µl	10 µl	10 µl

Bam HI (upstream) and *Xho* I (downstream) restriction sites were used in all cloning experiments described in this thesis. The pGEX-6P-2 vector was used in all cases. However, since the *Bam* HI site is in-frame with the promoter in all three vectors in the pGEX-6P series (pGEX-6P-1-3), identical results would have been obtained with any of the other vectors. The *Bam* HI site was used on account of it being the closest cloning site to the PreScission[™] Protease site, thereby producing the smallest number of artifactual residues at the beginning of the protein. The residues Gly-Pro-Leu-Gly-Ser were appended in all cases.

pGEX-6P-2 (27-4598-01)

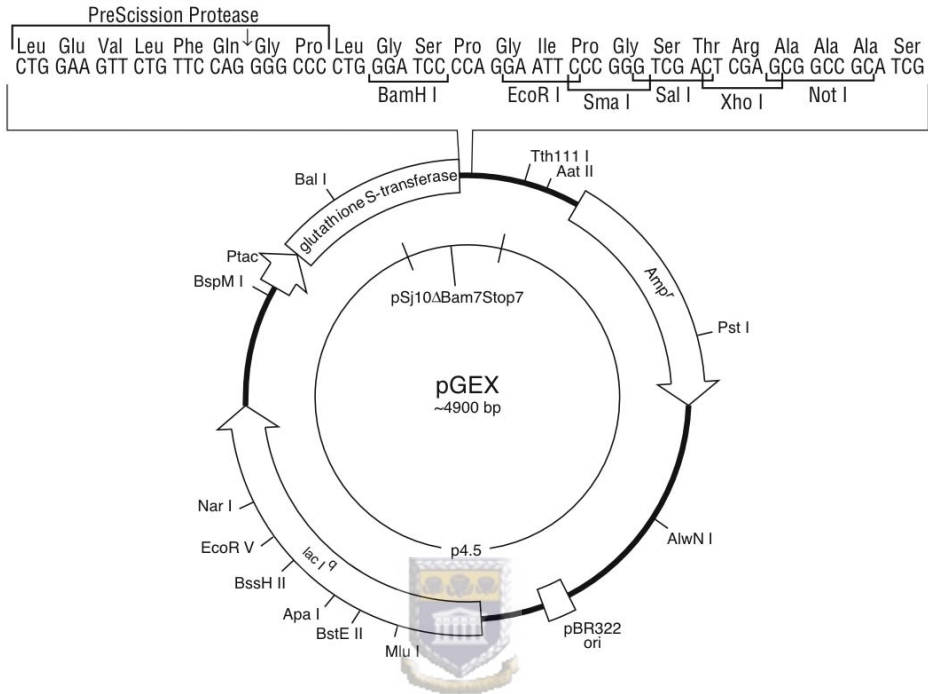


Fig. 2.2: A circular map of the pGEX-6P-2 vector. The PreScission™ Protease recognition motif is situated between GST and the multiple cloning cassette. Cloning into the *Bam* HI and *Xho* I sites results in five extra amino acids (Gly-Pro-Leu-Gly-Ser) being appended to the N-terminus of the protein following removal of GST using PreScission™ Protease. (Diagram courtesy of Amersham Pharmacia).

2.4 Bacterial transformation

The chosen strain of competent cells was thawed on ice for 10 minutes after which 10 μl of plasmid DNA was added to 100 μl of competent cells and gently mixed on ice for 30 min. The cells were heat shocked at 42°C for 45 s and then placed on ice for 2 min to allow for recovery of the cells. 900 μl of pre-warmed LB broth was added and the cells incubated at 37°C for 1 hour. 100 μl of the transformed cells were then plated onto pre-warmed LB agar plates containing 100 $\mu\text{g}/\mu\text{l}$ ampicillin and incubated at 37°C overnight.

2.5 Preparation of plasmid DNA

Both small and large-scale methods for preparation of plasmid DNA were based on the alkaline lysis method [86].



2.5.1 Small-scale preparation of plasmid DNA

A single discrete colony was picked from an overnight plate and grown in 10 ml of LB broth with 100 $\mu\text{g}/\mu\text{l}$ ampicillin at 37°C overnight with vigorous shaking. A glycerol stock was made by transferring 500 μl of the overnight culture to an eppendorf tube, adding an equal amount of 80% glycerol and storing at -80°C until required.

The remaining cell suspension was centrifuged at 10 000 x g for 10 min. The supernatant was discarded and 200 μl of 10x GTE added to re-suspend the cells at room temperature for 5 min. The cells were then lysed with 400 μl NaOH/SDS (Lysis Solution) with gentle swirling and allowed to incubate for 5 min at room temperature. 300 μl of 1.5 M KOAc (Neutralising Solution) was added and incubated on ice for 5 min and then centrifuged at

10 000 x g for 15 min, after which all of the supernatant was transferred into a fresh eppendorf tube. The DNA was precipitated with 0.6 volumes of isopropanol for 1 hr at -20°C, and then centrifuged for 10 min at 10 000 x g. The pellet was washed with 250 µl of 70% ethanol (EtOH) and air-dried. The pellet was then re-suspended in 100 µl of 1X TE.

An equal volume of phenol/chloroform (PC) was added to the plasmid DNA and vortexed for 1 min. The DNA was centrifuged at 10 000 x g for 10 min after which the aqueous top phase was transferred to a fresh 1.5 ml tube. The DNA was precipitated with 1/10 volumes of 3 M NaOAc pH 5.5 and 2.5 volumes of 100% EtOH for 30 min at -20°C and then centrifuged at 10 000 x g for 10 min. The pellet was washed twice with 70% EtOH and finally re-suspended in 50 µl 1x TE.



2.5.2 Large-scale preparation of plasmid DNA

A single colony from an overnight plate was inoculated into 250 ml of LB containing 100 µg/µl ampicillin. The cells were grown overnight at 37°C with constant shaking, after which the cells were collected by centrifugation in 250 ml polypropylene tubes at 6 000 x g for 10 min.

The supernatant was decanted and the cells re-suspended in 4 ml of 10x GTE and incubated on ice for 5 min. 8 ml of NaOH/SDS was added and mixed gently and allowed to incubate on ice for 5 min. 6 ml of 1.5 M KOAc pH 4.8 was added to the sample and centrifuged at 10 000 x g for 15 min. The supernatant was then filtered through

Miracloth™ (Calbiochem) into a 50 ml falcon tube. The DNA was precipitated by addition of 0.6 volumes of isopropanol, incubated at -20°C for 30 min and then centrifuged at 10 000 x g for 15 min. The pellet was washed with 500 µl of 70% EtOH, air-dried and dissolved in 4.5 ml of 1x TE containing 5.57 g of cesium chloride (CsCl) and 400 µl of 100 mg/ml ethidium bromide (EtBr₂) and centrifuged at 10 000 x g for 5 min at room temperature. The supernatant was filtered through glass wool and the density adjusted to 1.61 g/ml before loading into 11.2 ml Beckman OptiSeal™ Polyallomer centrifuge tubes. The tubes were loaded into a Vti65 rotor and centrifuged overnight at 50 000 x g at 22°C in a Beckman L7-80 ultracentrifuge.

The tubes were carefully removed from the rotor and visualised using a 360 nm UV lamp. The tubes were pierced at the top and the lower band (representing the plasmid DNA) drawn off using a 1 ml syringe and transferred to a 2 ml eppendorf tube. One volume of salt-saturated isopropanol was added and shaken vigorously to extract EtBr₂. The DNA was centrifuged at 6 000 x g for 5 min to separate the phases, and the organic phase was drawn off using a pipette. The EtBr₂ extraction was repeated three times. Following the third extraction, two volumes of dH₂O and three volumes of isopropanol were added and incubated on ice for 10 min to precipitate the DNA. The DNA was then centrifuged at 10 000 x g for 15 min at 4°C. The pellet was washed twice with 200 µl of 70% EtOH and air-dried. The pellet was finally dissolved in 100 µl of 1x TE and 10 µl electrophoresed on a 1% agarose gel to determine the quality of the DNA.

2.6 Agarose gel electrophoresis of DNA

Electrophoresis of DNA samples was carried out using 1% agarose gels containing 0.5 $\mu\text{g/ml}$ EtBr₂ at a field strength of 10 V/cm in 1x TBE electrophoresis buffer. 10 μl of DNA was added to 10 μl of DNA loading buffer before being loaded into the wells. A DNA molecular weight marker was also loaded onto the gel to facilitate estimation of the size of the DNA fragments. The DNA was visualized on a WHITE/UV TRANSILLUMINATOR and the gel images were captured using an Ultra Violet Products (UVP) image capture system.

2.7 DNA quantification

The DNA concentration was determined by measuring the optical density at 260 nm (OD₂₆₀) using a spectrophotometer. The following formula was then used to estimate the concentration of double stranded DNA (dsDNA):

$$[\text{dsDNA}] = 50 \mu\text{g/ml} \times \text{OD}_{260} \times \mu$$

where μ represent the dilution factor.

2.8 Manipulation of DNA

2.8.1 Restriction enzyme digestion

Restriction digests were carried out at 37°C for 2 hrs using the appropriate buffer. In the case of multiple digests in incompatible buffers, a single enzyme was used in the appropriate buffer, followed by heat inactivation or phenol/chloroform extraction, depending on the enzyme. The DNA was then precipitated and re-suspended in 1x TE

and the second digestion was then performed using the second enzyme with its compatible buffer.

2.8.2 Cloning of DNA

The ligations of DNA were carried out in 1x ligase buffer (3 mM Tris-Cl pH 7.8, 1 mM ATP, 1mM MgCl₂, 1mM DTT) using T4 DNA ligase. Sticky-ended ligations were incubated at 22°C for 3 hrs or 4°C for 16 hrs, and blunt ended ligations were incubated at 20°C for 16 hrs. Following ligation, T4 DNA ligase was heat inactivated at 70°C for 10 min.

2.9 PCR amplification of DNA fragments

Amplification of DNA was carried out using the Polymerase Chain Reaction (PCR) using the following sequence of steps: melting temperature T_m for 30 s followed by annealing temperature T_a for 30 s, repeated 30 times. 0.2 U of *Taq* polymerase (Takara Biotechnology) was used per reaction. The primers were added to a final concentration of 1 μ M and the concentration of DNA template varied between 1 and 10 ng/ μ l per reaction. The values of T_a , T_m and [MgCl₂] can be found in Table 2.

2.10 Gel purification of DNA and PCR products

DNA fragments were electrophoresed on 1% agarose gels in 1x TBE buffer with 0.5 μ g/ml EtBr₂ and visualized using a long wave (360 nm) UV lamp to avoid damage to the DNA. The fragment of interest was excised from the gel and weighed. The DNA was

then recovered by purification using the GFX™ PCR DNA and Gel Band Purification Kit (Amersham Biosciences) according to the manufactures instructions.

Table 2. PCR conditions

Domain	T _m	T _a	[MgCl ₂]
RbBD	94°C	64°C	2 mM
p53BD	94°C	64°C	2 mM
p53BDb	94°C	68°C	2 mM
p53	94°C	66°C	2 mM
RING	94°C	55°C	2 mM
zinc	94°C	60°C	2 mM



2.11 DNA sequencing

DNA sequencing reactions was carried out using the BigDye™ Terminator V3.0 Sequencing Ready Reaction kit (Applied Biosystems). The final reaction volume of 10 µl contained 3.2 pmol of sequencing primers, 2 µl of Terminator Ready Reaction Mix (TRM) and 1 µl of 5x sequencing buffer. The concentration of the plasmid DNA was 500 ng/µl, while for PCR fragments the concentration was dependant on the size of the PCR fragment.

The following conditions were used in sequencing reactions: melting temperature of 96°C for 30 sec followed by annealing temperature of 60°C for 4 min, repeated for 25 cycles. After amplification, DNA fragments were precipitated using 8 µl of de-ionised

water and 32 μ l of 95% EtOH. The samples were then incubated for 30 min at room temperature and centrifuged at 10 000 x g for 15 min. The supernatant was discarded and the pellet was washed twice in 250 μ l 70% EtOH and the DNA recovered by centrifugation at 10 000 x g for 15 min. The pellet was air-dried and re-suspended in 20 μ l of Template Suppression buffer from the BigDye™ Terminator V3.0 Sequencing Ready Reaction kit (Applied Biosystems). The samples were denatured by boiling at 95°C for 2 min and transferred to sequencing tubes for loading onto the ABI 310 PRISM™ Genetic Analyser for analysis.

2.12 Colony PCR

Single colonies were picked from an overnight LB agar plate and re-suspended in 10 μ l of de-ionised water. PCR reactions were performed as described in Section 2.9. For each reaction, 1 μ l of the colony suspension was used as the template DNA. The products of the colony PCR were then analysed by electrophoresis on a 1% agarose gel.

2.13 Expression and purification of GST fusion proteins

2.13.1 Expression screen

After transformation into *E. coli* BL21 (DE3) *pLys S*, as described in Section 2.4, transformants were screened for expression of the recombinant protein. Single discrete colonies were picked from an overnight LB agar plate and used to inoculate 1 ml of LB broth containing 100 μ g/ μ l ampicillin in a 15 ml falcon tube, which was then shaken at 37°C for 6 hrs. Half of the culture was transferred into a fresh tube and designated as the “un-induced” sample. IPTG was added to the remaining 500 μ l to a final concentration of

0.3 mM and both the un-induced and the induced cultures were shaken for a further 4 hrs at 37°C. Both cultures were then centrifuged at 10 000 x g for 10 min and the pellets dissolved in 50 µl lysis buffer and vortexed. 20 µl was removed from each sample and 20 µl of 2x sample buffer was added and boiled for 5 min at 95°C to disrupt cells. The lysates were analysed using SDS-PAGE as described in Section 2.14.

2.13.2 Large-scale expression

Strongly expressing clones were identified and plasmid DNA was extracted as described in Section 2.8.1. Freshly transformed colonies were used for inoculation because expression levels were found to be higher than in colonies taken from mature plates. A single colony was inoculated into 10 ml of NZ Amine A media containing 100 µg/µl ampicillin and grown overnight at 37°C with vigorous shaking. 10 ml of the overnight culture was used to inoculate 2l of fresh NZ Amine A media containing 100 µg/µl ampicillin in a 5l flask and incubated with vigorous shaking at 37°C until the OD₆₀₀ reached 0.5 – 0.6. Cultures were induced by addition of IPTG to a final concentration of 1.5 mM and grown further at 30°C for 16 hrs. The cells were harvested by centrifugation for 10 min at 10 000 x g. The pellet was resuspended in 15 ml of lysis buffer and lysed through 3 cycles of freezing at -80°C followed by thawing at 37°C. The lysate was then centrifuged at 10 000 x g for 30 min at 4°C. The supernatant containing the soluble protein was transferred into a 50 ml Falcon tube. 30 µl of the total cell lysate was analysed for the expression of recombinant protein on a SDS-PAGE gel. Sodium azide was added to the remaining total cell lysate to a concentration of 0.02% to prevent bacterial growth and stored at 4°C until further purified.

2.13.3 Glutathione affinity chromatography

5 ml glutathione-linked agarose columns were prepared by swelling 0.5 g of glutathione agarose beads (SIGMA) overnight in 100 ml of distilled water, after which they were poured into 15x1 cm Econo chromatography columns (Amersham Biosciences). After equilibration with 5 column volumes of PBS operated using gravity flow, the total cell lysate was loaded onto the column and allowed to incubate at 4°C for 5 min, whereafter the flow-through was collected. 20 µl of the flow-through was reserved for SDS-PAGE analysis. The column was washed with 10 column volumes of PBS and then bound proteins were eluted in three 5 ml fractions using Elution Buffer. 20 µl from each fraction was set aside for SDS-PAGE analysis. Fractions containing the protein of interest were pooled, 5 µl of PreScissionTM Protease (Amersham Biosciences) was added, DTT was added to a final concentration of 1 mM and the sample dialysed overnight at 4°C in Cleavage Buffer. 20 µl of the cleaved sample was reserved for SDS-PAGE analysis and the rest re-loaded onto the glutathione-linked agarose column to remove GST, uncleaved fusion protein and PreScissionTM Protease. Proteins of interest in the flow-through were taken forward into further purification

2.14 Cation exchange chromatography

Cation exchange chromatography was carried out using a 1.6 ml column packed with 20HS POROS media (Amersham Biosciences) operated at a flow rate of 15 ml/min on a BioCAD Sprint Perfusion Chromatography system (Perseptive Biosystems). The column was equilibrated with 50 mM Tris pH 7.0 and samples loaded into the column using a 20 ml sample loop. Proteins retained by the column were eluted using a 0-500 mM NaCl

gradient, which was followed by a 2 M NaCl wash to remove any remaining proteins from the column. 1 ml fractions were collected using a Gilson FC-203B fraction collector using a pre-programmed automated procedure. Fractions were subjected to SDS-PAGE analysis and those containing proteins of interest were pooled together.

2.15 SDS-PAGE analysis

Protein samples were analysed on an SDS-polyacrylamide gel according to Laemmli's protocol [87], which utilises a stacking gel to concentrate the proteins into a thin line before they enter the separating gel which then separates them according to their molecular weight. 8.6 x 6.8 cm gels of 1 mm thickness were cast using Hoefer Mighty Small™ SE 245 Dual Gel casters (Hoefer), using a 40% pre-mixed acrylamide: bisacrylamide 37,5:1 solution. 16% separating gels were made up as follows: 1.268 ml dH₂O, 1.6 ml 40% pre-mixed acrylamide: bisacrylamide 37,5:1, 1.05 ml of 1.5 M Tris pH 8.8, 42 µl 10% SDS, 20 µl of 10% ammonium persulphate (APS) and 2 µl TEMED (N, N, N', N'-tetramethylethylenediamine). 4% stacking gels were prepared from 1.268 ml dH₂O, 0.2 ml 40% pre-mixed acrylamide: bisacrylamide 37,5:1, 0.5 ml of 0.5 M Tris pH 6.8, 10 µl of 10% APS and 2 µl TEMED.

Samples were diluted with an equal amount of 2x sample buffer and boiled at 95°C for 5 min. Pre-mixed protein molecular marker was diluted 20 times before being subjected to the same treatment. Electrophoresis was carried out in 1x SDS electrophoresis buffer at a field of 20 V/cm using a Hoefer Mighty Small II Gel Electrophoresis System (Hoefer).

After electrophoresis the gel was stained for 30 min in Staining Solution and rinsed with sterile water and de-stained in De-staining Solution.

2.16 Determination of protein concentration using the Bradford assay

The concentration of the protein was determined using the Bradford Assay [88] adapted for microtitre plates. The Bradford reagent stock solution was diluted five times with de-ionised water and 50 µl of 1M NaOH was added. Samples of Bovine Serum Albumin (BSA) at the following concentrations were prepared using serial dilution to serve as standards: 0.006 mg/ml, 0.012mg/ ml, 0.025 mg/ml, 0.05 mg/ml and 0.1 mg/ml. Serial dilutions of the protein of interest were also made. 20 µl of each dilution of the standard protein, 20 µl the diluted protein of interest and 20 µl of protein buffer to serve as a blank were added to separate wells of the microtitre plate. 180 µl of the Bradford reagent was then added to each sample whereafter the plate was incubated at room temperature for 5 min and the absorbance of each sample was taken at 620 nm using the Multiskan[®] BIOCHROMATIC plate reader (Labsystems).

2.17 Nuclear Magnetic Resonance (NMR) analysis

The protein sample was dialysed overnight into NMR buffer (100 mM phosphate buffer pH 6.0, 150 mM NaCl, 1 mM DTT and 0.02% Sodium azide) at 4°C and then concentrated to 600 µl using 5,000 MWCO VIVASPIN concentrators (VIVASCIENCE). Deuterium oxide (D₂O) was added to a final concentration of 7% to act as a lock signal and the sample was then transferred to a 5 mm NMR tube. 1D proton spectra were

collected using the 600 MHz Varian Inova Spectrometer at Stellenbosch University.
Water suppression was effected using pre-saturation.



Chapter 3: Cloning, expression and purification of the pRb and p53 binding domains from human RBBP6

3.1 Introduction

This chapter describes the generation of recombinant DNA constructs for the expression of the p53 binding domain and the pRb binding domain (denoted p53BD and RbBD respectively) from human RBBP6 (GenBank accession number NP_008841) (Appendix 1). These expression constructs were amplified using Polymerase Chain Reaction (PCR) from a full-length RBBP6 cDNA clone generated by Dr Amanda Skepu of the University of the Western Cape and cloned into pGEX-6P-2 expression vectors. The constructs were sequenced to confirm that the coding sequence was in the correct reading frame and that no mutations had occurred during the amplification. The constructs were then used to express the target proteins as GST fusion proteins, after which the target domains were separated from the GST, purified to homogeneity and subjected to NMR analysis.

3.2 Construction of expression plasmids for the Rb and p53 binding domains

3.2.1 Amplification of RbBD and p53BD using PCR

PCR primers for p53BD and RbBD were designed based on the human RBBP6 cDNA sequence (Appendix 1). The RbBD was amplified from base pairs 3298–3766, corresponding to amino acids 753-908 of the P2P-R protein that was shown to precipitate pRb out of cellular extracts [4]. The p53BD was amplified from base pairs 4672-5700, corresponding to amino acids 1220-1562 of the PACT protein that was shown to interfere with the binding of p53 to DNA [1]. A truncated form of p53BD, excluding the poly-

lysine tail, was generated from base pairs 4672-5586 of the human RBBP6 gene. This construct, which was denoted “p53BDb”, was made in case the presence of the poly-lysine tail caused the full-length p53BD to be unstable.

In both cases, the forward primers were designed to incorporate a *Bam* HI restriction site while the reverse primers incorporated an *Xho* I restriction site (see Fig. 3.1A&B) for sub-cloning into the multiple cloning site of the pGEX-6P-2 expression vector. The *Bam* HI site was used because it leads to the smallest number of artifactual residues being added to the N-terminus of the protein following the removal of GST using Prescission™ Protease. Nevertheless five additional residues (Gly-Pro-Leu-Gly-Ser) were still added in each case. Two stop codons (TTA TCA) were incorporated into the reverse primer to ensure that no additional residues were added to the C-terminus of the protein. Fragments were amplified as described in Section 2.9 with the annealing temperature of 64°C and resulted in fragments of 468 bp for the RbBD and 914 and 1028 bp for the p53BDb and p53BD respectively (see Fig. 3.2).

3.2.2 Cloning of the pRb and p53 binding domains into pGEM®-T Easy

PCR-amplified fragments of RbBD and p53BD were cloned into the pGEM®-T Easy vector as described in Section 2.3.1 and transformed into *E. coli* M1061 competent cells as described in Section 2.4. Transformants were screened for the presence of an insert using colony PCR as described in Section 2.12. M13 primers were used because there are M13 sites flanking the multiple cloning site of the pGEM®-T Easy vector. Due to the additional 200 bp on either side of the multiple cloning site, colony PCR was expected to

RbBD F'



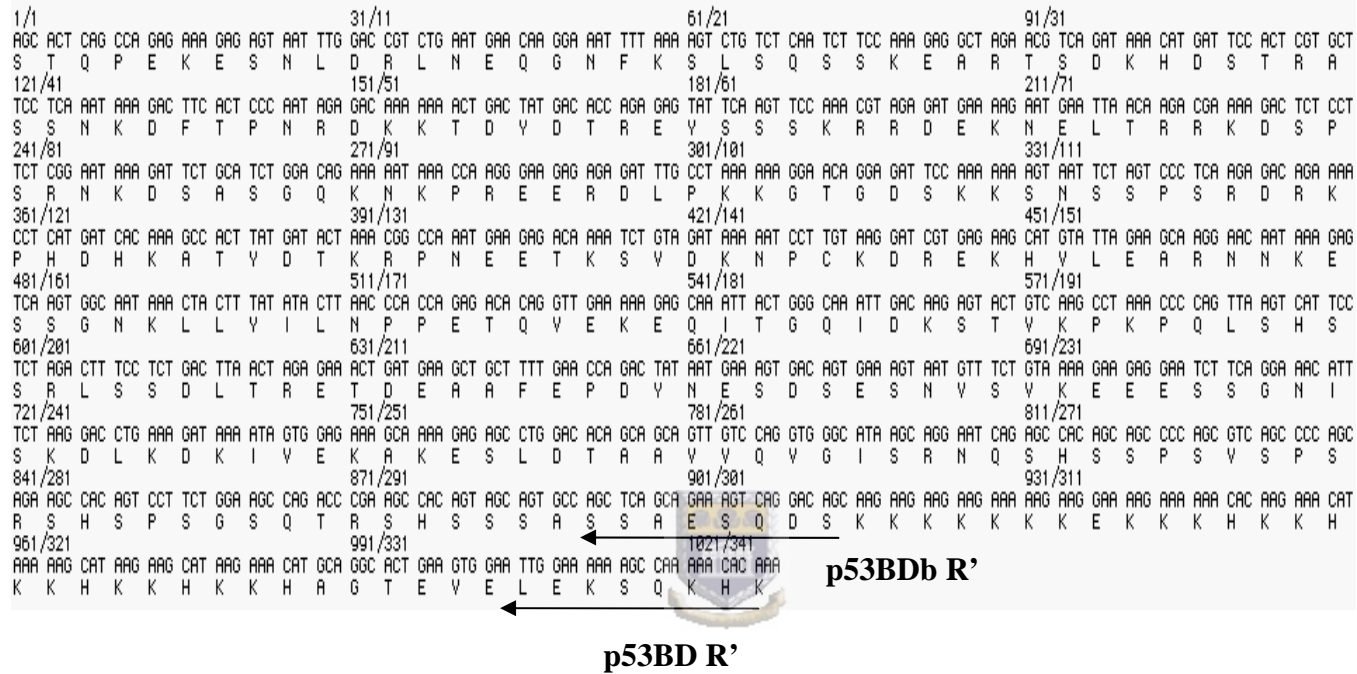
RbBD F': GAGGCG**GGATCC**CACAGGTGTTGAAGAAAATAAAACAGAC

RbBD R':GAGGCG**CTCGAG**TTATCATTTGACATCTTTGGAATAGTCCTTCTT

* *

Fig. 3.1A: Sequence of the pRb binding domain from human RBBP6. The RbBD F' and RbBD R' primers were designed from the above sequence and their positions are indicated on the sequence by arrows. The bold and underlined sequences represent the restriction enzyme sites (*Bam* HI and *Xho* I) and the asterisks represent the two stop codons.

p53BD F'



p53BD F': GAGGCGGGATCCAGCACTCAGCCAGAGAAAGAGAGT

p53BD R': GAGGCGCTCGAGTTATCATTTGTGTTTTTGGCTTTTTTCCAA

* *

p53BDb R': GAGGCGCTCGAGTTATCAGCTGTACTGACTTTCTGCTGAGCT

* *

Fig. 3.1B: Sequence of the p53 binding domain from human RBBP6. The p53BD F', p53BD R' and p53BDb R' primers were designed from the above sequence and their positions are indicated on the sequence by arrows. The underlined sequences represent the restriction enzyme sites (*Bam* H I and *Xho* I) and the asterisks represent the two stop codons.

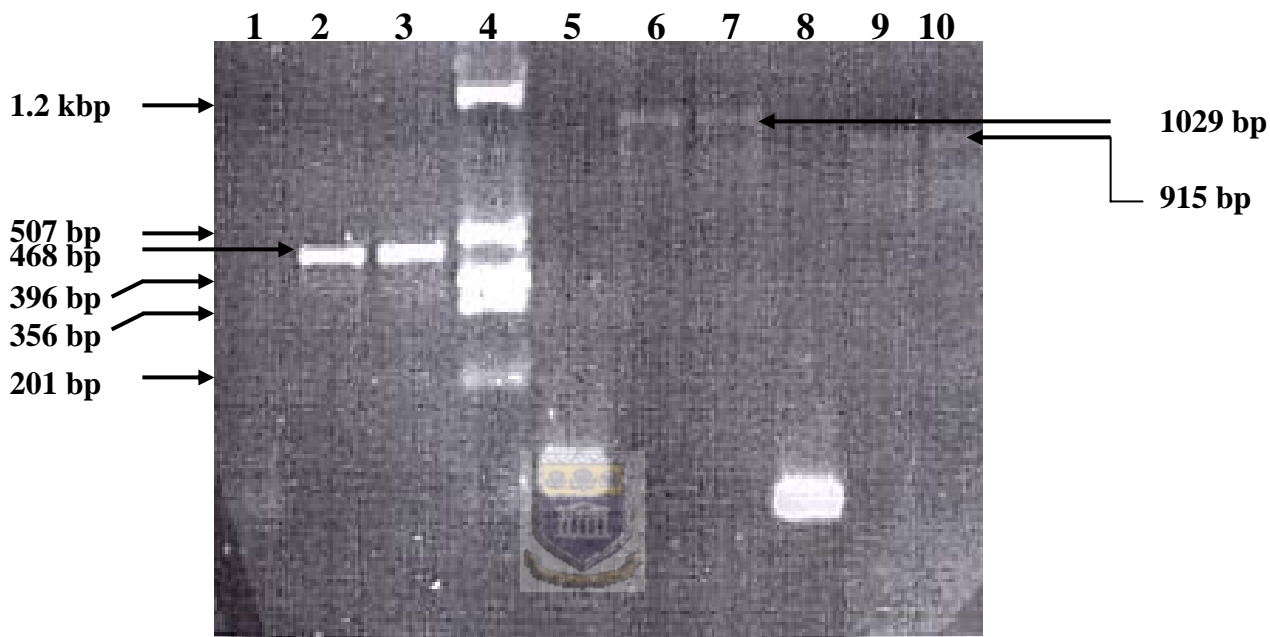


Fig. 3.2: PCR amplification of RbBD and p53BD from human RBBP6 cDNA. Lane 1: negative control of RbBD containing no DNA template and showing no product; lanes 2-3: RbBD fragments with the expected size of 468 bp; lane 4: DNA molecular weight marker. Lane 5: negative control containing no template and showing a primer dimer; lanes 6-7: p53BD fragments with the expected size of 1029 bp. Lane 8: negative control showing only a primer dimer. Lanes 9-10: p53BDb fragments with the expected size of 915 bp.

produce fragments of 668 bp in the case of the RbBD and 1114 and 1228 bp respectively in the case of p53BDb and p53BD.

Clones containing PCR fragments of the expected size were used to extract plasmid DNA as described in Section 2.5.1. In all three cases digestion of the plasmid DNA with *Bam* HI and *Xho* I released a fragment of the expected size (see Fig. 3.3A-C).

3.2.3 Sub-cloning of the pRb and p53 binding domains into pGEX-6P-2

The RbBD, p53BD and p53BDb fragments released from the pGEM[®]-T Easy positive clones after digestion with *Bam* HI and *Xho* I were gel purified as described in Section 2.10 and sub-cloned into pGEX-6P-2 that had been pre-digested with *Bam* HI and *Xho* I and transformed directly into *E. coli* BL21 (DE3) *pLys S* cells as described in Section 2.4. The colonies were screened for the expression of the GST fusion protein as described in Section 2.13.1. Colonies showing expression of RbBD and p53BD were grown in 500 ml of LB broth supplemented with 100 µg/µl ampicillin at 37°C overnight and plasmid DNA extracted as described in Section 2.5.2. The plasmid DNA was then digested with *Bam* HI and *Xho* I to confirm the presence of an insert of the correct size in each case (see Fig. 3.4A&B).

The expression constructs of the RbBD and p53BD were sequenced as described in Section 2.11 using pGEX-6P-2 sequencing primers. The sequences were aligned with human RBBP6 to check for possible mutations that could have been introduced by PCR. The alignment shown in Fig. 3.5 shows the first 145 amino acids of the RbBD to be 100% identical to the human RBBP6 when sequenced with the pGEX sequencing primer

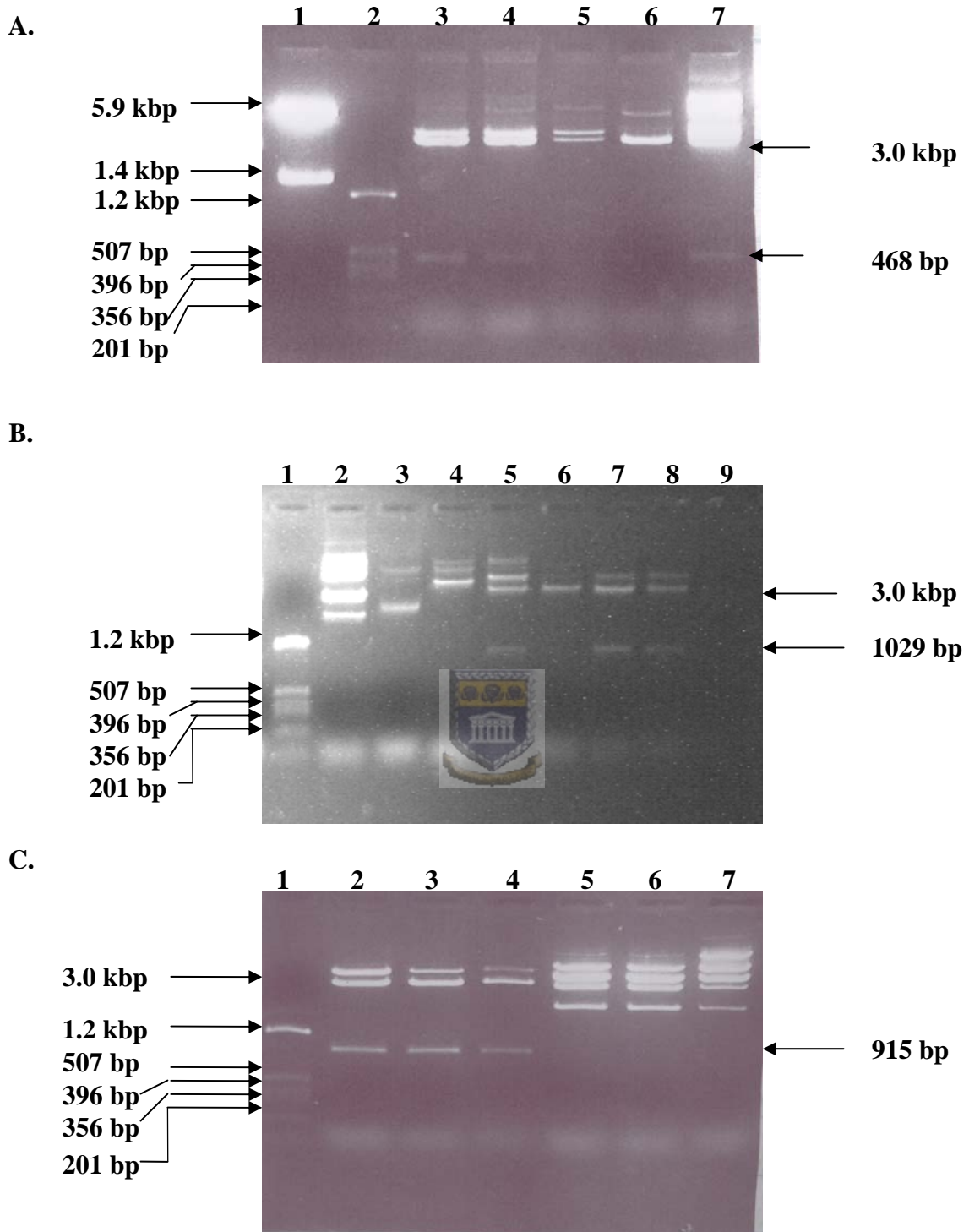
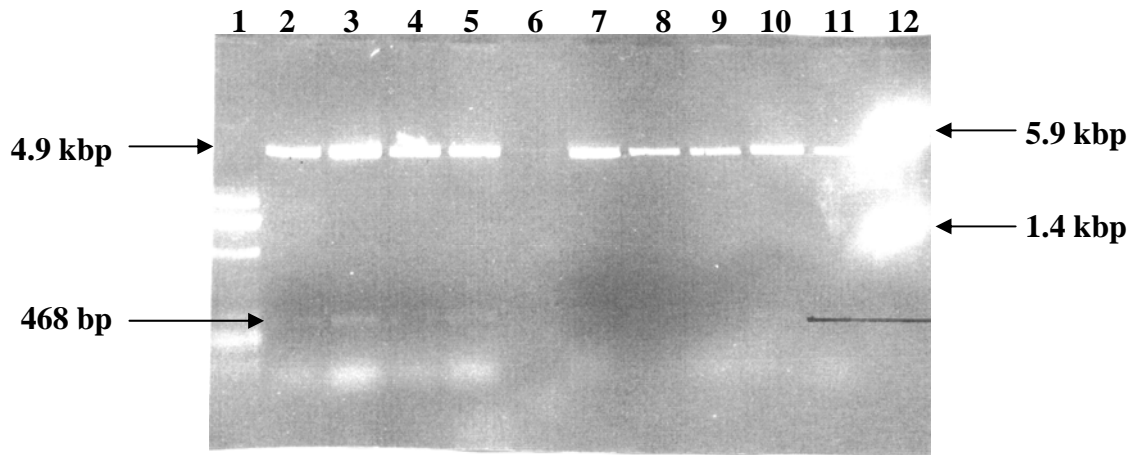


Fig. 3.3: Cloning of the RbBD (A), p53BD (B) and p53BDb (C) into the pGEM[®]-T Easy vector. (A) Restriction digestion of RbBD clones. All clones were positive as they all released a fragment with the expected size of 468 bp as indicated by the arrow in lanes 3-7. Lanes 1-2: molecular weight markers. (B) Restriction digest of p53BD clones. Lane 1: molecular weight marker. Lanes 2-4: uncut plasmid; lanes 5-8: positive clones as the expected fragment of 1029 bp was released. Lane 9 is a negative clone as no insert is released. (C) Restriction digestion of p53BDb clones. All three clones were positive as they all released an expected fragment of 915 bp insert as indicated by the arrow in lanes 2-4. Lanes 5-7: uncut clones; lane 1: molecular weight marker.

A.



B.

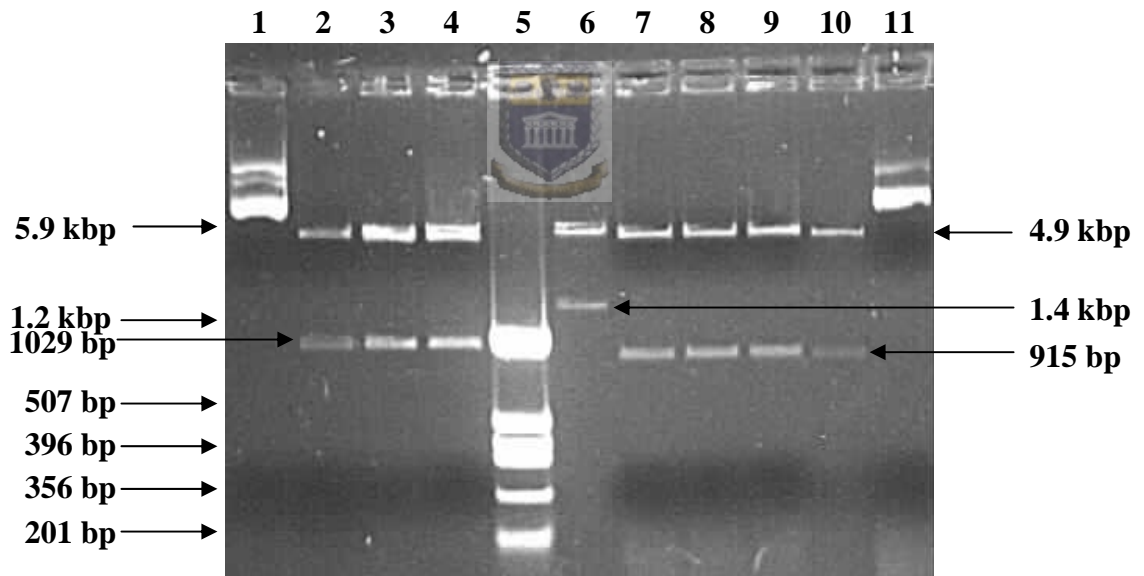


Fig. 3.4: Sub-cloning of RbBD and p53BD into the pGEX-6P-2 vector. (A) Restriction digestion of RbBD clones with *Bam* HI and *Xho* I. Lanes 1 and 12: molecular weight markers; lanes 2-11: positive clones as the expected fragment of 468 bp was released in each case. (B) Restriction digestion of p53BD and p53BDb clones with *Bam* HI and *Xho* I. Lanes 5-6: molecular weight markers; lanes 1 and 11: uncut plasmid of p53BD and p53BDb respectively. Lanes 2-4 shows that the expected 1029 bp fragment is released from the p53BD clones. Lanes 7-10 shows that the expected 915 bp fragment is released from the p53BDb clones.

Score = 842 bits (438), Expect = 0.0
Identities = 441/443 (99%)
Strand = Plus / Minus



```
Query: 1  ggatccacaggtgttgaagaaaaataaacagactcattgttgttctccaagtagagat 60
      |||
Sbjct: 448 ggatccacaggtgttgaagaaaaataaacagactcattgttgttctccaagtagagat 389

Query: 61  gatgccacacctgttagagatgaaccaatggatgcagaatcaatcacttttaaatcagtg 120
      |||
Sbjct: 388 gatgccacacctgttagagatgaaccaatggatgcagaatcaatcacttttaaatcagtg 329

Query: 121 tctgaaaaagacaagagagaaagggataaaccaaaagcaaagggtgataaaaccaaacgg 180
      |||
Sbjct: 328 tctgaaaaagacaagagagaaagggataaaccaaaagcaaagggtgataaaaccaaacgg 269

Query: 181 aagaatgatggatctgctgtgtccaaaaaagaaaatattgtaaaacctgctaaggacc 240
      |||
Sbjct: 268 aagaatgatggatctgctgtgtccaaaaaagaaaatattgtaaaacctgctaaggacc 209

Query: 241 caagaaaaagtagatggagaacgtgagagatctcctcgatctgaacctccaattaaaaa 300
      |||
Sbjct: 208 caagaaaaagtagatggagaacgtgagagatctcctcgatctgaacctccaattaaaaa 149

Query: 301 gccaaagaggagactccgaagactgacaataactaatcatcatcttctctcagaaggat 360
      |||
Sbjct: 148 gccaaagaggagactccgaagactgacaataactaatcatcatcttctctcagaaggat 89

Query: 361 gaaaaaatcactggaacccccagaaaagctcactctaatacagcaaaagaacaccaagaa 420
      |||
Sbjct: 88  gaaaaaatcactggaacccccagaaaagctcactctaatacagcaaaagaacaccnagaa 29

Query: 421 acaaaaccagtcaaagaggaaaa 443
      |||
Sbjct: 28  acaaaactagtcaaagaggaaaa 6
```

Fig. 3.5: Sequence alignment of the pRb binding domain (sbjct) against the expected *in-silico* sequence made using DNA Strider 1.2 (query). The two mismatches in the last two lanes are due to errors in the automated base-calling procedure, manual examination of the traces shows that the agreement is 100% identical to the human RBBP6.

from the N-terminal end. The p53BD sequence data shows that there is only one mutation, which is a silent mutation, in which CCC changes to CCT, which remains as a Proline residue (data not shown).

3.3 Expression and purification of the pRb and p53 binding domains

3.3.1 Expression screen of the pRb and p53 binding domains

The transformants from Section 3.2.3 were screened for the expression of GST fusion proteins as described in Section 2.13.1. Figs. 3.6A&B illustrate the total bacterial cell lysate with and without induction with 0.3 mM of IPTG at 37°C for 4 hrs. The induced samples show that proteins of 45 kDa, 60 kDa and 65 kDa are induced, which correspond to RbBD, p53BD_b and p53BD respectively.

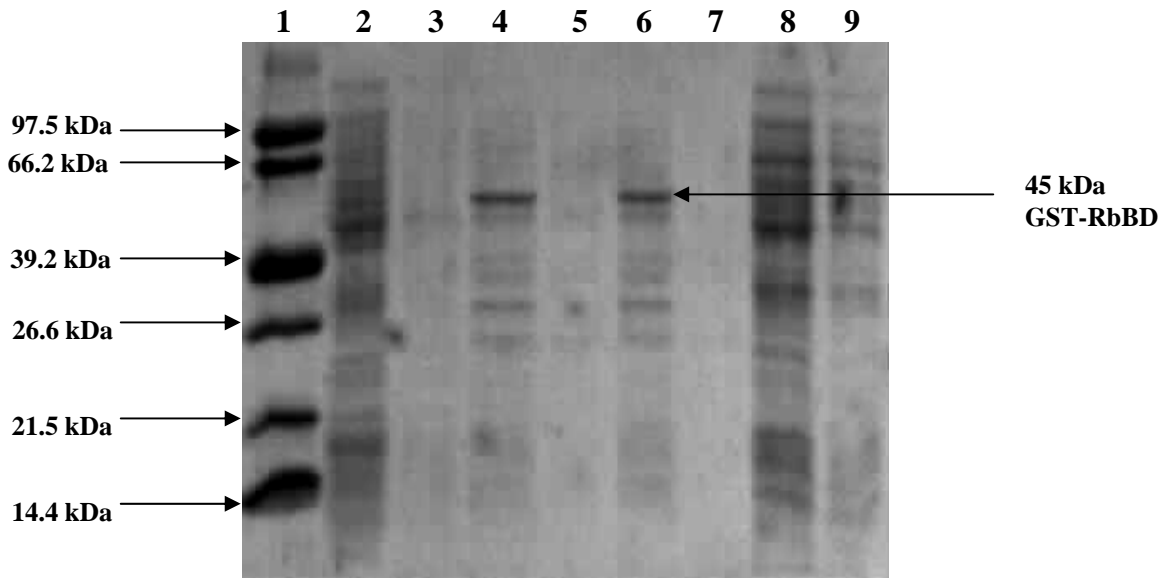


3.3.2 Large-scale expression and purification of the pRb and p53 binding domains

Clones that showed expression of recombinant GST fusion proteins in Section 3.3.1 were used for large-scale expression as described in Section 2.13.2. GST-RbBD and GST-p53 fusion proteins were purified using a glutathione-linked agarose column as described in Section 2.13.3. Fig 3.7A shows a single strong band of approximately 45 kDa in lanes 6-10 corresponding to GST-RbBD. Fig 3.7B shows three bands in the region of 60-65 kDa, which are most likely to correspond to proteolytic fragments of GST-p53BD. This could be due to non-specific proteolysis due to instability caused by the lysine residues at the C-terminus of the protein.

Fractions containing purified fusion proteins were pooled together and cleaved with PreScission™ Protease as described in Section 2.13.3. Fig 3.8A (Lane 2) shows almost

A.



B.

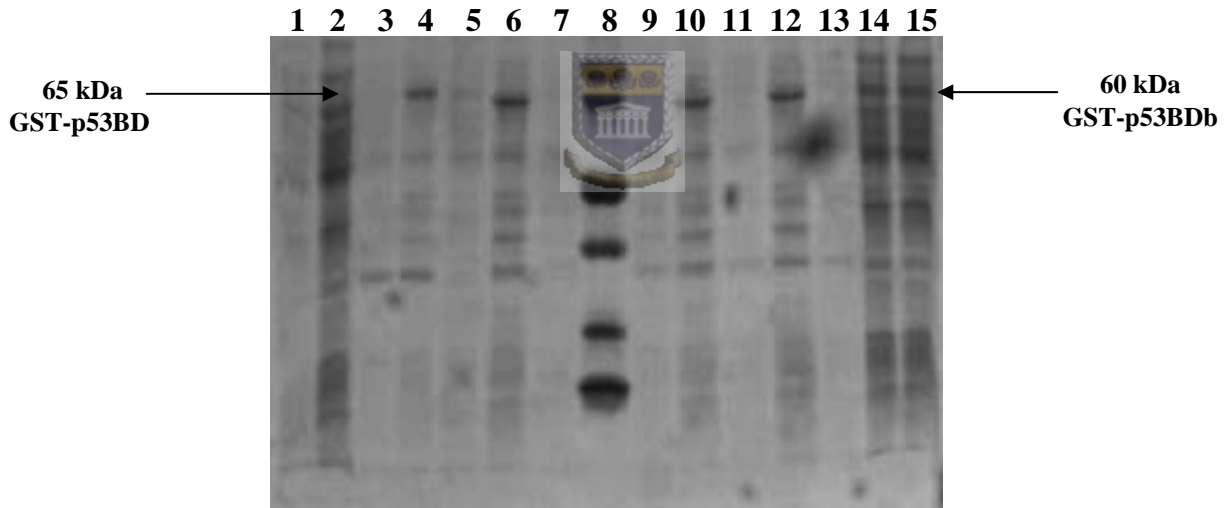
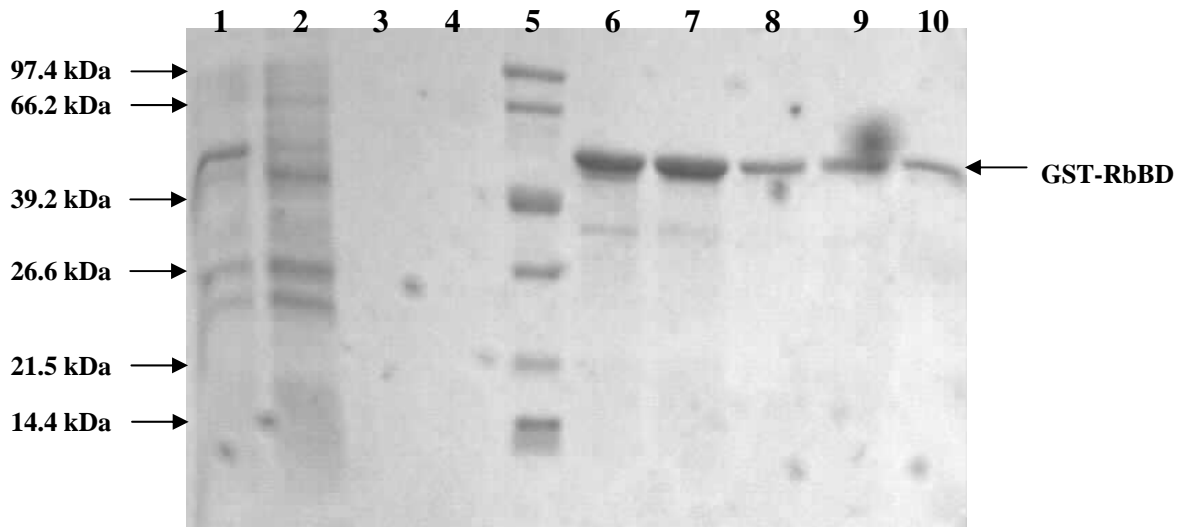


Fig. 3.6: Induction of RbBD (**A**), p53BD and p53BDb (**B**) as GST fusion proteins. (**A**) Expression screen of colonies transformed with the RbBD clone. Lane 1: protein molecular weight marker; lanes 2, 3, 5 and 7: total bacterial lysate from un-induced cells. Lanes 4 and 6 are positive clones as they show an expression of the RbBD fusion protein 45 kDa following induction. Lanes 8-9 are negative clones as they show no expression of RbBD fusion protein. (**B**) Expression screen of colonies transformed with p53BD and p53BDb. Lane 8: protein molecular weight marker. Lane 2, 4 and 6: induced samples of p53BD fusion protein as the 65 kDa fusion protein is induced while lane 1, 3, 5 and 7 are un-induced samples of p53BD. Lane 10, 12, 14 and 15: expression of the p53BDb fusion protein with an expected size fragment of 60 kDa. Lane 9, 11 and 13: un-induced samples of p53BDb.

A.



B.

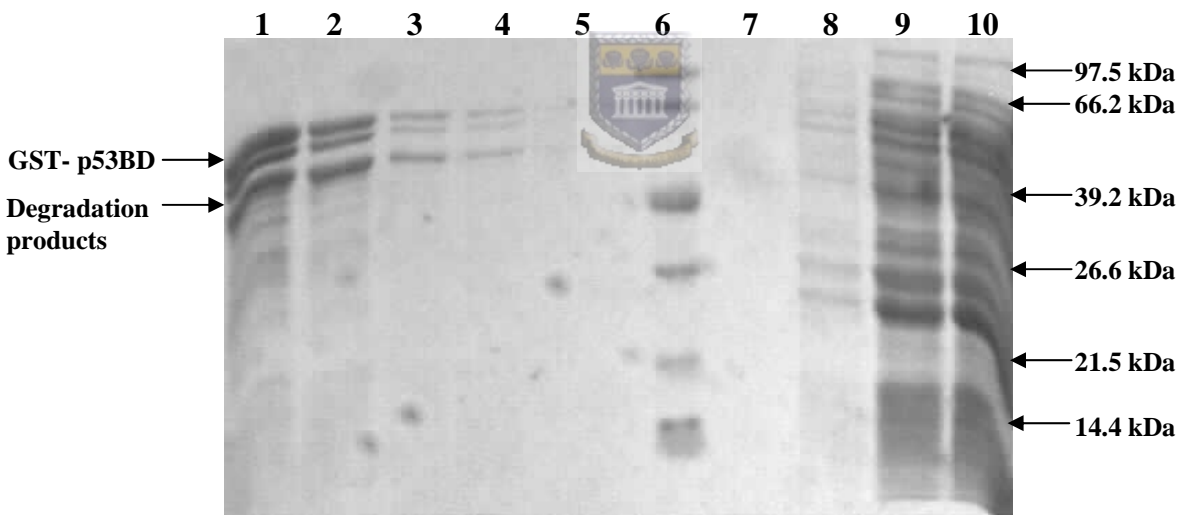


Fig. 3.7: Purification of RbBD (A) and p53BD (B) using a glutathione-linked agarose column. (A) Lane 1: total bacterial cell lysate; lane 2: flow-through; lanes 3-4: PBS wash before elution of the protein. Lane 5: protein molecular weight marker; lanes 6-10: purified RbBD fusion protein with the expected size of 45 kDa. The amount of protein loaded into each of lanes 6-10 represents 1/1000th of the amount present in each fraction. (B) Lanes 1-5: p53BD fusion protein at approximately 65kDa, as well as lower molecular weight products, which may represent degradation products; lane 6: protein molecular weight marker. Lanes 7-8: PBS wash. Lane 9: flow-through. Lane 10: bacterial lysate of p53BD. The amount of protein loaded into each of lanes 1-5 represents 1/1000th of the amount in each fraction.

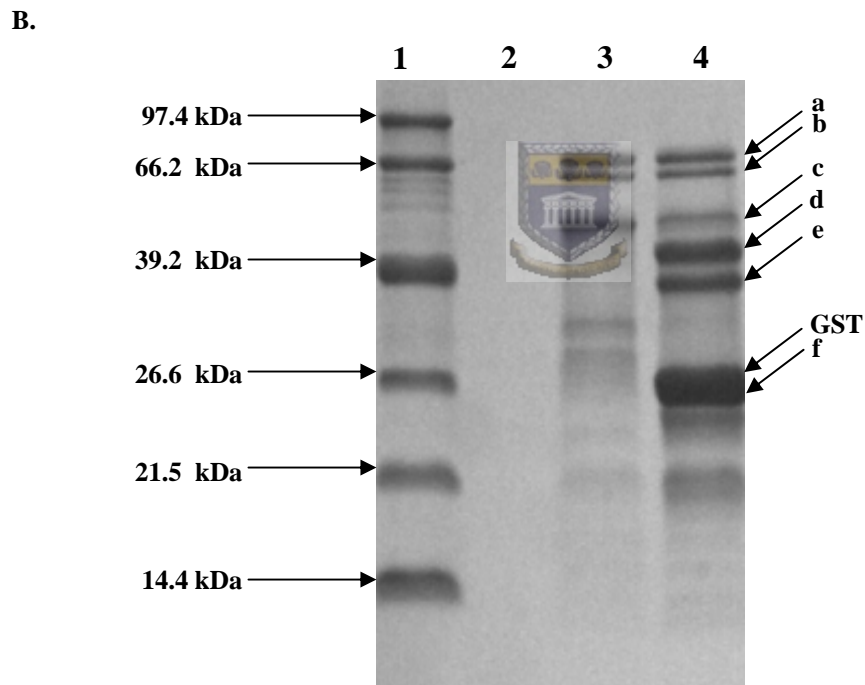
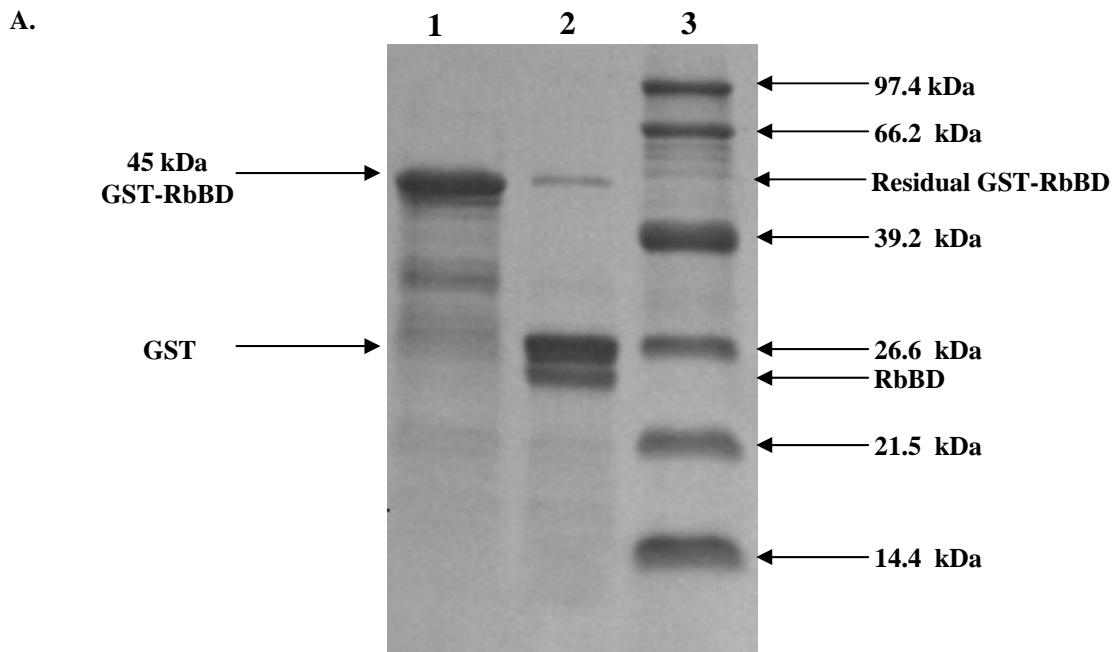


Fig. 3.8: Cleavage of GST-RbBD (**A**) and GST-p53BD (**B**) using PreScissionTM Protease. (**A**) Lane 1 contains the 45 kDa GST-RbBD fusion protein before cleavage; lane 2 shows the same protein after cleavage. The 26.6 kDa band corresponds to GST and the 26 kDa band corresponds to the RbBD, which runs at an apparent molecular weight of almost 26 kDa instead of its actual molecular weight of 18kDa. Lane 3: protein molecular weight marker. (**B**) Lane 1: protein molecular weight marker. Lane 3: p53BD fusion protein ('a', 'b' and 'c'). Lane 4 shows the fusion protein after partial cleavage. Bands 'd', 'e' and 'f' correspond to bands 'a', 'b' and 'c' respectively after removal of GST. Since GST remains as a single band we concluded that 'e' and 'f' represent C-terminal cleavage products, possibly due to proteolysis of the lysine rich region.

complete cleavage of GST-RbBD, to yield a band at approximately 26.6 kDa, corresponding to GST, and another band, corresponding to the RbBD, running at an apparent molecular weight of approximately 26 kDa, in contrast to its actual molecular weight of 18 kDa. Fig 3.8B (Lane 4) shows partial cleavage of the GST-p53BD shown in lane 3. Cleavage of bands 'a', 'b' and 'c' clearly gives rise to bands 'd', 'e' and 'f', and a single band for GST at 27 kDa, from which we conclude that band 'd' corresponds to full-length p53BD, and bands 'e' and 'f' represent C-terminal degradation products of p53BD. This is confirmed in Fig 3.8C, which shows the result of loading the now completely cleaved sample (Lane 3) back onto the glutathione-linked agarose column. The GST, which was retained by the column, is now in lane 7. The p53BD and its two C-terminal degradation products of p53BD were found in the flow-through (Lanes 4 and 5).



RbBD and p53BD were purified further to remove any remaining traces of GST using 20HS cation exchange chromatography as described in Section 2.14. At pH 7.0 RbBD and p53BD should both be retained on a cation column, since their pI's are 9.50 and 9.65 respectively. GST on the other hand should not be retained as it has a pI of 4.9 and should therefore be found in the flow-through. These predictions are confirmed in Fig. 3.9A&B.

3.4 Physical analysis of the RbBD

Due to the fact that the RbBD was expressed as a single species, whereas p53BD was expressed in a number of fragments, combined with the difficulty of expressing full-length p53, it was decided at this stage to focus on the RbBD/pRb system and discontinue characterisation of the p53BD/p53 system.

C.

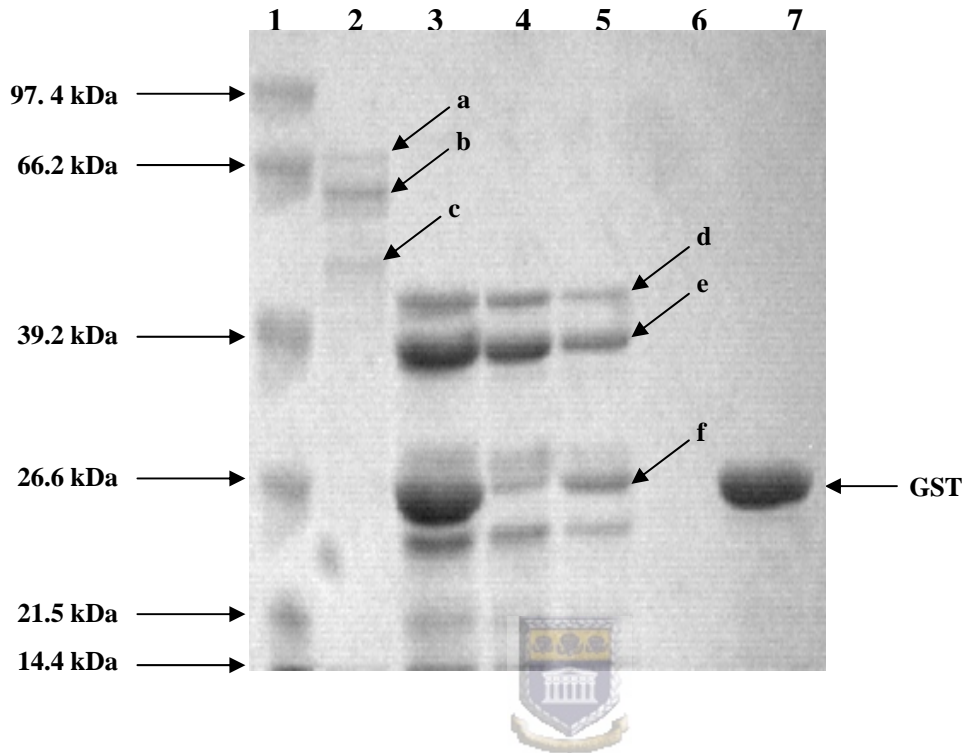
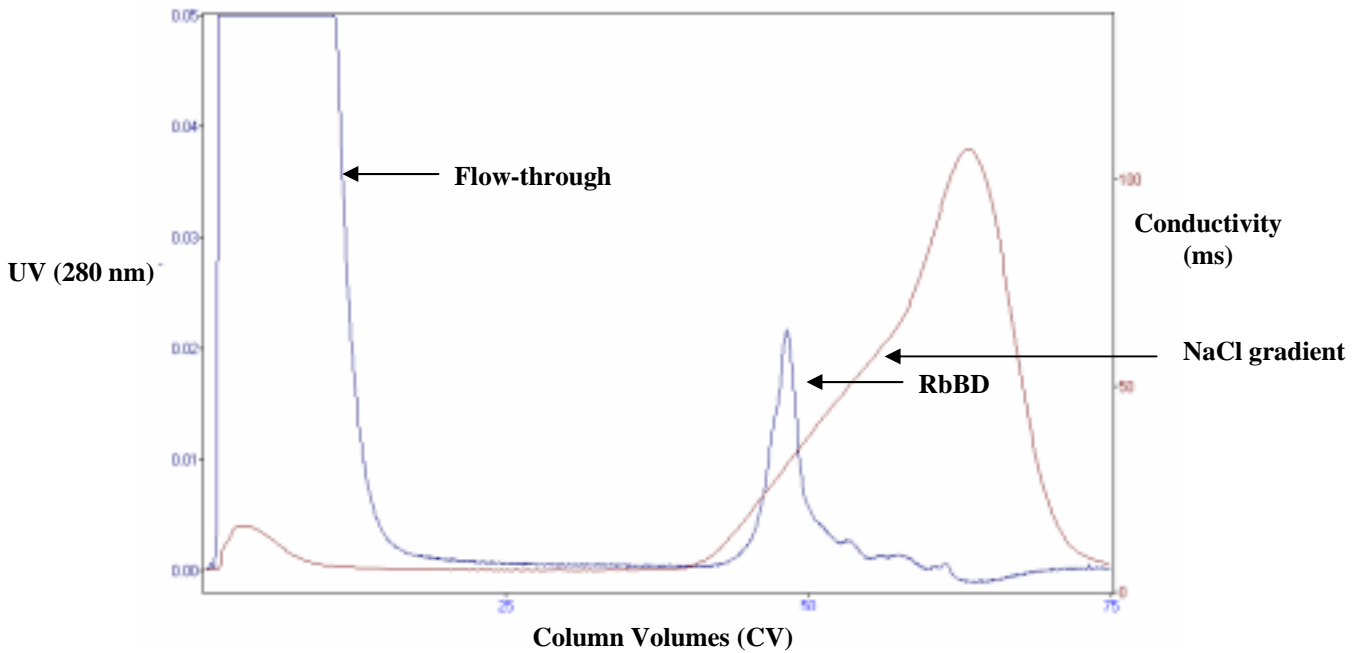


Fig. 3.8(C): Removal of GST from the p53BD preparation using a glutathione-linked agarose column. Lane 1: protein molecular weight marker. Lane 2: p53BD fusion protein ('a', 'b' and 'c'). Lane 3 shows fully cleaved fusion protein: bands 'a', 'b' and 'c' in Fig. 3.8B (lane 4) have disappeared, leaving only bands 'd', 'e' and 'f' as well as GST. Lanes 4-5: cleaved protein after removal of GST with some degradation products at lower molecular weight. Lane 7 shows the eluted GST corresponding to 26.6 kDa as expected. The fact that GST is a single band lead us to conclude that the bands 'e' and 'f' are C-terminal truncations of the p53BD, possibly due to proteolysis of the lysine rich region.

A.



B.

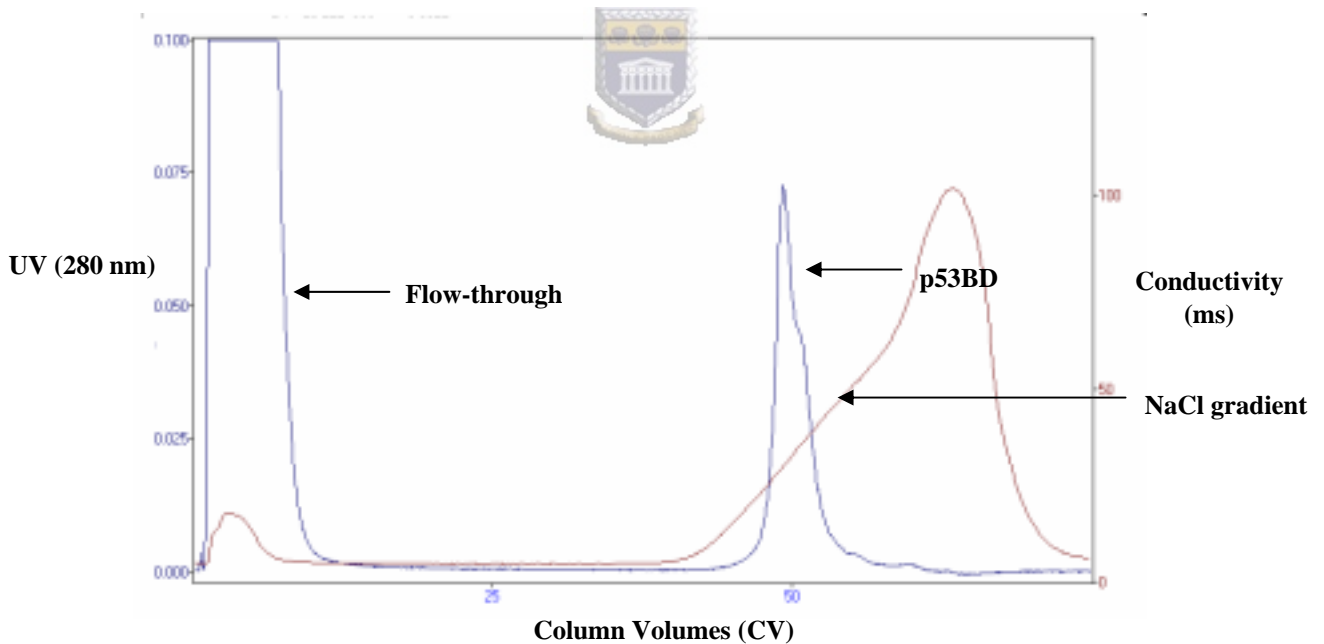


Fig. 3.9: Removal of GST using a 20HS cation exchange column at pH 7.0. **(A)** Purification of RbBD. The GST does not bind to the column because it has a pI of 4.9 and is only found in the flow-through while the RbBD, which has a pI of 9.50, is retained on the column and eluted with a NaCl gradient. **(B)** Purification of p53BD, which has a pI of 9.65, is retained on the 20HS cation column and is eluted with a NaCl gradient. GST is not retained on the column as it has a pI of 4.9, and instead is found in the flow-through.

3.4.1 Mass spectrometric analysis

It can be seen from Fig 3.8A that the RbBD runs on SDS-PAGE at an apparent molecular weight that is significantly higher than its actual molecular weight of 18 kDa. Nevertheless MALDI-TOF mass spectrometry (see Fig 3.10) confirmed that the molecular weight of the protein is 18058 Da, compared to the expected value of 17503.51 Da. The presence of a sizeable peak at 36 kDa suggests that the protein may have a tendency to form homo-dimers.

3.4.2 Determination of the concentration of the pRb binding domain

The concentration of the RbBD was determined using the Bradford Assay, as described in Section 2.16. The concentration was determined by measuring the absorbance readings of the protein sample and comparing it with the absorbance readings of a standard protein BSA. A standard curve constructed using BSA is shown in Chart 1. The absorbance of the RbBD sample following 10-fold dilution was 0.12, as indicated by the horizontal dashed line. The corresponding concentration was 0.053 mg/ml, from which we conclude that the concentration of the un-diluted sample was 0.53 mg/ml. Since the volume of the un-diluted sample was 15 ml, the total yield of RbBD was 7.95 mg.

PerSeptive Biosystems

Original Filename: c:\voyager\data\dpugh\52_03_2.ms
This File # 4 = C:\VOYAGER\DATA\DPUGH\52_03_2.MS
Comment: Frac. 45 / Sin Acid

Method: HCD1004
Mode: Linear
Accelerating Voltage: 25000
Grid Voltage: 91.500 %
Guide Wire Voltage: 0.300 %
Delay: 750 ON
Sample: 54

Laser: 2350
Scans Averaged: 178
Pressure: 2.27e-07
Low Mass Gate: 2000.0
Timed Ion Selector: 24.9 OFF
Negative Ions: OFF
Collected: 6/24/03 11:33 AM

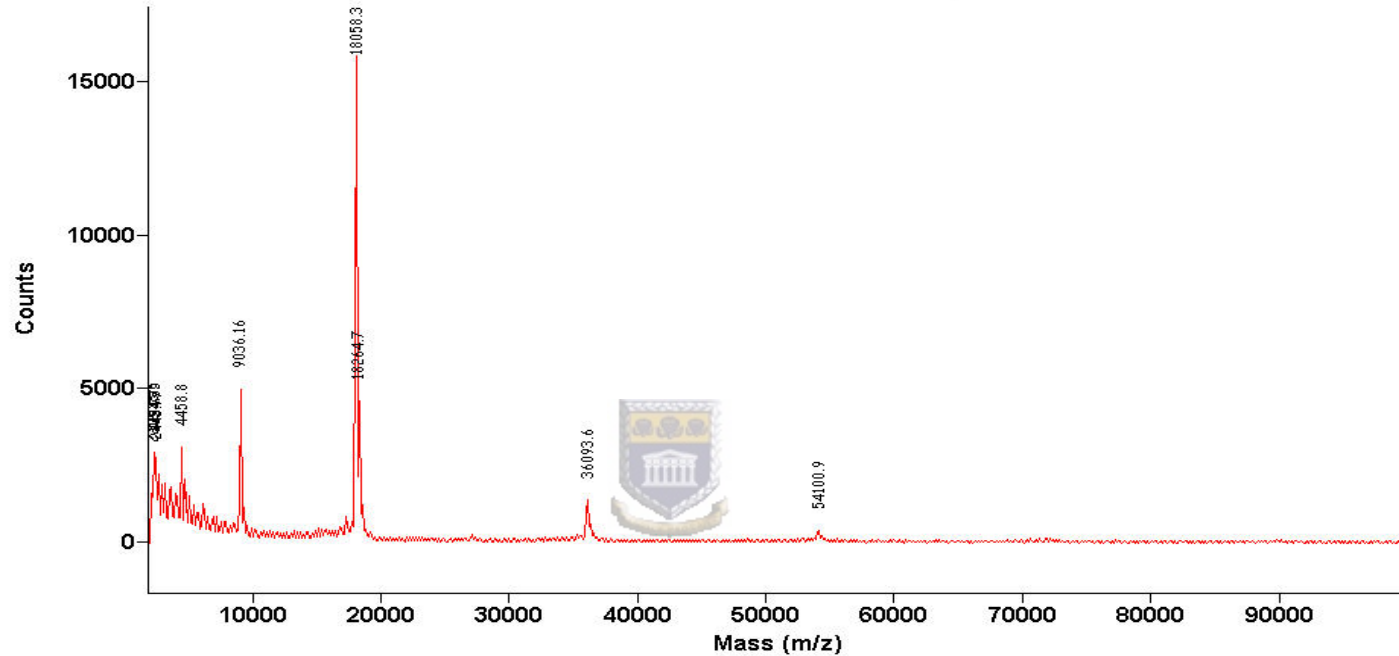


Fig. 3.10: Mass spectrogram of RbBD showing a major peak at 18 kDa protein, which corresponds to the expected size of the RbBD. The peaks at 36 and 54 kDa suggest that the RbBD protein may have the propensity to form homo-dimers and homo-trimers.

Absorbance readings at 620 nm	Concentration of BSA in mg/ml
0.013	0.00625
0.027	0.0125
0.067	0.025
0.125	0.05
0.217	0.1

Table 3: Absorbance at 620 nm for five different concentrations of the standard protein BSA.

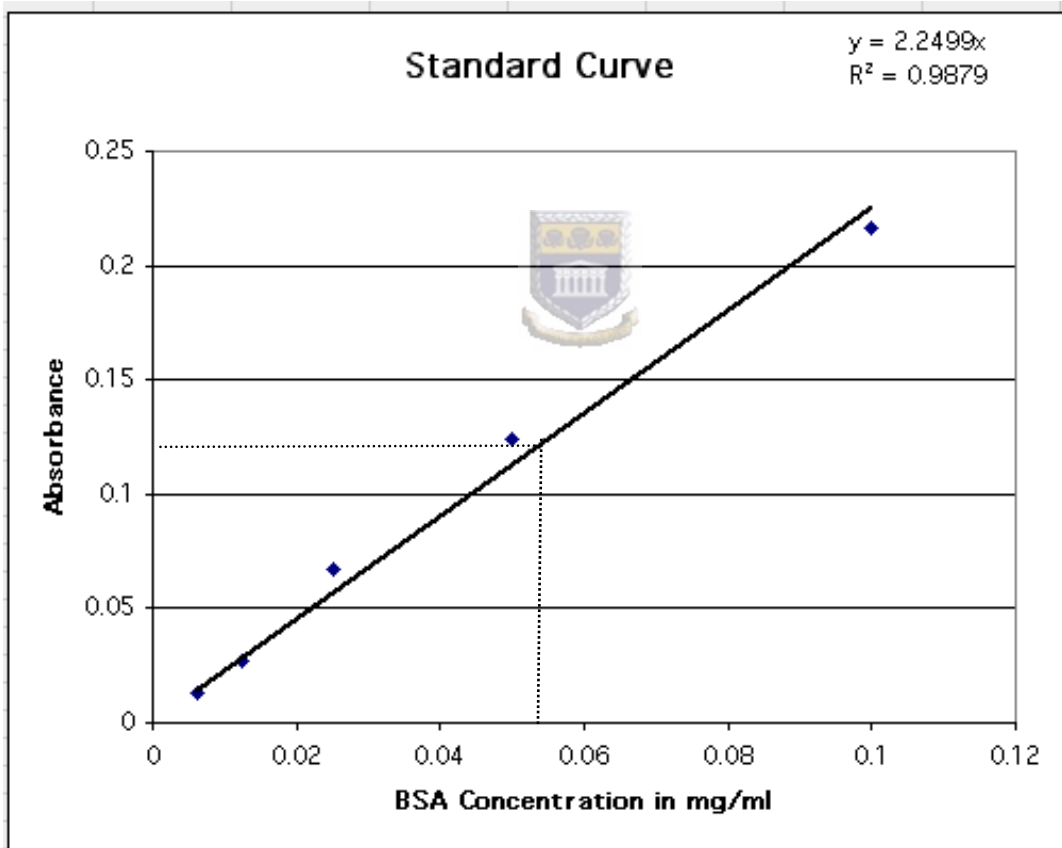


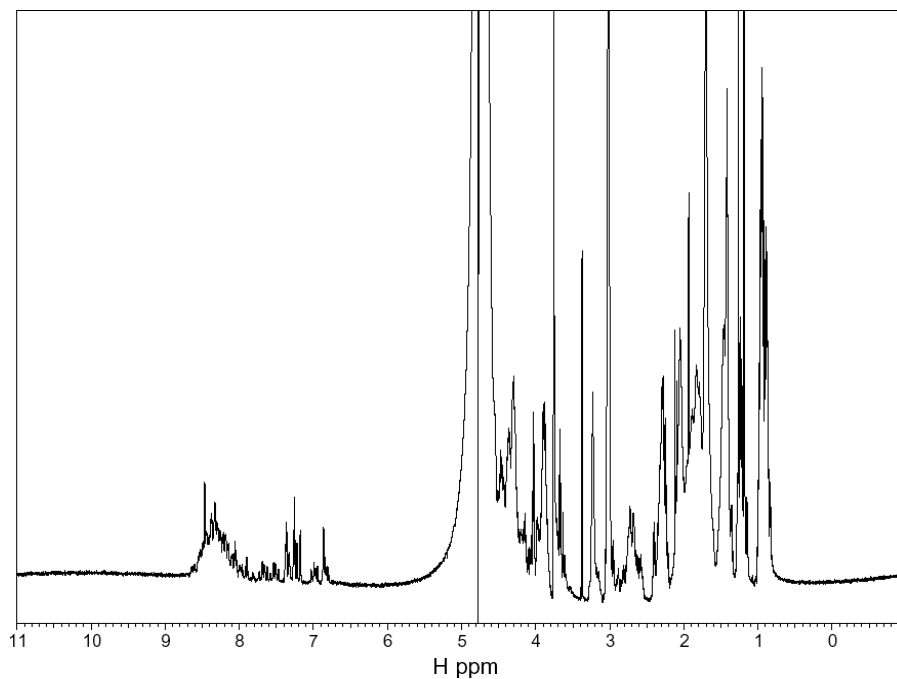
Chart 1: BSA standard curve used to determine the concentration of the RbBD. The absorbance of the RbBD at 10x dilution (0.12) is indicated by the horizontal dashed line. The corresponding concentration of the diluted sample was 0.053 mg/ml, giving a value for [RbBD] of 0.53 mg/ml and a total yield of 7.95 mg.

3.4.3 1D NMR analysis of pRb binding domain

The protein was dialysed into NMR Buffer (100 mM phosphate buffer, pH 6.0, 150 mM NaCl, 1 mM DTT and 0.02% Azide) and concentrated into 600 μ l, giving an expected concentration of 13.25 mg/ml. Since the MW of the domain is 18.06 kDa, this corresponds to 0.73 mM, which is sufficiently concentrated for NMR. The sample was transferred to a 5 mm NMR tube (Wilmad) and a 1D spectrum recorded as shown in Fig 3.11A. The 1D proton spectrum is poorly dispersed, suggesting that the protein is in an unfolded state. Most of the amide proton resonances are clustered around 8.3 ppm, which corresponds to random coil configuration. There is also no evidence of any resonances between 0.5 and -1.0 ppm, or between 4.7 and 6.5, which are usually taken as evidence of folding. For comparison, the folded 1D spectrum of a commercial Ubiquitin sample (VLI Research), recorded under the same conditions, is shown in Fig 3.11B.



A.



B.

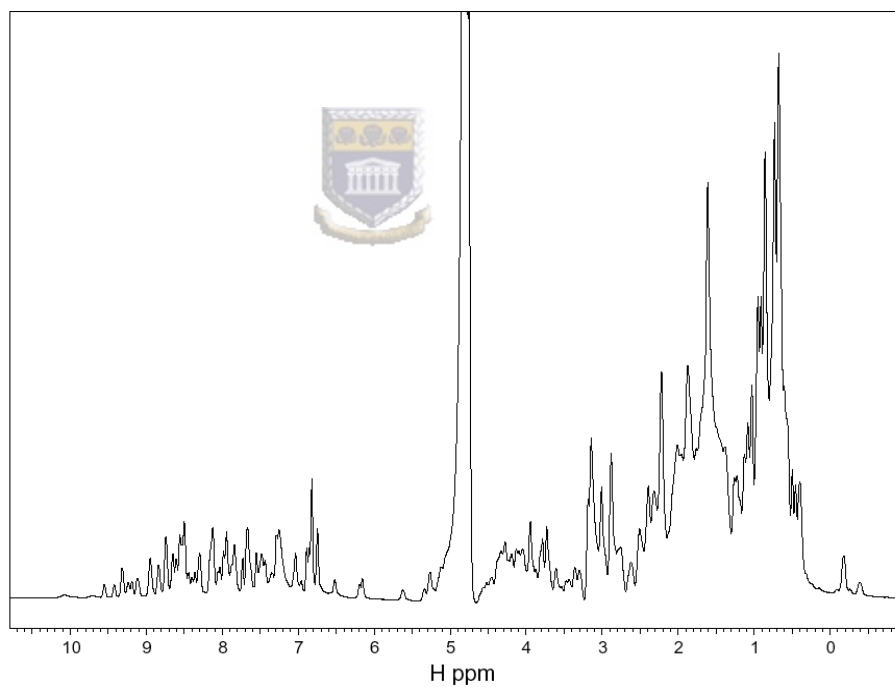


Fig. 3.11: 1D spectra of the RbBD (**A**) at pH 6.0, 25°C, and a commercial Ubiquitin sample (**B**) at pH 5.8, 25°C, both recorded at 600 MHz at Stellenbosch University. The RbBD protein is likely to be unfolded because there are no peaks to the right of 0.5 ppm or to the left of 8.7 ppm. The spectrum of ubiquitin, in contrast, is well dispersed.

Chapter 4: Recombinant expression of p53 and Rb A/B

4.1 Introduction

This chapter describes our attempts to recombinantly express full-length p53 and the pocket domain of the pRb for future *in vitro* binding studies with the p53 binding domain and the pRb binding domain described in the previous chapter.

A construct coding for wild-type p53 (GenBank accession number M14695) (Appendix 2) cloned into a pUC19 plasmid vector was a kind gift from Prof Iqbal Parker of the University of Cape Town. The p53 expression construct was amplified using PCR and cloned into a pGEM[®]-T Easy vector and from there sub-cloned into a pGEX-6P-2 expression vector.



A pGEX-2T plasmid vector coding for the pocket domain of human pRb was kindly supplied by Dr Anne-Laure Gall of Cambridge University. The construct was the same as that used to solve the structure of the pRb pocket domain in complex with a peptide from HPV E7 [84]. The expressed protein included residues 379-589 from the A box and residues 635-787 of the B box of the pocket domain of pRb (see Fig. 1.2B), but did not include the 46 residues of the linker region which is the least conserved region of the pocket domain amongst the pRb-related proteins [84]. The expressed protein will be referred to in the following as Rb A/B. The Rb A/B was expressed from the supplied vector without the need for sub-cloning.

4.2 Construction of an expression plasmid for full-length p53

4.2.1 Amplification of p53 using PCR

Wild-type p53 cDNA (Appendix 2) cloned into a pUC19 plasmid vector was used as the template for the amplification of full-length p53 wild-type by PCR using the primers shown in Fig 4.1. The forward primer included a *Bam* HI restriction site and the reverse primer included a single stop codon and an *Xho* I restriction site to enable it to be cloned into a pGEX-6P-2 vector digested with *Bam* HI and *Xho* I. The PCR reaction using these primers generated the expected product of 1.2 kbp (see Fig. 4.2A).

4.2.2 Cloning of p53 into pGEM[®]-T Easy

The PCR products from Section 4.2.1 were purified as described in Section 2.10 and cloned into a pGEM[®]-T Easy vector as described in Table 1 and Section 2.8.2. Colony PCR carried out using M13 primers yielded the expected 1.4 kbp fragment for a number of colonies, as shown in Fig. 4.2B. Small-scale plasmid isolation was performed from one of the positive clones.

4.2.3 Sub-cloning of p53 into pGEX-6P-2

Digestion of the plasmid DNA produced in Section 4.2.2 released a fragment of 1.2 kbp (data not shown), which was purified as described in Section 2.10. The purified fragment was sub-cloned into pGEX-6P-2 that had been pre-digested with *Bam* HI and *Xho* I as described in Section 2.8.2 and transformed into competent *E. coli* BL21 (DE3) *pLys S* cells as described in Section 2.4. The colonies were screened for the expression of the 80 kDa GST-p53 fusion protein and large-scale plasmid preparation was carried out using

p53 F'

1/1 31/11 61/21 91/31
 ATG GAG GAG CCG CAG TCA GAT CCT AGC GTC GAG CCC CCT CTG AGT CAG GAA ACA TTT TCA GAC CTA TGG AAA CTA CTT CCT GAA AAC AAC GTT CTG TCC CCC TTG CCG TCC CAA GCA ATG
 M E E P Q S D P S V E P P L S Q E T F S D L W K L L P E N N V L S P L P S Q A M
 121/41 151/51 181/61 211/71
 GAT GAT TTG ATG CTG TCC CCG GAC GAT ATT GAA CAA TGG TTC ACT GAA GAC CCA GGT CCA GAT GAA GCT CCC AGA ATG CCA GAG GCT GCT CCC CGC GTG GCC CCT GCA CCA GCA GCT CCT
 D D L M L S P D D I E Q W F T E D P G P D E A P R M P E A A P R V A P A P A A P
 241/81 271/91 301/101 331/111
 ACA CCG GCG GCC CCT GCA CCA GCC CCC TCC TGG CCC CTG TCA TCT TCT GTC CCT TCC CAG AAA ACC TAC CAG GGC AGC TAC GGT TTC CGT CTG GGC TTC TTG CAT TCT GGG ACA GCC AAG
 T P A A P A P A P S W P L S S S V P S Q K T Y Q G S Y G F R L G F L H S G T A K
 361/121 391/131 421/141 451/151
 TCT GTG ACT TGC AGC TAC TCC CCT GCC CTC AAC AAG ATG TTT TGC CAA CTG GCC AAG ACC TGC CCT GTG CAG CTG TGG GTT GAT TCC ACA CCC CGC CCC GGC ACC CGC GTC CGC GCC ATG
 S V T C T Y S P A L N K M F C Q L A K T C P V Q L W V D S T P P P G T R V R A M
 481/161 511/171 541/181 571/191
 GCC ATC TAC AAG CAG TCA CAG CAC ATG ACG GAG GTT GTG AAG CGC TGC CCC CAC CAT GAG CGC TGC TCA GAT AGC GAT GGT CTG GCC CCT CCT CAG CAT CTT ATC CGA GTG GAA GGA AAT
 A I Y K Q S Q H M T E V V R R C P H H E R C S D S D G L A P P Q H L I R V E G N
 601/201 631/211 661/221 691/231
 TTG CGT GTG GAG TAT TTG GAT GAC AGA AAC ACT TTT CGA CAT AGT GTG GTG GTG CCC TAT GAG CCG CCT GAG GTT GGC TCT GAC TGT ACC ACC ATC CAC TAC AAC TAC ATG TGT AAC AGT
 L R V E Y L D D R N T F R H S V V V P Y E P P E V G S D C T T I H Y N Y M C N S
 721/241 751/251 781/261 811/271
 TCC TGC ATG GGC GGC ATG AAC CCG AGG CCC ATC CTC ACC ATC ATC ACA CTG GAA GAC TCC AGT GGT AAT CTA CTG GGA CCG AAC AGC TTT GAG GTG CGT GTT TGT GCC TGT CCT GGG AGA
 S C M G G M N R R P I L T I I T L E D S S G N L L G R N S F E V R V C A C P G R
 841/281 871/291 901/301 931/311
 GAC CGG CGC ACA GAG GAA GAG AAT CTC CGC AAG AAA GGG GAG CCT CAC CAC GAG CTG CCC CCA GGG AGC ACT AAG CGA GCA CTG CCC AAC AAC ACC AGC TCC TCT CCC CAG CCA AAG AAG
 D R R T E E E N L R K K G E P H H E L P P G S T K R A L P N N T S S S P Q P K K
 961/321 991/331 1021/341 1051/351
 AAA CCA CTG GAT GGA GAA TAT TTC ACC CTT CAG ATC CGT GGG CGT GAG CGC TTC GAG ATG TTC CGA GAG CTG AAT GAG GCC TTG GAA CTC AAG GAT GCC CAG GCT GGG AAG GAG CCA GGG
 K P L D G E Y F T L Q I R G R E R F E M F R E L N E A L E L K D A Q A G K E P G
 1081/361 1111/371 1141/381 1171/391
 GGG AGC AGG GCT CAC TCC AGC CAC CTG AAG TCC AAA AAG GGT CAG TCT ACC TCC CGC CAT AAA AAA CTC ATG TTC AAG ACA GAA GGG CCT GAC TCA GAC TGA
 G S R A H S S H L K S K K G Q S T S R H K K L M F K T E G P D S D *

←

p53F': 5'-CGAGAATTCGGATCCCATGGAGGAGCCGCAGTCAGAT-3'

p53 R'

p53R': 5'-CAGTTTCTCGAGTCAGTCTGAGTCAGGCCCTTC-3'

*

Fig. 4.1: The coding sequence of p53 showing the forward and reverse primers indicated by arrows. The underlined sequences indicate the Bam HI and Xho I restriction sites in the forward and reverse primer, respectively. The asterisk indicates the position of the stop codon.

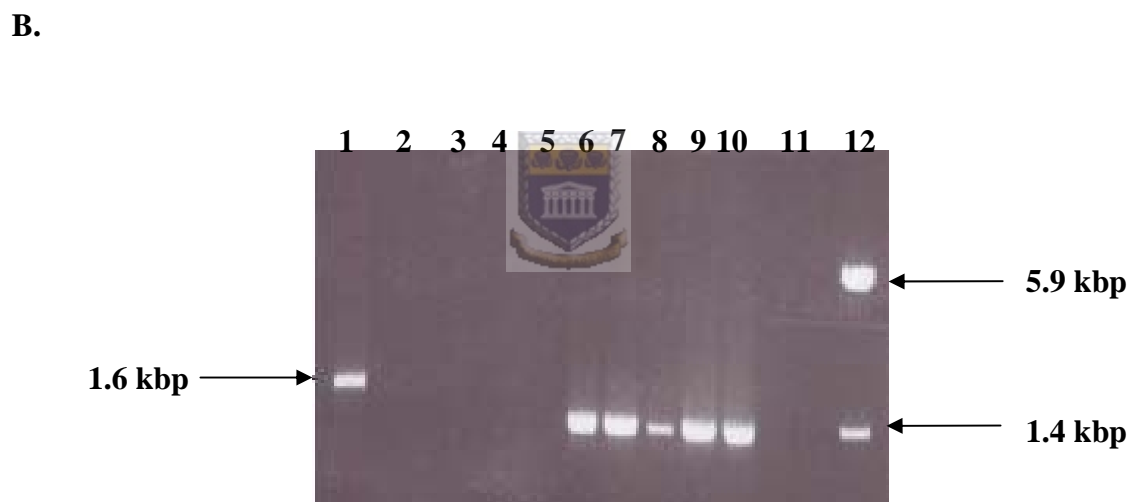
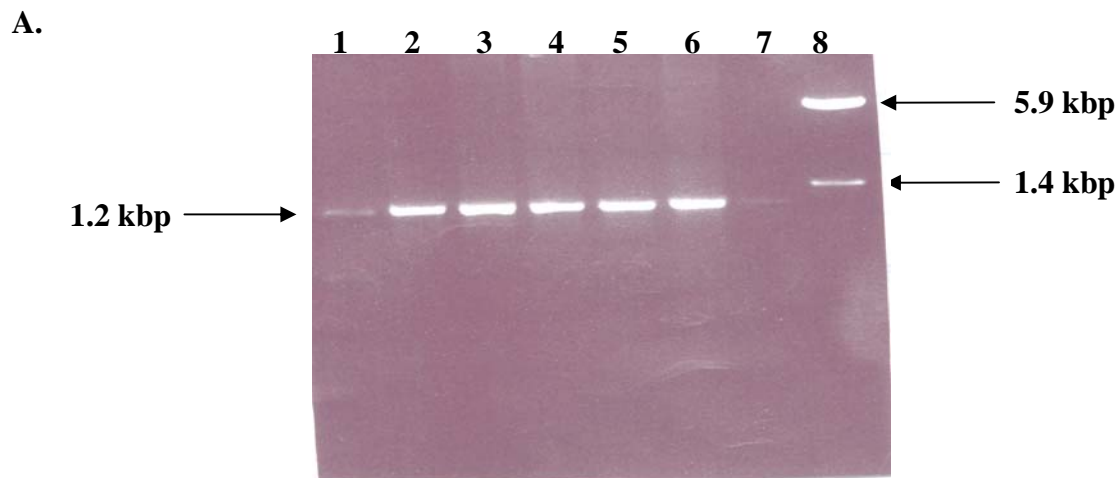


Fig. 4.2: Cloning of p53 into the pGEM[®]-T Easy vector. **(A)** Lanes 1-6 show the expected PCR product of 1.2 kbp. Lane 7 is the negative control and lane 8 is the DNA molecular weight marker. **(B)** Colony PCR to confirm the presence of the cloned PCR product. Amplification M13 primers generated the expected 1.4 kbp product as indicated in lanes 6-10. Lane 11: negative control; lane 12: DNA molecular weight marker. Lanes 1-5 are negative clones as they do not produce the expected 1.4 kbp product.

four of the positive clones. Digestion with *Bam* HI and *Xho* I released the expected fragment of 1.2 kbp (see Fig. 4.3)

4.3 Expression and purification of p53 and Rb A/B

4.3.1 Expression screen of the p53 and Rb A/B

The p53 transformants were screened for the expression of the GST-p53 fusion protein as described in Section 2.13.1. Fig. 4.4A shows the results of the expression screen with and without induction with 0.3 mM IPTG. The presence of an 80 kDa band in the induced but not in the un-induced sample is evidence that p53 is being expressed.

The Rb A/B construct was received in a pGEX-2T expression vector, which contains a thrombin site for cleavage of the GST from the target protein. The construct was transformed into competent *E. coli* BL21 (DE3) *pLys* S cells and a small-scale expression study demonstrated that expression of a protein with the expected size of 68 kDa could be induced (see Fig. 4.4B).

4.3.2 Large-scale expression of and purification of p53 and Rb A/B

Colonies showing the highest levels of expression of both p53 and Rb A/B were used for large-scale expression as described in Section 2.13.2. The cells were induced at 25°C as expression was found to be better at this temperature than at 30°C (data not shown). The GST-p53 fusion protein was found to be insoluble as it was found in the pellet after centrifugation of the cell lysate rather than in the supernatant (data not shown). Several attempts were made to refold the protein using sarkosyl and urea, but on dialysis back into native conditions the protein did not remain in solution (data not shown).

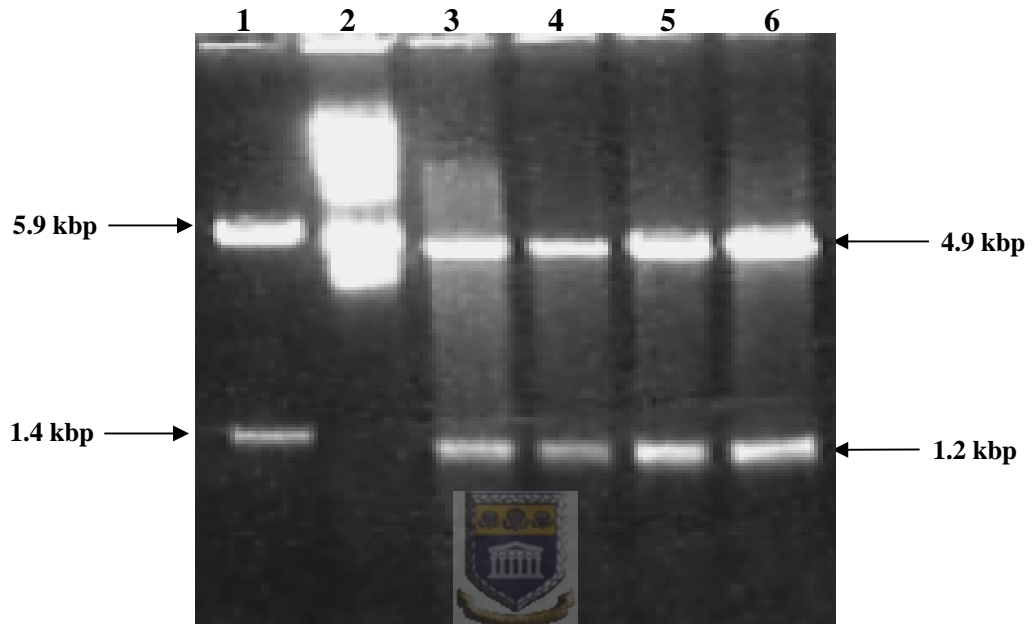


Fig. 4.3: Sub-cloning of p53 into the pGEX-6P-2 vector. Digestion of the p53 pGEX-6P-2 clones using *Bam* HI and *Xho* I. Lanes 3-6 show the 1.2 kbp insert that is released after digestion with *Bam* HI and *Xho* I. Lane 2: uncut p53 clone. Lane 1: DNA molecular weight marker.

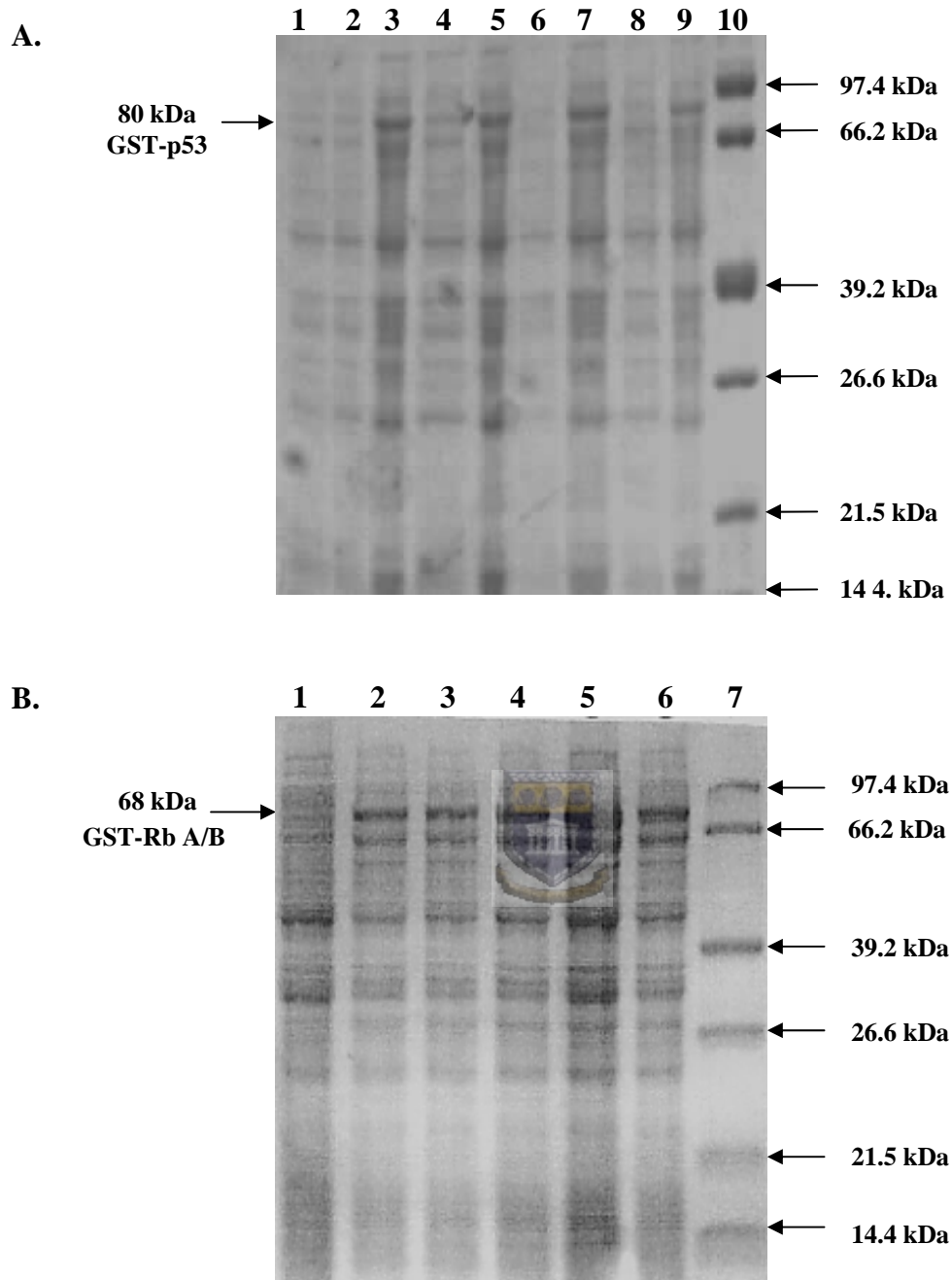


Fig. 4.4: Small-scale expression of p53 (**A**) and Rb A/B (**B**) fusion proteins. (**A**) Expression screen of p53 constructs showing induction of GST-p53 fusion protein. The gel shows the results of an expression screen before and after induction with 0.3 mM IPTG at 37°C for 4 hrs. Lanes 1-2, 4, 6 and 8: un-induced samples. Lane 3, 5, 7 and 9 show induction of 80 kDa GST-p53 fusion protein as indicated by the arrow. (**B**) Expression screen of Rb A/B constructs showing induction of GST-Rb A/B fusion protein. Lane 1: un-induced sample. Lanes 2-6 show induction of a 68 kDa GST-Rb A/B fusion protein as indicated by the arrow. Lane 7: protein molecular weight marker.

The GST-Rb A/B fusion protein was solubly expressed and purified using a glutathione-linked agarose column as described in Section 2.13.3. The presence of a protein with the expected size of 68 kDa was confirmed using SDS-PAGE (see Fig. 4.5).



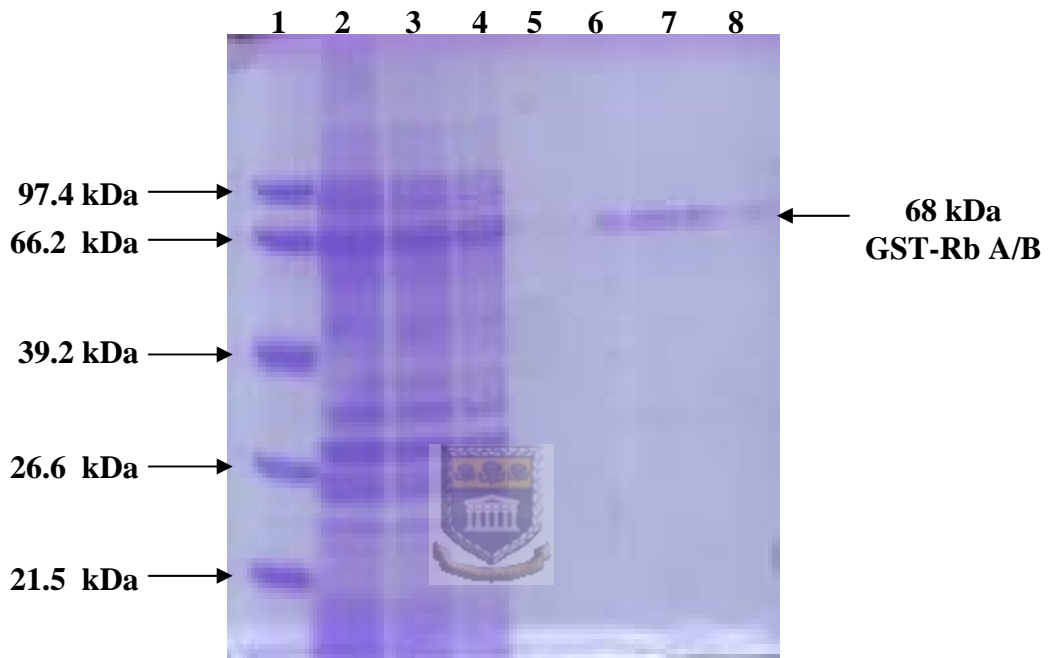


Fig. 4.5: Purification of GST-Rb A/B using a glutathione-linked agarose column. Lane 1: molecular weight marker. Lane 2: bacterial cell lysate; lane 3: flow-through; lanes 4-5: PBS wash. Lanes 6-8: purified GST-Rb A/B fusion protein with the expected size of 68 kDa.

Chapter 5: Generation of recombinant expression constructs for the RING and zinc finger domains from human RBBP6

5.1 Introduction

This chapter describes the generation of expression constructs for the RING and zinc finger domains from human RBBP6 for future structural analysis. RING finger domains are found in proteins involved in a diverse range of cellular processes, including apoptosis, oncogenesis, ubiquitination and viral infections [12]. They have also been shown to be essential for the ubiquitination of proteins [12]. Zinc knuckles have been found in viral proteins and proteins involved in mRNA processing. The presence of these domains within the human RBBP6 protein has led to the hypothesis that RBBP6 may be involved in the regulation of mRNA processing through the ubiquitination-associated mechanism (Pugh *et al.*, unpublished data). Further insights into the function of these domains may therefore be gained from structural analysis of their structures.

Both constructs were amplified from a complete cDNA of human RBBP6 (Appendix 1) using PCR. The amplified fragments were first cloned into a pGEM[®]-T Easy vector and then sub-cloned into a pGEX-6P-2 expression vector. The RING finger domain was sequenced to determine whether the sequence was correct and in the correct reading frame.

5.2 PCR amplification of RING and zinc finger domains

The region corresponding to base pairs 1114–1414 of the human RBBP6 sequence was amplified using PCR to produce a 300 bp fragment containing the RING finger consensus sequence.

Since there was uncertainty regarding the start of the zinc finger domain, two different zinc finger constructs were made, differing only in their start position, and termed the “long” and “short” forms respectively. The long form, which starts immediately following the C-terminal end of the DWNN domain, was amplified from base pairs 646-1143 to generate a 497 bp fragment. The short form was amplified from base pairs 838-1143 to generate a 305 bp fragment.



The primers were designed to incorporate *Bam* HI and *Xho* I sites at the 5' and 3' ends respectively for the purpose of cloning into pGEX-6P-2 (see Fig. 5.1A&B). Two stop codons, TTA and TCA, were incorporated into the reverse primer to prevent the incorporation of artifactual amino acids at the C-terminus of the protein. The PCR reactions were carried out as described in Section 2.9 and produced the expected fragments in all three cases (see Fig. 5.2A-C).

5.3 Cloning of RING and zinc finger domains into pGEM[®]-T Easy

The PCR fragments of both the RING and the zinc finger domains were cloned into the pGEM[®]-T Easy vector as described in Section 2.3.1. Colony PCR carried out using M13 primers was used to identify a number of positive transformants (data not shown).



Zinc 1F': GAGGCGGGATCCGTAAATCTACAAGCAAGACA

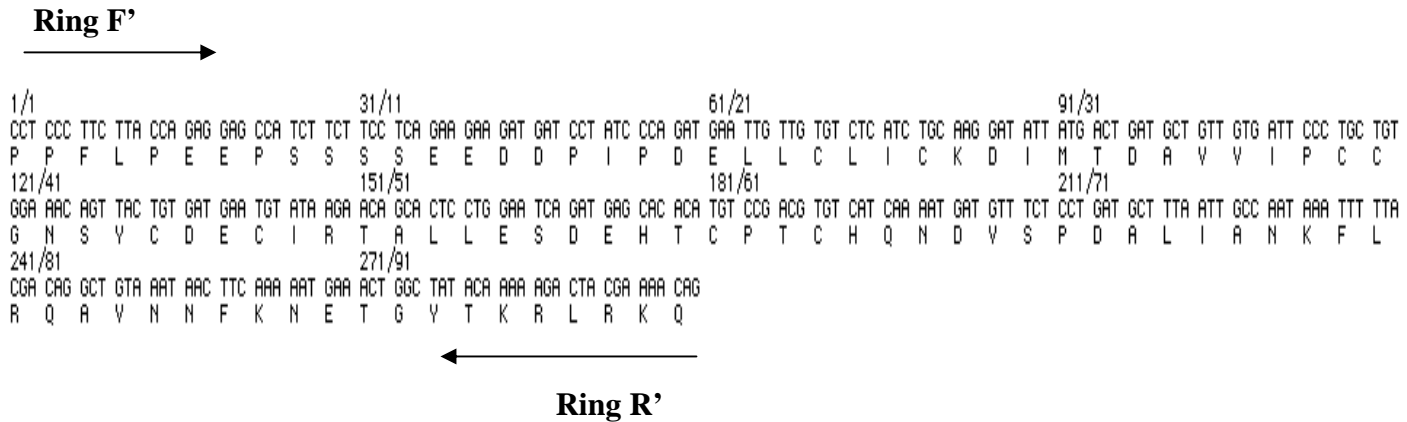
Zinc 2F': GAGGCGGGATCCCCAATCAATTACATGAAGAAA

Zinc R': GAGGCGGCTCGAGTTATCAAGAAGATGGCTCCTCTGG

* *

Fig. 5.1A: Sequence of the zinc finger domain from human RBBP6 and associated PCR primers. The underlined sequences are the recognition footprints for *Bam* HI in the case of forward primer and for *Xho* I in the case of the reverse primer. The positions of the two stop codons are indicated with asterisks.

B.



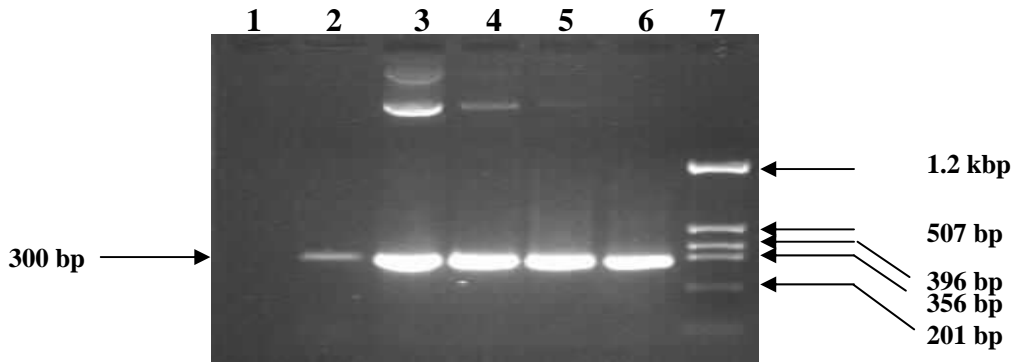
Ring F': GCTGGATCCCCCTCCCTTCTTACCAGAG

Ring R': GCTCTCGAGTCATTACTGTTTTCGTAGTCTTTTTGTATA

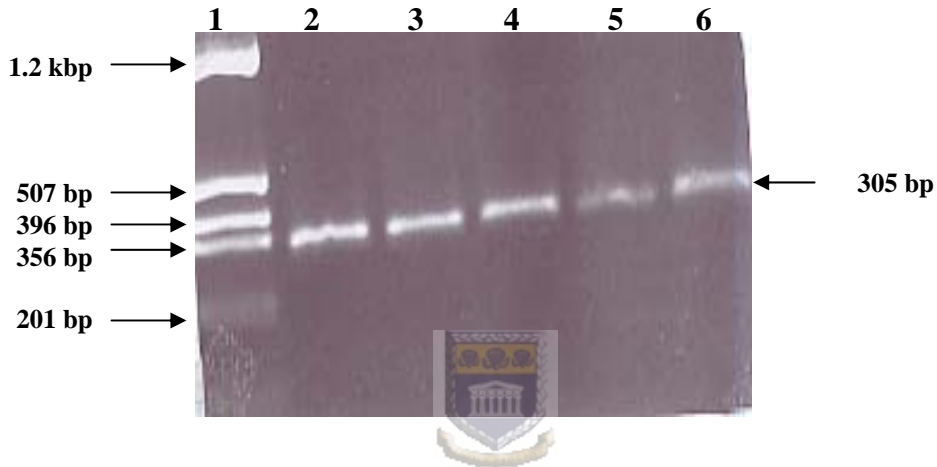
* *

Fig. 5.1B: Sequence of the RING finger domain from human RBBP6 and associated PCR primers. The underline sequences are the recognition footprints for *Bam* HI in the case of the forward primer and *Xho* I in the case of the reverse primer. The positions of the two stop codons are marked with asterisks.

A.



B.



C.

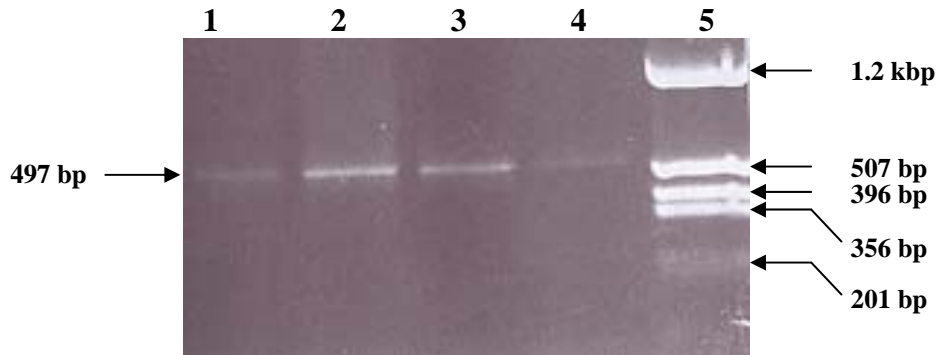


Fig. 5.2: PCR amplification of the RING and zinc finger domains from human RBBP6. (A) Lane 1: negative control where H₂O was used as a template instead of RBBP6 cDNA. Lanes 2-6: PCR products with the expected size of 300 bp for the RING finger domain. Lane 7: molecular weight marker. (B) PCR amplification of the short form zinc finger domain showing the expected fragment of 305 bp in lanes 2-6. Lane 1: molecular weight marker. (C) PCR amplification of the long form zinc finger domain showing the expected fragment of 497 bp in Lanes 1-4 . Lane 5: molecular weight marker.

Positive clones were grown overnight at 37°C in 5 ml of LB broth containing 100 µg/µl ampicillin. Plasmid DNA was extracted as described in Section 2.5.1 and digested with *Bam* HI and *Xho* I as described in Section 2.8.1 to release the fragment from the pGEM[®]-T Easy constructs. The fragments were found to have the expected sizes using 1% agarose electrophoresis (see Fig. 5.3A&B).

5.4 Sub-cloning the RING and zinc finger domains into pGEX-6P-2

The fragments described in Section 5.3 were purified and sub-cloned into pGEX-6P-2. Plasmid DNA was extracted and digested with *Bam* HI and *Xho* I to confirm the presence of inserts of the correct size (data not shown). The RING finger was sequenced using pGEX sequencing primers. The alignment of the sequenced RING finger domain against the expected *in-silico* sequence made using the DNA Strider 1.2 showed a 100% identity, as shown in Fig. 5.4.



5.5 Expression screen of RING and zinc finger constructs

The expression constructs of both RING and zinc finger domains from Section 5.4 were screened for the expression of GST fusion proteins (see Fig. 5.5A&B). Proteins of the expected sizes of 38 kDa, 45 kDa and 38 kDa were induced in the RING finger and the “long” and “short” zinc finger cultures respectively. The “short” form of the zinc finger domain was found to be insoluble and subsequent investigation of it was discontinued.

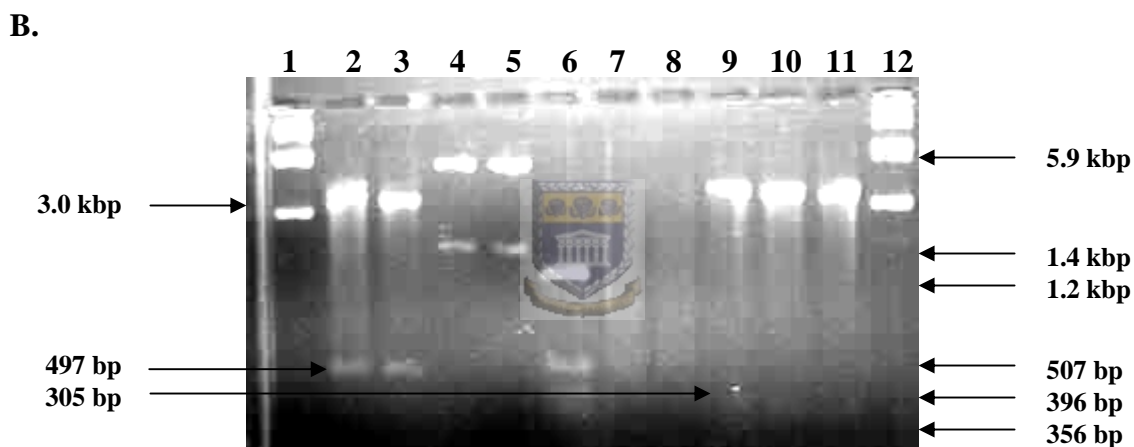
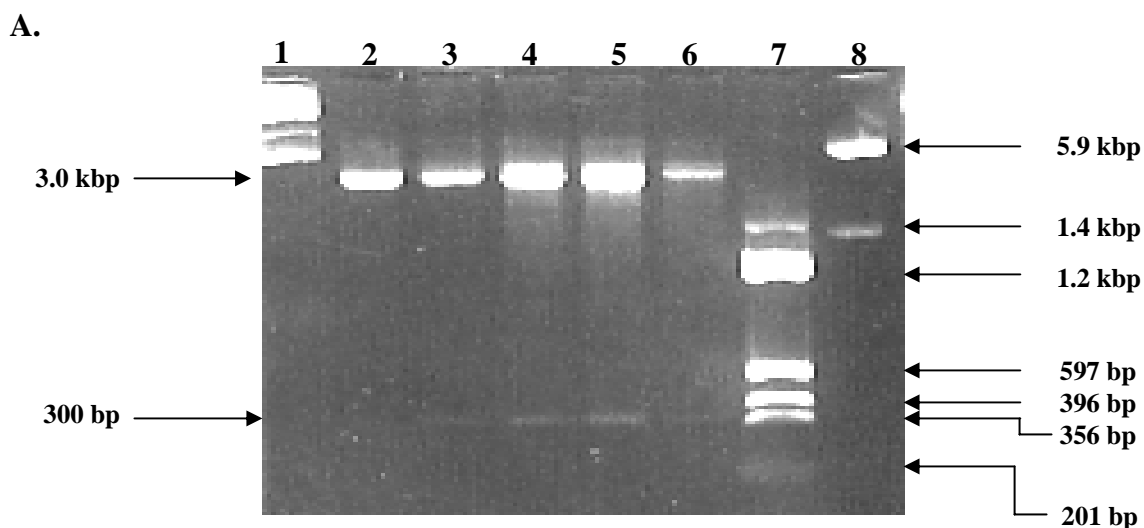


Fig. 5.3: Cloning of the RING and zinc finger domains into the pGEM[®]-T Easy vector. **(A)** Restriction digestion of the positive clones of the RING finger domain with *Bam* HI and *Xho* I. Lane 1: uncut RING clone. Lanes 2-6 represent the digested clones, showing the 3.0 kbp of the vector and the expected 300 bp fragment of the RING finger domain. Lanes 7-8: DNA molecular weight markers. **(B)** Restriction digestion of both “long” and “short” forms of the zinc finger domain. Lanes 1 and 12: uncut plasmid clones of the “long” and “short” forms respectively. Lanes 2-3: positive clones of the long form zinc finger domain showing the release of the expected fragment of 497 bp. Lanes 4-6: molecular weight markers. Lanes 9-11 are positive clones of the short form zinc finger domain showing the release of the expected fragment of 305 bp.

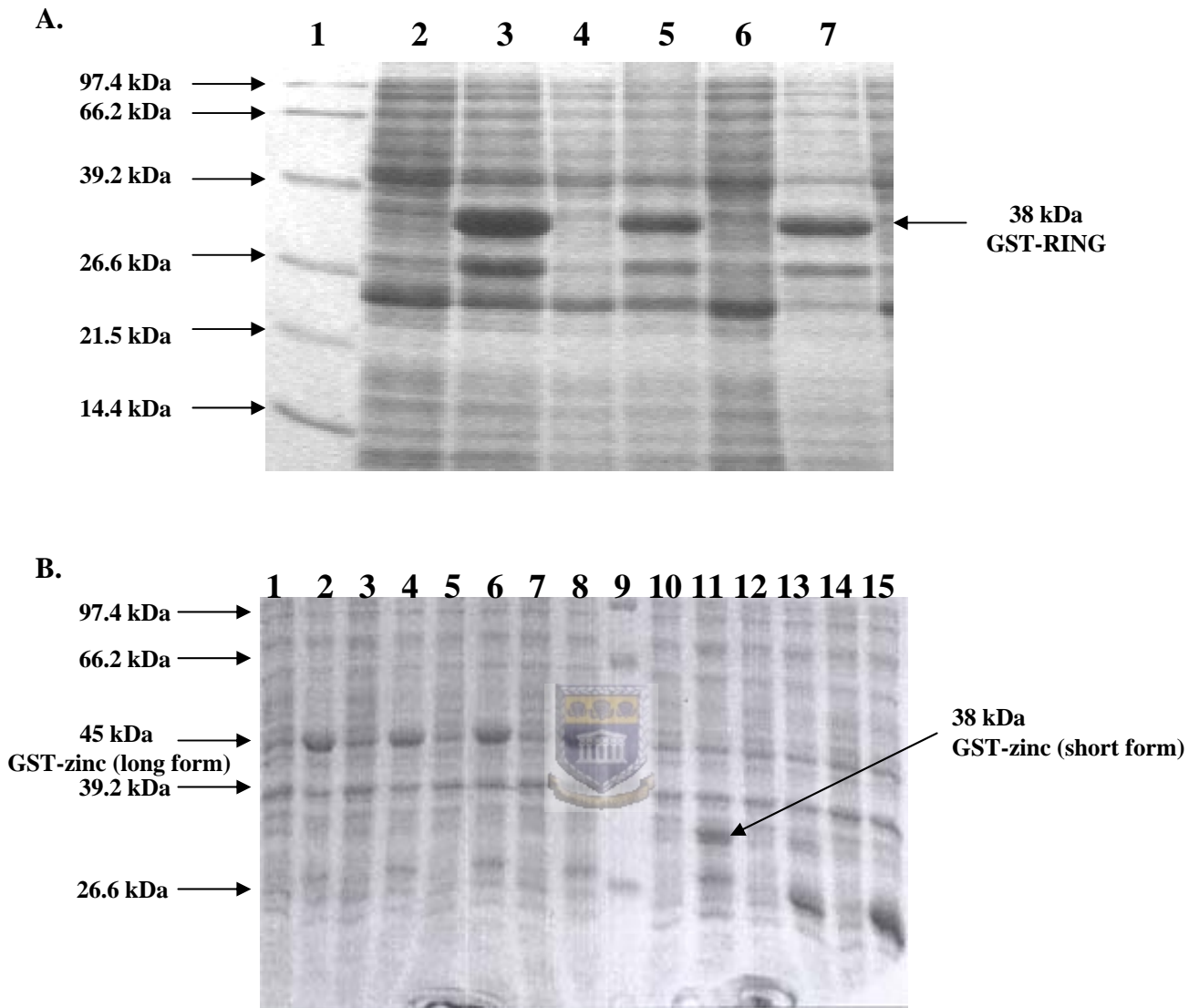



Fig. 5.5: Expression screen of the RING finger (**A**) and zinc finger (**B**) domains. (**A**) Lane 1: protein molecular weight marker. Lane 2, 4 and 6: un-induced samples. Lane 3, 5 and 7: induced samples showing induction of the 38 kDa GST-RING finger fusion protein. (**B**) Lane 1, 3, 5 and 7: un-induced samples of the long form clones; Lane 2, 4, 6 and 8: induced samples showing the expression of the 45 kDa fusion protein. Lane 9: protein molecular weight marker. Lane 10, 12 and 14: un-induced samples of the short form zinc finger construct. Lane 11, 13 and 15: induced samples of the short form zinc finger domain. Only lane 11 shows the induction of the GST-zinc (short form) as indicated by an arrow at 38 kDa.

Score = 612 bits (318), Expect = e-172
Identities = 318/318 (100%)
Strand = Plus / Plus



```
Query: 1  ggatccccctcccttcttaccagaggagccatcttcttcctcagaagaagatgatcctatc 60
      |||
Sbjct: 44  ggatccccctcccttcttaccagaggagccatcttcttcctcagaagaagatgatcctatc 103

Query: 61  ccagatgaattgtgtgtctcatctgcaaggatattatgactgatgctgttgtgattccc 120
      |||
Sbjct: 104  ccagatgaattgtgtgtctcatctgcaaggatattatgactgatgctgttgtgattccc 163

Query: 121  tgctgtggaacagttactgtgatgaatgtataagaacagcactcctggaatcagatgag 180
      |||
Sbjct: 164  tgctgtggaacagttactgtgatgaatgtataagaacagcactcctggaatcagatgag 223

Query: 181  cacacatgtccgacgtgtcatcdaaatgatgtttctcctgatgctttaattgccataaa 240
      |||
Sbjct: 224  cacacatgtccgacgtgtcatcdaaatgatgtttctcctgatgctttaattgccataaa 283

Query: 241  ttttacgacaggctgtaaataacttcaaaaatgaaactggctatacaaaaagactacga 300
      |||
Sbjct: 284  ttttacgacaggctgtaaataacttcaaaaatgaaactggctatacaaaaagactacga 343

Query: 301  aaacagtaatgactcgag 318
      |||
Sbjct: 344  aaacagtaatgactcgag 361
```

Fig. 5.4: Sequence alignment of the RING finger domain (sbjct) against the expected *in-silico* sequence made using DNA Strider 1.2 (query) showing 100% identity. Alignment was performed using the BLAST 2 server (NCBI).

Chapter 6: Discussion and Conclusion

6.1 Introduction

In the post-genomic era, determination of the function of the protein products of uncharacterised genes is a major challenge currently facing biologists. *In vitro* protein-protein interaction studies is a commonly adopted approach. The aim of this thesis was to produce DNA expression constructs and use them to investigate the feasibility of recombinantly expressing proteins for future interaction studies between human RBBP6 and p53 and pRb proteins, with which it was previously shown to interact *in vivo* using co-immunoprecipitation [1]. Regions shown to interact with p53 and pRb (denoted p53BD and RbBD respectively) were amplified out of the human RBBP6 using PCR. These were then sub-cloned into the pGEX expression system for recombinant expression as GST fusions to facilitate purification using a glutathione-linked agarose column. p53 and pRb proteins were themselves also recombinantly expressed as GST fusion proteins. Domains containing the zinc finger and RING finger domains were also cloned into the pGEX expression system for expression and future structural studies.

6.2 Expression and purification of the pRb binding domain from human RBBP6 and the pocket domain from pRb

RbBD was successfully expressed as a GST-RbBD fusion protein and purified using a glutathione-linked agarose column. After proteolytic removal of the GST fusion partner, the RbBD was purified to homogeneity using 20HS cation exchange chromatography. The RbBD appeared on SDS-PAGE at an apparent molecular weight of 26 kDa fragment, instead of the expected molecular weight of 18 kDa, although mass spectrometry

confirmed the mass of the protein to be 18 kDa. Other peaks were also visible at 36 and 54 kDa, suggesting that the RbBD could have the tendency to form homo-dimers and homo-trimers. The total yield of the RbBD was determined as 7.95 mg, which when concentrated into 600 μ l produced an NMR sample of 0.73 mM. However a 1D proton NMR spectrum of the protein showed it to be unfolded as the spectrum was very poorly dispersed. This gave rise to the hypothesis that the protein may require the binding of pRb in order to fold. Confirmation of this hypothesis will have to await the completion of *in vitro* binding studies, which is beyond the scope of this thesis.

The pocket domain of pRb was also expressed as a GST fusion protein and purified on a glutathione-linked agarose column. Expression and purification yielded a protein of the expected size of 68 kDa.

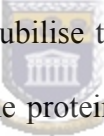


On the basis of this study, we conclude that the pRb binding domain and the pocket domain from pRb can be expressed in sufficient quantities for *in vitro* binding studies using NMR. However, additional investigation should be undertaken to investigate the state of folding of the pRb binding domain.

6.3 Generation of recombinant expression constructs for the p53 binding domain from human RBBP6 and for full-length p53

The p53 binding domain from human RBBP6 was successfully expressed as a GST fusion protein and purified using a glutathione-linked agarose column. The level of expression appeared to be less significantly than that for the RbBD although the exact

extent was not quantified. The domain also appeared to be sensitive to C-terminal proteolysis, the evidence for this being that both the fusion protein and the cleaved p53BD ran as three bands on the SDS-PAGE, whereas after cleavage GST ran as a single tight band. We conclude from this that the C-terminus of the domain is most probably unstructured, possibly due to the presence of the poly-lysine tail at the C-terminus of the domain. The domain was further purified using 20HS cation chromatography.

p53 was amplified using PCR and sub-cloned into a pGEX-6P-2 expression vector and successfully expressed in a small-scale expression as a GST-p53 fusion protein of 80 kDa. The protein was found to be insoluble when expressed in large volumes as the expressed fusion protein was found only in the pellet rather than in the supernatant (data not shown). Attempts were made to solubilise the protein using urea but it precipitated immediately on removal of the urea.  The protein could therefore not be purified further and the interaction studies were discontinued.

On the basis of this study we conclude that the p53 binding domain can be recombinantly expressed for NMR-based interaction studies. With more careful handling it may be possible to reduce the amount of C-terminal degradation. Alternatively expression of the short form p53BD_b, which lacks the C-terminal poly-lysine tail, could be pursued further. However, since the binding to p53 was originally demonstrated using the full-length p53 binding domain, it is possible that use of the short form of p53BD would reduce the binding to p53.

Instead of using full-length p53, we suggest that only the core DNA binding domain be expressed in future studies since this is the part of p53 involved in the interaction with RBBP6 [1]. The core domain of p53 has been successfully used in similar NMR-based studies by Fersht and co-workers [89, 90].

6.4 Generation of reagents for structural analysis of the RING and zinc finger domains of the human RBBP6

Three pGEX expression plasmids, encoding the RING and a short and a long forms of the zinc finger domain from human RBBP6, were also generated as part of this work, for future structural studies. The RING finger construct was sequenced and shown to be correct. The zinc finger constructs were not sequenced. Expression studies showed that proteins of the correct size could be induced in all three cases, of which the RING finger and the long form of the zinc finger were found to be soluble, whereas the short form of the zinc finger was found to be insoluble.

We conclude that the RING finger construct and the long form of the zinc finger are suitable for structural analysis

References:

1. Simons, A., et al., *PACT: cloning and characterization of a cellular p53 binding protein that interacts with Rb*. *Oncogene*, 1997. **14**(2): p. 145-55.
2. Saijo, M., et al., *Molecular cloning of a human protein that binds to the retinoblastoma protein and chromosomal mapping*. *Genomics*, 1995. **27**(3): p. 511-9.
3. Sakai, Y., et al., *cDNA sequence and chromosomal localization of a novel human protein, RBQ-1 (RBBP6), that binds to the retinoblastoma gene product*. *Genomics*, 1995. **30**(1): p. 98-101.
4. Witte, M.M. and R.E. Scott, *The proliferation potential protein-related (P2P-R) gene with domains encoding heterogeneous nuclear ribonucleoprotein association and Rb1 binding shows repressed expression during terminal differentiation*. *Proc Natl Acad Sci U S A*, 1997. **94**(4): p. 1212-7.
5. Scott, R.E., et al., *Functional potential of P2P-R: a role in the cell cycle and cell differentiation related to its interactions with proteins that bind to matrix associated regions of DNA?* *J Cell Biochem*, 2003. **90**(1): p. 6-12.
6. Vo, L.T., et al., *Mpe1, a zinc knuckle protein, is an essential component of yeast cleavage and polyadenylation factor required for the cleavage and polyadenylation of mRNA*. *Mol Cell Biol*, 2001. **21**(24): p. 8346-56.
7. Yoshitake, Y., et al., *Proliferation potential-related protein, an ideal esophageal cancer antigen for immunotherapy, identified using complementary DNA microarray analysis*. *Clin Cancer Res*, 2004. **10**(19): p. 6437-48.
8. Pugh, D.J., et al., *DWNN, a novel ubiquitin-like domain, implicates RBBP6 in mRNA processing and ubiquitin-like pathways*. *BMC Struct Biol*, 2006. **6**(1): p. 1.
9. Matthews, J.M. and M. Sunde, *Zinc fingers--folds for many occasions*. *IUBMB Life*, 2002. **54**(6): p. 351-5.
10. Bae, K.H., et al., *Human zinc fingers as building blocks in the construction of artificial transcription factors*. *Nat Biotechnol*, 2003. **21**(3): p. 275-80.
11. Kentsis, A. and K.L. Borden, *Construction of macromolecular assemblages in eukaryotic processes and their role in human disease: linking RINGs together*. *Curr Protein Pept Sci*, 2000. **1**(1): p. 49-73.
12. Borden, K.L., *RING domains: master builders of molecular scaffolds?* *J Mol Biol*, 2000. **295**(5): p. 1103-12.
13. Borden, K.L. and P.S. Freemont, *The RING finger domain: a recent example of a sequence-structure family*. *Curr Opin Struct Biol*, 1996. **6**(3): p. 395-401.
14. Tyers, M. and A.R. Willems, *One ring to rule a superfamily of E3 ubiquitin ligases*. *Science*, 1999. **284**(5414): p. 601, 603-4.
15. Vogelstein, B., D. Lane, and A.J. Levine, *Surfing the p53 network*. *Nature*, 2000. **408**(6810): p. 307-10.
16. Macleod, K., *Tumor suppressor genes*. *Curr Opin Genet Dev*, 2000. **10**(1): p. 81-93.
17. Chin, L., G. Merlino, and R.A. DePinho, *Malignant melanoma: modern black plague and genetic black box*. *Genes Dev*, 1998. **12**(22): p. 3467-81.
18. Rodrigues, N.R., et al., *p53 mutations in colorectal cancer*. *Proc Natl Acad Sci U S A*, 1990. **87**(19): p. 7555-9.

19. Steller, H., *Mechanisms and genes of cellular suicide*. Science, 1995. **267**(5203): p. 1445-9.
20. Abrams, J.M., *An emerging blueprint for apoptosis in Drosophila*. Trends Cell Biol, 1999. **9**(11): p. 435-40.
21. Vaux, D.L. and A. Strasser, *The molecular biology of apoptosis*. Proc Natl Acad Sci U S A, 1996. **93**(6): p. 2239-44.
22. Iwahashi, H., et al., *Synergistic anti-apoptotic activity between Bcl-2 and SMN implicated in spinal muscular atrophy*. Nature, 1997. **390**(6658): p. 413-7.
23. Benoist, C. and D. Mathis, *Cell death mediators in autoimmune diabetes--no shortage of suspects*. Cell, 1997. **89**(1): p. 1-3.
24. Levine, A.J., *p53, the cellular gatekeeper for growth and division*. Cell, 1997. **88**(3): p. 323-31.
25. Weinberg, R.A., *The retinoblastoma protein and cell cycle control*. Cell, 1995. **81**(3): p. 323-30.
26. Guillouf, C., et al., *p53 involvement in control of G2 exit of the cell cycle: role in DNA damage-induced apoptosis*. Oncogene, 1995. **10**(11): p. 2263-70.
27. Clarke, A.R., et al., *Thymocyte apoptosis induced by p53-dependent and independent pathways*. Nature, 1993. **362**(6423): p. 849-52.
28. Vousden, K.H., *p53: death star*. Cell, 2000. **103**(5): p. 691-4.
29. Shimizu, S., et al., *Involvement of ICE family proteases in apoptosis induced by reoxygenation of hypoxic hepatocytes*. Am J Physiol, 1996. **271**(6 Pt 1): p. G949-58.
30. Bennett, M., et al., *Cell surface trafficking of Fas: a rapid mechanism of p53-mediated apoptosis*. Science, 1998. **282**(5387): p. 290-3.
31. Ashkenazi, A. and V.M. Dixit, *Death receptors: signaling and modulation*. Science, 1998. **281**(5381): p. 1305-8.
32. Hsieh, J.K., et al., *RB regulates the stability and the apoptotic function of p53 via MDM2*. Mol Cell, 1999. **3**(2): p. 181-93.
33. Lundberg, A.S. and R.A. Weinberg, *Functional inactivation of the retinoblastoma protein requires sequential modification by at least two distinct cyclin-cdk complexes*. Mol Cell Biol, 1998. **18**(2): p. 753-61.
34. Harbour, J.W., et al., *Cdk phosphorylation triggers sequential intramolecular interactions that progressively block Rb functions as cells move through G1*. Cell, 1999. **98**(6): p. 859-69.
35. Lane, D.P. and L.V. Crawford, *T antigen is bound to a host protein in SV40-transformed cells*. Nature, 1979. **278**(5701): p. 261-3.
36. Hainaut, P. and M. Hollstein, *p53 and human cancer: the first ten thousand mutations*. Adv Cancer Res, 2000. **77**: p. 81-137.
37. Vogelstein, B. and K.W. Kinzler, *p53 function and dysfunction*. Cell, 1992. **70**(4): p. 523-6.
38. Shaulsky, G., A. Ben-Ze'ev, and V. Rotter, *Subcellular distribution of the p53 protein during the cell cycle of Balb/c 3T3 cells*. Oncogene, 1990. **5**(11): p. 1707-11.
39. Polyak, K., et al., *A model for p53-induced apoptosis*. Nature, 1997. **389**(6648): p. 300-5.

40. Oren, M., *Regulation of the p53 tumor suppressor protein*. J Biol Chem, 1999. **274**(51): p. 36031-4.
41. Oren, M. and V. Rotter, *Introduction: p53--the first twenty years*. Cell Mol Life Sci, 1999. **55**(1): p. 9-11.
42. Ryan, K.M., A.C. Phillips, and K.H. Vousden, *Regulation and function of the p53 tumor suppressor protein*. Curr Opin Cell Biol, 2001. **13**(3): p. 332-7.
43. Jayaraman, L. and C. Prives, *Covalent and noncovalent modifiers of the p53 protein*. Cell Mol Life Sci, 1999. **55**(1): p. 76-87.
44. Fields, S. and S.K. Jang, *Presence of a potent transcription activating sequence in the p53 protein*. Science, 1990. **249**(4972): p. 1046-9.
45. Raycroft, L., H.Y. Wu, and G. Lozano, *Transcriptional activation by wild-type but not transforming mutants of the p53 anti-oncogene*. Science, 1990. **249**(4972): p. 1049-51.
46. Unger, T., et al., *p53: a transdominant regulator of transcription whose function is ablated by mutations occurring in human cancer*. Embo J, 1992. **11**(4): p. 1383-90.
47. el-Deiry, W.S., et al., *Definition of a consensus binding site for p53*. Nat Genet, 1992. **1**(1): p. 45-9.
48. Hupp, T.R., D.P. Lane, and K.L. Ball, *Strategies for manipulating the p53 pathway in the treatment of human cancer*. Biochem J, 2000. **352 Pt 1**: p. 1-17.
49. Martin, S.J., *Apoptosis: suicide, execution or murder?* Trends Cell Biol, 1993. **3**(5): p. 141-4.
50. Thut, C.J., et al., *p53 transcriptional activation mediated by coactivators TAFII40 and TAFII60*. Science, 1995. **267**(5194): p. 100-4.
51. Liu, X., et al., *The p53 activation domain binds the TATA box-binding polypeptide in Holo-TFIID, and a neighboring p53 domain inhibits transcription*. Mol Cell Biol, 1993. **13**(6): p. 3291-300.
52. Woods, D.B. and K.H. Vousden, *Regulation of p53 function*. Exp Cell Res, 2001. **264**(1): p. 56-66.
53. Ashcroft, M. and K.H. Vousden, *Regulation of p53 stability*. Oncogene, 1999. **18**(53): p. 7637-43.
54. Haupt, Y., et al., *Mdm2 promotes the rapid degradation of p53*. Nature, 1997. **387**(6630): p. 296-9.
55. Honda, R., H. Tanaka, and H. Yasuda, *Oncoprotein MDM2 is a ubiquitin ligase E3 for tumor suppressor p53*. FEBS Lett, 1997. **420**(1): p. 25-7.
56. Hershko, A. and A. Ciechanover, *The ubiquitin system*. Annu Rev Biochem, 1998. **67**: p. 425-79.
57. Maki, C.G., *Oligomerization is required for p53 to be efficiently ubiquitinated by MDM2*. J Biol Chem, 1999. **274**(23): p. 16531-5.
58. Freedman, D.A. and A.J. Levine, *Nuclear export is required for degradation of endogenous p53 by MDM2 and human papillomavirus E6*. Mol Cell Biol, 1998. **18**(12): p. 7288-93.
59. Giannakakou, P., et al., *p53 is associated with cellular microtubules and is transported to the nucleus by dynein*. Nat Cell Biol, 2000. **2**(10): p. 709-17.
60. Colman, M.S., C.A. Afshari, and J.C. Barrett, *Regulation of p53 stability and activity in response to genotoxic stress*. Mutat Res, 2000. **462**(2-3): p. 179-88.

61. Shieh, S.Y., et al., *The human homologs of checkpoint kinases Chk1 and Cds1 (Chk2) phosphorylate p53 at multiple DNA damage-inducible sites.* Genes Dev, 2000. **14**(3): p. 289-300.
62. Chehab, N.H., et al., *Chk2/hCds1 functions as a DNA damage checkpoint in G(1) by stabilizing p53.* Genes Dev, 2000. **14**(3): p. 278-88.
63. Prives, C., *Signaling to p53: breaking the MDM2-p53 circuit.* Cell, 1998. **95**(1): p. 5-8.
64. Lambert, P.F., et al., *Phosphorylation of p53 serine 15 increases interaction with CBP.* J Biol Chem, 1998. **273**(49): p. 33048-53.
65. Sakaguchi, K., et al., *DNA damage activates p53 through a phosphorylation-acetylation cascade.* Genes Dev, 1998. **12**(18): p. 2831-41.
66. Luo, J., et al., *Deacetylation of p53 modulates its effect on cell growth and apoptosis.* Nature, 2000. **408**(6810): p. 377-81.
67. Gostissa, M., et al., *Activation of p53 by conjugation to the ubiquitin-like protein SUMO-1.* Embo J, 1999. **18**(22): p. 6462-71.
68. Gu, W. and R.G. Roeder, *Activation of p53 sequence-specific DNA binding by acetylation of the p53 C-terminal domain.* Cell, 1997. **90**(4): p. 595-606.
69. Meek, D.W., *Mechanisms of switching on p53: a role for covalent modification?* Oncogene, 1999. **18**(53): p. 7666-75.
70. Rodriguez, M.S., et al., *SUMO-1 modification activates the transcriptional response of p53.* Embo J, 1999. **18**(22): p. 6455-61.
71. Buchhop, S., et al., *Interaction of p53 with the human Rad51 protein.* Nucleic Acids Res, 1997. **25**(19): p. 3868-74.
72. Zhang, Y., Y. Xiong, and W.G. Yarbrough, *ARF promotes MDM2 degradation and stabilizes p53: ARF-INK4a locus deletion impairs both the Rb and p53 tumor suppression pathways.* Cell, 1998. **92**(6): p. 725-34.
73. Knudson, A.G., Jr., *Genetics of human cancer.* Annu Rev Genet, 1986. **20**: p. 231-51.
74. Hickman, E.S., M.C. Moroni, and K. Helin, *The role of p53 and pRB in apoptosis and cancer.* Curr Opin Genet Dev, 2002. **12**(1): p. 60-6.
75. Sellers, W.R., J.W. Rodgers, and W.G. Kaelin, Jr., *A potent transrepression domain in the retinoblastoma protein induces a cell cycle arrest when bound to E2F sites.* Proc Natl Acad Sci U S A, 1995. **92**(25): p. 11544-8.
76. Kim, H.Y., B.Y. Ahn, and Y. Cho, *Structural basis for the inactivation of retinoblastoma tumor suppressor by SV40 large T antigen.* Embo J, 2001. **20**(1-2): p. 295-304.
77. Morris, E.J. and N.J. Dyson, *Retinoblastoma protein partners.* Adv Cancer Res, 2001. **82**: p. 1-54.
78. Xiao, B., et al., *Crystal structure of the retinoblastoma tumor suppressor protein bound to E2F and the molecular basis of its regulation.* Proc Natl Acad Sci U S A, 2003. **100**(5): p. 2363-8.
79. Ko, L.J. and C. Prives, *p53: puzzle and paradigm.* Genes Dev, 1996. **10**(9): p. 1054-72.
80. Adams, P.D., *Regulation of the retinoblastoma tumor suppressor protein by cyclin/cdks.* Biochim Biophys Acta, 2001. **1471**(3): p. M123-33.

81. Adams, P.D., et al., *Retinoblastoma protein contains a C-terminal motif that targets it for phosphorylation by cyclin-cdk complexes*. Mol Cell Biol, 1999. **19**(2): p. 1068-80.
82. Bartek, J., J. Bartkova, and J. Lukas, *The retinoblastoma protein pathway in cell cycle control and cancer*. Exp Cell Res, 1997. **237**(1): p. 1-6.
83. Shiiio, Y., T. Yamamoto, and N. Yamaguchi, *Negative regulation of Rb expression by the p53 gene product*. Proc Natl Acad Sci U S A, 1992. **89**(12): p. 5206-10.
84. Lee, J.O., A.A. Russo, and N.P. Pavletich, *Structure of the retinoblastoma tumour-suppressor pocket domain bound to a peptide from HPV E7*. Nature, 1998. **391**(6670): p. 859-65.
85. Smith, D.B. and K.S. Johnson, *Single-step purification of polypeptides expressed in Escherichia coli as fusions with glutathione S-transferase*. Gene, 1988. **67**(1): p. 31-40.
86. Birnboim, H.C. and J. Doly, *A rapid alkaline extraction procedure for screening recombinant plasmid DNA*. Nucleic Acids Res, 1979. **7**(6): p. 1513-23.
87. Laemmli, U.K., *Cleavage of structural proteins during the assembly of the head of bacteriophage T4*. Nature, 1970. **227**(5259): p. 680-5.
88. Bradford, M.M., *A rapid and sensitive method for the quantitation of microgram quantities of protein utilizing the principle of protein-dye binding*. Anal Biochem, 1976. **72**: p. 248-54.
89. Friedler, A., et al., *A peptide that binds and stabilizes p53 core domain: chaperone strategy for rescue of oncogenic mutants*. Proc Natl Acad Sci U S A, 2002. **99**(2): p. 937-42.
90. Weinberg, R.L., et al., *Regulation of DNA binding of p53 by its C-terminal domain*. J Mol Biol, 2004. **342**(3): p. 801-11.

1/1 31/11 61/21 91/31
CGG CCG CGC TAT GGA CCC CTG ACC CCG TGg gGT Cgc TCG GAC TCT TAA CGT GTG GAC TGA CCG cTA CTG ACT GCA CCG CCA ATC CCC CCG TCT CTG CCG GCC CCT TAG CAT GAG CGA GGG

121/41 151/51 181/61 211/71
GGA Ccc aGC CGG GTG ACA TTG TGC CCG TTG GCG GAT TCT CGA TTT CCC CTC TTC CCC gTc Ctc GtC Ctc Ctc cTC ccC caT gaA GtG Att CtG aGt atC GGG GGG TCT CTG GAT TAT TGT

241/81 271/91 301/101 331/111
TCT GAC GAA CCC CTG CTT GTG GTT GGG GGG TAT TTA ATC TGA GGC CTT AGG GTC CTT CGG TGT Ctt TGA GTG TTT TGT GTG TAC ATA TTT TGC TCT TAA AGT TTA TAA ATA TAC GTA TAT

361/121 391/131 421/141 451/151
TGA GAG TGT CCA CGT CTC CTC GCT GAA CCT TAG GAA TCC CTT GGC ACC ATG TCC TGT GTg CAT TAT AAA tTT TCC tCT AAA CTC AAC TAt GAT ACC GTC ACC TTT Gat GGG CTC CAC ATC
M S C V H Y K F S S K L N Y D T V T F D G L H I

481/161 511/171 541/181 571/191
TCC CTC tGC GAC TTA aAG AAG CAG ATT ATG GgG AGA GAG AAG CTG aAA GCT GCC GAC TGC GAC CTG CAG ATC ACC AAT GCG CAG ACg Aaa gAA gAa TAT ACT GAT GAT AAT GCT CTG ATT
S L C D L K K Q I M G R E K L K A A D C D L Q I T N A Q T K E E Y T D D N A L I

601/201 631/211 661/221 691/231
CcT AAG AAT TCT Tct GTA ATT GTT agA aga ATt cCT ATT GGA GGT GTT AAA TCT ACA AGC AAG Aca TAT GTT aTA AGT CGA ACT GAA CCa GCg ATG Gca ACT Aca AAA Gca ATT GAT GAC
P K N S S V I V R R I P I G G V K S T S K T Y V I S R T E P A M A T T K A I D D

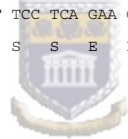
Appendix 1: Human RBBP6 sequence

721/241 751/251 781/261 811/271
TCT TCC GCG TCT ATT TCT CTG GCC CAG CTT ACA AAG GCT GCC AAT CTG GCT GAA GCC AAT GCT TCT GAA GAA GAT AAA ATT AAA GCA ATG ATG CCG CAA TCT GGC CAT GAA TAC TAC CCA
S S A S I S L A Q L T K A A N L A E A N A S E E D K I K A M M P Q S G H E Y Y P

841/281 871/291 901/301 931/311
ATC AAT TAC ATG AAG AAA CCT CTA GGT CCA CCA CCT CCA TCT TAC ACG TGT TTC CGT TGT GGT AAA CCT GGA CAT TAT ATT AAG AAT TGC CCA ACA AAT GGG GAT AAA AAC TTT GAA TCT
I N Y M K K P L G P P P P S Y T C F R C G K P G H Y I K N C P T N G D K N F E S

961/321 991/331 1021/341 1051/351
GGT CCT AGG ATT AAA AAG AGC ACT GGA ATT CCC AGA AGT TTC ATG ATG GAA GTG AAA GAT CCT AAT ATG AAA GGT GCA ATG CTT ACC AAC ACT GGA AAA TAT GCA ATA CCA ACT ATA GAT
G P R I K K S T G I P R S F M M E V K D P N M K G A M L T N T G K Y A I P T I D

1081/361 1111/371 1141/381 1171/391
GCA GAA GCA TAT GCA ATT GGG AAG AAA GAG AAA CCT CCC TTC TTA CCA GAG GAG CCA TCT TCT TCC TCA GAA GAA GAT GAT CCT ATC CCA GAT GAA TTG TTG TGT CTC ATC TGC AAG GAT
A E A Y A I G K K E K P P F L P E E P S S S S E E D D P I P D E L L C L I C K D



1201/401 1231/411 1261/421 1291/431
ATT ATG ACT GAT GCT GTT GTG ATT CCC TGC TGT GGA AAC AGT TAC TGT GAT GAA TGT ATA AGA ACA GCA CTC CTG GAA TCA GAT GAG CAC ACA TGT CCG ACG TGT CAT CAA AAT GAT GTT
I M T D A V V I P C C G N S Y C D E C I R T A L L E S D E H T C P T C H Q N D V

1321/441 1351/451 1381/461 1411/471
TCT CCT GAT GCT TTA ATT GCC AAT AAA TTT TTA CGA CAG GGT GTA AAT AAC TTC AAA AAT GAA ACT GGC TAT ACA AAA AGA CTA CGA AAA CAG TTA CCT CCT CCA CCA CCC CCA ATA CCA
S P D A L I A N K F L R Q A V N N F K N E T G Y T K R L R K Q L P P P P P P I P

1441/481 1471/491 1501/501 1531/511
CCT CCG AGA CCA CTG ATT CAG AGG AAC CTA CAA CCT CTG ATG AGA TCT CCG ATA TCA AGA CAA CAA GAT CCT CTT ATG ATT CCA GTG ACA TCT TCA TCA ACT CAC CCA GCT CCG TCT ATA
P P R P L I Q R N L Q P L M R S P I S R Q Q D P L M I P V T S S S T H P A P S I

2281/761 2311/771 2341/781 2371/791
TCA AAT ACC ATC CCA ACA ACA CAA GCA CCA CCT TTG TCC AGG GAA GAA TTC TAT AGA GAG CAG CGA CGA CTA AAA GAA GAG GAA AAG AAA AAG TCC AAG CTA GAT GAG TTT ACA AAT GAT
S N T I P T T Q A P P L S R E E F Y R E Q R R L K E E E K K K S K L D E F T N D

2401/801 2431/811 2461/821 2491/831
TTT GCT AAG GAA TTG ATG GAA TAC AAA AAG ATT CAA AAG GAG CGT AGG CGC TCA TTT TCC AGG TCT AAA TCT CCC TAT AGT GGT TCT TCG TAT TCA AGA AGT TCA TAT ACT TAT TCT AAA
F A K E L M E Y K K I Q K E R R R S F S R S K S P Y S G S S Y S R S S Y T Y S K

2521/841 2551/851 2581/861 2611/871
TCA AGA TCT GGG TCA ACA CGT TCA CGC TCT TAT TCT CGA TCA TTC AGC CGC TCA CAT TCT CGT TCC TAT TCA CGG TCA CCT CCA TAC CCC AGA AGA GGC AGA GGC AAG AGC CGC AAT TAC
S R S G S T R S R S Y S R S F S R S H S R S Y S R S P P Y P R R G R G K S R N Y



2641/881 2671/891 2701/901 2731/911
CGT TCA CGG TCT AGA TCT CAT GGA TAT CAT CGA TCT AGG TCA AGG TCA CCC CCT TAC AGA CGC TAT CAT TCA CGA TCA AGA TCT CCT CAA GCG TTT AGG GGA CAG TCT CCT AAT AAA CGT
R S R S R S H G Y H R S R S R S P P Y R R Y H S R S R S P Q A F R G Q S P N K R

2761/921 2791/931 2821/941 2851/951
AAT GTA CCT CAA GGG GAA ACA GAA CGT GAA TAT TTT AAT AGA TAC AGA GAA GTT CCA CCA CCA TAT GAC ATG AAA GCA TAT TAT GGG AGA AGT GTT GAC TTT AGA GAC CCA TTT GAA AAA
N V P Q G E T E R E Y F N R Y R E V P P P Y D M K A Y Y G R S V D F R D P F E K

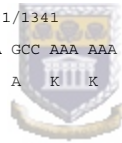
2881/961 2911/971 2941/981 2971/991
GAA CGC TAC CGA GAA TGG GAG AGA AAA TAT AGA GAG TGG TAT GAA AAA TAT TAT AAA GGT TAT GCT GCT GGA GCA CAG CCT AGA CCC TCA GCA AAT AGA GAG AAC TTT TCT CCA GAG AGA
E R Y R E W E R K Y R E W Y E K Y Y K G Y A A G A Q P R P S A N R E N F S P E R

E T P K T D N T K S S S S S Q K D E K I T G T P R K A H S K S A K E H Q E T K P

3721/1241 3751/1251 3781/1261 3811/1271
GTC AAA GAG GAA AAA GTG AAG AAG GAC TAT TCC AAA GAT GTC AAA TCA GAA AAG CTA ACA ACT AAG GAA GAA AAG GCC AAG AAG CCT AAT GAG AAA AAC AAA CCA CTT GAT AAT AAG GGA
V K E E K V K K D Y S K D V K S E K L T T K E E K A K K P N E K N K P L D N K G

3841/1281 3871/1291 3901/1301 3931/1311
Gaa aaa aga aaa aga aaa act gaa gaa aaa ggc gta gat aaa gat ttt gag tct tct tca atg aaa atc tCG AAA CTA GAA GTG ACT GAA ATA GTG AAA CCA TCA CCA AAG CGC AAA ATG
E K R K R K T E E K G V D K D F E S S S M K I S K L E V T E I V K P S P K R K M

3961/1321 3991/1331 4021/1341 4051/1351
GAA CCT GAT ACT GAA AAA ATG GAT AGG ACC CCT GAA AAG GAC AAA ATT TCT TTA AGT GCG CCA GCC AAA AAA ATC AAA CTC AAC AGA GAA ACT GGG AAG AAA ATT GGA AGT ACA GAA AAT
E P D T E K M D R T P E K D K I S L S A P A K K I K L N R E T G K K I G S T E N



4081/1361 4111/1371 4141/1381 4171/1391
ATA TCA AAC ACA AAA GAA CCC TCT GAA AAA TTG GAG TCA ACA TCT AGC AAA GTT AAA CAA GAA AAA GTC AAA GGA AAG GTC AGA CGA AAA GTG ACT GGA ACT GAA GGA TCC AGC TCA ACT
I S N T K E P S E K L E S T S S K V K Q E K V K G K V R R K V T G T E G S S S T

4201/1401 4231/1411 4261/1421 4291/1431
CTG GTG GAT TAC ACC AGT ACG AGC TCA ACT GGA GGC AGT CCT GTG CGG AAA TCT GAA GAA AAA ACA GAT ACA AAG CGA ACT GTG ATT AAA ACG ATG GAA GAA TAT AAT AAT GAC AAT ACC
L V D Y T S T S S T G G S P V R K S E E K T D T K R T V I K T M E E Y N N D N T

4321/1441 4351/1451 4381/1461 4411/1471
GCG CCA GCT GAA GAT GTT ATC ATT ATG ATT CAG GTT CCT CAA TCC AAA TGG GAT AAA GAT GAC TTT GAA TCT GAA GAA GAA GAT GTT AAA TCC ACA CAG CCT ATA TCA AGT GTA GGA AAA


1/1 31/11 61/21 91/31
GGC ACG AGC CAC CGT CCA GGG AGC AGG TAG CTG CTG GGC TCC GGG GAC ACT TTG CGT TCG GGC TGG GAG CGT GCT TTC CAC GAC GGT GAC ACG CTT CCC TGG ATT GGC AGC CAG ACT GCC
121/41 151/51 181/61 211/71
TTC CGG GTC ACT GCC ATG GAG GAG CCG CAG TCA GAT CCT AGC GTC GAG CCC CCT CTG AGT CAG GAA ACA TTT TCA GAC CTA TGG AAA CTA CTT CCT GAA AAC AAC GTT CTG TCC CCC TTG
M E E P Q S D P S V E P P L S Q E T F S D L W K L L P E N N V L S P L
241/81 271/91 301/101 331/111
CCG TCC CAA GCA ATG GAT GAT TTG ATG CTG TCC CCG GAC GAT ATT GAA CAA TGG TTC ACT GAA GAC CCA GGT CCA GAT GAA GCT CCC AGA ATG CCA GAG GCT GCT CCC CGC GTG GCC CCT
P S Q A M D D L M L S P D D I E Q W F T E D P G P D E A P R M P E A A P R V A P
361/121 391/131 421/141 451/151
GCA CCA GCA GCT CCT ACA CCG GCG GCC CCT GCA CCA GCC CCC TCC TGG CCC CTG TCA TCT TCT GTC CCT TCC CAG AAA ACC TAC CAG GGC AGC TAC GGT TTC CGT CTG GGC TTC TTG CAT
A P A A P T P A A P A P A P S W P L S S S V P S Q K T Y Q G S Y G F R L G F L H
481/161 511/171 541/181 571/191
TCT GGG ACA GCC AAG TCT GTG ACT TGC ACG TAC TCC CCT GCC CTC AAC AAG ATG TTT TGC CAA CTG GCC AAG ACC TGC CCT GTG CAG CTG TGG GTT GAT TCC ACA CCC CCG CCC GGC ACC
S G T A K S V T C T Y S P A L N K M F C Q L A K T C P V Q L W V D S T P P P G T
601/201 631/211 661/221 691/231
CGC GTC CGC GCC ATG GCC ATC TAC AAG CAG TCA CAG CAC ATG ACG GAG GTT GTG AGG CGC TGC CCC CAC CAT GAG CGC TGC TCA GAT AGC GAT GGT CTG GCC CCT CCT CAG CAT CTT ATC
R V R A M A I Y K Q S Q H M T E V V R R C P H H E R C S D S D G L A P P Q H L I
721/241 751/251 781/261 811/271
CGA GTG GAA GGA AAT TTG CGT GTG GAG TAT TTG GAT GAC AGA AAC ACT TTT CGA CAT AGT GTG GTG GTG CCC TAT GAG CCG CCT GAG GTT GGC TCT GAC TGT ACC ACC ATC CAC TAC AAC
R V E G N L R V E Y L D D R N T F R H S V V V P Y E P P E V G S D C T T I H Y N
841/281 871/291 901/301 931/311
TAC ATG TGT AAC AGT TCC TGC ATG GGC GGC ATG AAC CCG AGG CCC ATC CTC ACC ATC ATC ACA CTG GAA GAC TCC AGT GGT AAT CTA CTG GGA CGG AAC AGC TTT GAG GTG CGT GTT TGT
Y M C N S S C M G G M N R R P I L T I I T L E D S S G N L L G R N S F E V R V C
961/321 991/331 1021/341 1051/351
GCC TGT CCT GGG AGA GAC CCG CGC ACA GAG GAA GAG AAT CTC CGC AAG AAA GGG GAG CCT CAC CAC GAG CTG CCC CCA GGG AGC ACT AAG CGA GCA CTG CCC AAC AAC ACC AGC TCC TCT
A C P G R D R R T E E E N L R K K G E P H H E L P P G S T K R A L P N N T S S S
1081/361 1111/371 1141/381 1171/391
CCC CAG CCA AAG AAG AAA CCA CTG GAT GGA GAA TAT TTC ACC CTT CAG ATC CGT GGG CGT GAG CGC TTC GAG ATG TTC CGA GAG CTG AAT GAG GCC TTG GAA CTC AAG GAT GCC CAG GCT
P Q P K K K P L D G E Y F T L Q I R G R E R F E M F R E L N E A L E L K D A Q A
1201/401 1231/411 1261/421 1291/431
GGG AAG GAG CCA GGG GGG AGC AGG GCT CAC TCC AGC CAC CTG AAG TCC AAA AAG GGT CAG TCT ACC TCC CGC CAT AAA AAA CTC ATG TTC AAG ACA GAA GGG CCT GAC TCA GAC TGA CAT
G K E P G G S R A H S S H L K S K K G Q S T S R H K K L M F K T E G P D S D *
1321/441 1351/451 1381/461 1411/471
TCT CCA CTT CTT GTT CCC CAC TGA CAG CCT CCC ACC CCC ATC TCT CCC TCC CCT GCC ATT TTG GGT TTT GGG TCT TTG AAC CCT TGC TTG CAA TAG GTG TGC GTC AGA AGC ACC CAG GAC
1441/481 1471/491 1501/501 1531/511
TTC CAT TTG CTT TGT CCC GGG GCT CCA CTG AAC AAG TTG GCC TGC ACT GGT GTT TTG TTG TGG GGA GGA GGA TGG GGA GTA GGA CAT ACC AGC TTA GAT TTT AAG GTT TTT ACT GTG AGG
1561/521 1591/531 1621/541 1651/551
GAT GTT TGG GAG ATG TAA GAA ATG TTC TTG CAG TTA AGG GTT AGT TTA CAA TCA GCC ACA TTC TAG GTA GGG GCC CAC TTC ACC GTA CTA ACC AGG GAA GCT GTC CCT CAC TGT TGA ATT
1681/561 1711/571 1741/581 1771/591
TTC TCT AAC TTC AAG GCC CAT ATC TGT GAA ATG CTG GCA TTT GCA CCT ACC TCA CAG AGT GCA TTG TGA GGG TTA ATG AAA TAA TGT ACA TCT GGC CTT GAA ACC ACC TTT TAT TAC ATG
1801/601 1831/611 1861/621 1891/631
GGG TCT AGA ACT TGA CCC CCT TGA GGG TGC TTG TTC CCT CTC CCT GTT GGT CGG TGG GTT GGT AGT TTC TAC AGT TGG GCA GCT GGT TAG GTA GAG GGA GTT GTC AAG TCT CTG CTG GCC
1921/641 1951/651 1981/661 2011/671
CAG CCA AAC CCT GTC TGA CCA CCT CTT GGT GAA CCT TAG TAC CTA AAA GGA AAT CTC ACC CCA TCC CAC ACC CTG GAG GAT TTC ATC TCT TGT ATA TGA TGA TCT GGA TCC ACC AAG ACT

Appendix 2: Human p53 sequence

Appendix 4: General chemicals and enzymes

40% 37.5:1 Acrylamide: bis-acrylamide	Promega
Agar	Merck
Agarose	Promega
Ammonium chloride	Sigma
Ammonium persulphate	Merck
Ampicillin	Roche Diagnostic
<i>Bam</i> HI	Promega
Boric acid	Merck
Buffered saturated phenol	Invitrogen
Bromophenol blue	Sigma
Calcium chloride (CaCl ₂)	Merck
Cesium chloride (CsCl ₂)	Roche Diagnostic
Chloroform	BDH
Complete protease inhibitors	Roche Diagnostic
Coomasie Brilliant Blue R 250	Sigma
DTT (Dithiothreitol)	Roche Diagnostic
EDTA (Ethylene diamine tetra acetic acid di-sodium salt)	Merck
Ethanol	BDH
EtBr ₂ (Ethidium bromide)	Sigma
Glacial acetic acid	Merck
Glucose	BDH
Glutathione	Sigma



Glutathione-Sepharose		Sigma
Glycerol		Merck
Glycine		Merck
Hydrochloric acid		Merck
IPTG (Isopropyl β - D – thiogalactopyranoside)		Roche Diagnostic
Isopropanol		Merck
MgCl ₂ (Magnesium Chloride)		Merck
Methanol		Merck
MOPS		Roche Diagnostic
NZ Amine A		Sigma
PMSF (Phenylmethylsulphonyl fluoride)		Roche Diagnostic
KOAc (Potassium acetate)		Merck
Premixed Protein Marker		Roche Diagnostic
SDS (Sodium Dodecyl Sulphate)		Promega
Sodium azide		Merck
Sodium chloride		Merck
Sodium hydroxide		Merck
Taq DNA Polymerase		Takara
TEMED (N, N, N', N' - tetramethylethylenediamine)		Promega
Tris (hydroxymethyl) amino methane		BDH
T4 DNA ligase		Promega
Triton X-100 (Iso- octylphenoxyethoxyethanol)		Roche Diagnostic
Tryptone powder		Merck

Xho I

Promega

Xylene cyanol

BDH

Yeast extract powder

Merck



Appendix 3: General stock solution and buffers

Ammonium persulphate:

10 % stock was prepared in de-ionised water and stored at -20°C.

Ampicillin:

100 mg/ml stock was prepared in de-ionised water and stored at 4°C.

Cleavage buffer:

50 mM Tris pH 8.0, 150 mM NaCl, 1 mM EDTA and 1 mM DTT.

De-staining Solution:

15% (v/v) acetic acid.

DNA Loading buffer:

30% (v/v) Glycerol, 0.25% (w/v) Bromophenol blue and 0.25% (w/v) Xylene cyanol.

DTT:

1 M stock in 0.01 M Sodium acetate, pH 5.2, filtered and stored at -20°C.

Elution Buffer:

16 mM Glutathione in 50 mM Tris pH 8 and 150 mM NaCl.

10x GTE:

50 mM Tris, 50 mM Glucose and 10 mM EDTA, pH 8.0 and stored at 4°C.

IPTG:

1M stock in de-ionised water filtered and stored at -20°C.

3 M KOAc:

3 M Potassium acetate, pH 5.2.

10x MOPS:

200 mM MOPS, 50 mM NaOAc, 10 mM EDTA, pH adjusted to 7.0 with 10 N NaOH.

LB agar:

10g/l Tryptone, 5g/l Yeast extract, 5 g/l NaCl and 14 g/l Bacteriological agar.

LB broth:

10 g/l Tryptone, 5 g/l Yeast extract and 5 g/l NaCl.

Lysis Buffer:

PBS containing 1 mM EDTA, 1 mM DTT, 1 mM PMSF, 1% (v/v) Triton X-100 and 1 pill of Ø complete free EDTA protease inhibitors.

10x M9 salts:

12.8g/l of $\text{Na}_2\text{HPO}_4 \cdot 7\text{H}_2\text{O}$, 0.5g/l NaCl, 3g/l KH_2PO_4 and 1g/l NH_4Cl

NaOH/SDS:

0.2 N NaOH and 1% SDS. Reagent was freshly prepared before use.

NZ Amine A:

10g of NZ Amine A and 5g of NaCl in 860ml of dH_2O and adjusted to 1L with 100ml of 10x M9 salt, 20% Glucose and 0.001 M Mg_2SO_4

PBS:

137 mM NaCl, 2.7 mM KCl, 8 mM Na_2HPO_4 , pH 7.4

PMSF:

0.1 M stock was prepared in isopropanol and stored at -20°C

Phenol: chloroform:

1 part buffered phenol and 1 part chloroform.

SDS Electrophoresis buffer:

25 mM Tris, 0.1% SDS and 250 mM Glycine, pH 8.3.

Separating buffer:

1.5 M Tris pH 8.8.

Sequencing buffer:

1 M Tris and 25 mM MgCl₂ and stored at -20°C.

Stacking buffer:

0.5 M Tris pH 6.8.

Staining Solution:

50% (v/v) Methanol, 10% (v/v) Acetic acid and 0.1625 M Coomassie brilliant blue R250.

10x TAE:

0.4 M Tris and 0.01 M EDTA, adjusted pH to pH 8.0 with glacial acetic acid and made up to 1L and autoclaved. Stock solution was diluted 10 fold for the running of agarose gels.



10x TBE:

0.9 M Tris, 0.89 M Boric acid and 25 mM EDTA pH 8.3, made up to 1L and autoclaved. Stock solution was diluted 10 fold with de-ionised water for the running of agarose gels.

10x TE:

100 mM Tris, 10 mM EDTA and adjusted the pH to 7.5 with HCl and autoclaved. Stock solution was diluted 10 fold with de-ionised water for DNA resuspension.

Tfb1:

30 mM Potassium acetate, 50 mM MnCl₂, 0.1 M KCl, 6.7 mM CaCl₂ and 15% (v/v) Glycerol.

Tfb2:

9 mM MOPS, 50 mM CaCl₂, 10 mM KCl and 15% (v/v) Glycerol.

TYM Broth:

20 g/l Tryptone, 5g/l Yeast extract, 3.5 g/l NaCl and 2 g/l MgCl₂.

